

1 **Systematic exploration of *Escherichia coli* phage-host interactions**
2 **with the BASEL phage collection**

3

4

5 Enea Maffei^{1,#}, Aisylu Shaidullina^{1,#}, Marco Burkolter¹, Valentin Druelle¹, Luc Willi¹, Fabienne
6 Estermann¹, Sarah Michaelis², Hubert Hilbi², David S. Thaler¹, Alexander Harms^{1*}

7

8

9 ¹Focal Area of Infection Biology, Biozentrum, University of Basel, Basel, Switzerland

10 ²Institute of Medical Microbiology, University of Zürich, Zürich, Switzerland

11 [#]These authors contributed equally.

12 ^{*}Correspondence should be addressed to Dr. Alexander Harms (alexander.harms@unibas.ch).

13 **Abstract**

14 Bacteriophages, the viruses infecting bacteria, hold great potential for the treatment of multidrug-
15 resistant bacterial infections and other applications due to their unparalleled diversity and recent
16 breakthroughs in their genetic engineering. However, fundamental knowledge of molecular mechanisms
17 underlying phage-host interactions is mostly confined to a few traditional model systems and did not keep
18 pace with the recent massive expansion of the field. The true potential of molecular biology encoded by
19 these viruses has therefore remained largely untapped, and phages for therapy or other applications are
20 often still selected empirically. We therefore sought to promote a systematic exploration of phage-host
21 interactions by composing a well-assorted library of 66 newly isolated phages infecting the model organism
22 *Escherichia coli* that we share with the community as the BASEL collection (BActeriophage SElection for
23 your Laboratory). This collection is largely representative of natural *E. coli* phage diversity and was
24 intensively characterized phenotypically and genomically alongside ten well-studied traditional model
25 phages. We experimentally determined essential host receptors of all phages, quantified their sensitivity to
26 eleven defense systems across different layers of bacterial immunity, and matched these results to the
27 phages' host range across a panel of pathogenic enterobacterial strains. Our results reveal clear patterns in
28 the distribution of phage phenotypes and genomic features that highlight systematic differences in the
29 potency of different immunity systems and point towards the molecular basis of receptor specificity in
30 several phage groups. Strong trade-offs were detected between fitness traits like broad host recognition and
31 resistance to bacterial immunity that might drive the divergent adaptation of different phage groups to
32 specific niches. We envision that the BASEL collection will inspire future work exploring the biology of
33 bacteriophages and their hosts by facilitating the discovery of underlying molecular mechanisms as the
34 basis for an effective translation into biotechnology or therapeutic applications.

35 Introduction

36 Bacteriophages, the viruses infecting bacteria, are the most abundant biological entities on earth
37 with key positions in all ecosystems and carry large part of our planet's genetic diversity in their genomes
38 [1-3]. Out of this diversity, a few phages infecting *Escherichia coli* became classical models of molecular
39 biology with roles in many fundamental discoveries and are still major workhorses of research today [4].
40 The most prominent of these are the seven "T phages" T1 – T7 [5, reviewed in reference 6] and
41 bacteriophage lambda [7]. Like the majority of known phages, these classical models are tailed phages or
42 *Caudovirales* that use characteristic tail structures to bind host surface receptors and to inject their genomes
43 from the virion head into the host cell. Three major virion morphotypes of *Caudovirales* are known,
44 myoviruses with a contractile tail, siphoviruses with a long and flexible tail, and podoviruses with a very
45 short, stubby tail [2] (Fig 1A). While the T phages are all so-called lytic phages and kill their host to replicate
46 at each infection event, lambda is a temperate phage and can either kill the host to directly replicate or
47 decide to integrate into the host's genome as a prophage for transient passive replication by vertical
48 transmission in the so-called lysogen [2, 8]. These two alternative lifestyles as lytic or temperate phages
49 have major implications for viral ecology and evolution: While lytic phages have primarily been selected
50 to overcome host defenses and maximize virus replication, temperate phages characteristically encode
51 genes that increase the lysogens' fitness, e.g., by providing additional bacterial immunity systems to fight
52 other phages [8, 9].

53 The ubiquity of phage predation has driven the evolution of a vast arsenal of bacterial immunity
54 systems targeting any step of phage infection [9, 10]. Inside host cells, phages encounter two lines of
55 defense of which the first primarily comprises restriction-modification (RM) systems or CRISPR-Cas, the
56 bacterial adaptive immunity, that directly attack viral genomes [11] (Fig 1B). A second line of defense is
57 formed by diverse abortive infection (Abi) systems that protect the host population by triggering an
58 altruistic suicide of infected cells when sensing viral infections [9-12] (Fig 1B). While RM systems and
59 CRISPR-Cas are highly abundant and have been successfully adapted for biotechnology (honored with

60 Nobel Prizes in 1978 and 2020, respectively), the molecular mechanisms underlying the function of
61 collectively abundant, but each individually rare, Abi systems have remained elusive with few exceptions
62 [9-12].

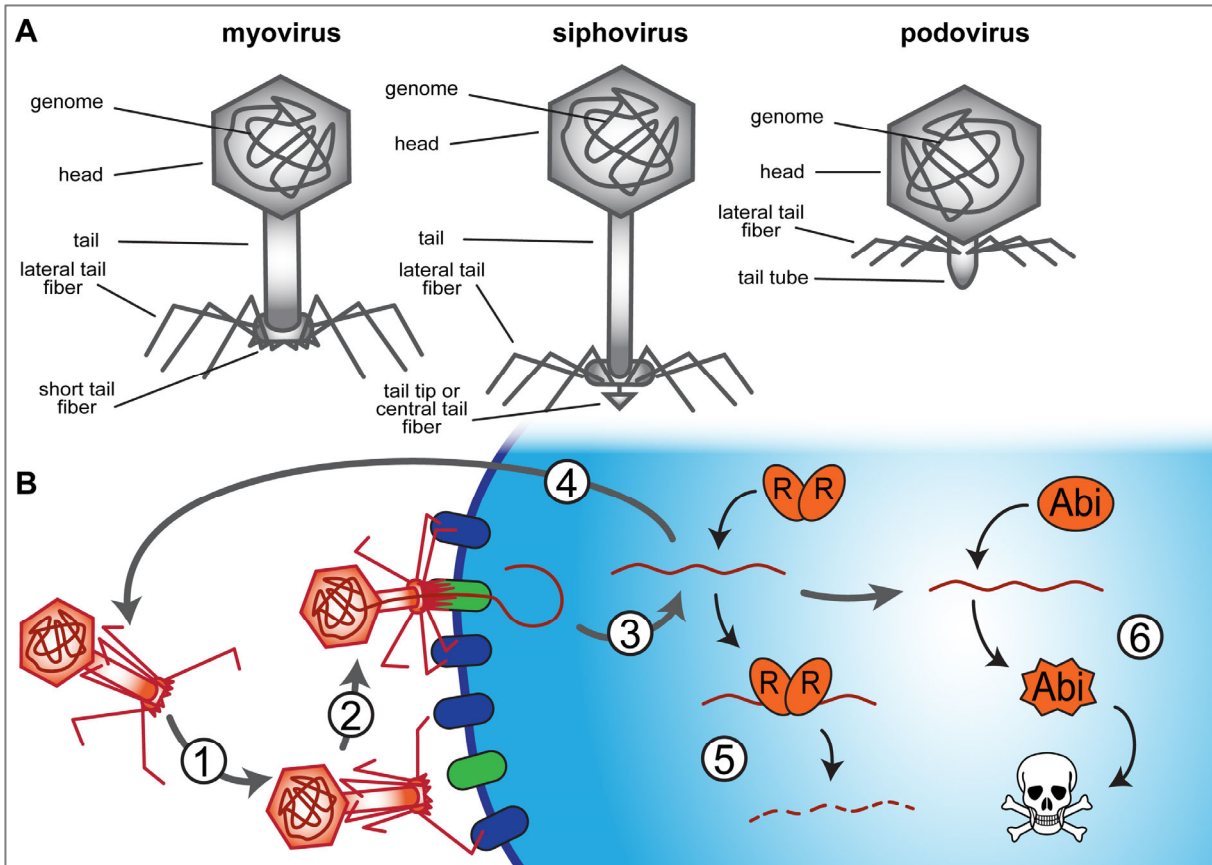


Fig 1. The three morphotypes of *Caudovirales* and two lines of defense in bacterial immunity.

(A) The virions of tailed phages or *Caudovirales* can be assigned to three general morphotypes including myoviruses (contractile tail), siphoviruses (long and flexible, non-contractile tail), and podoviruses (short and stubby tail). (B) The life cycle of a typical lytic phage begins with reversible attachment to a so-called primary receptor on the bacterial cell surface (1), usually via lateral tail fibers at the virion. Subsequently, irreversible attachment to secondary or terminal receptors usually depends on structures at the end of the tail, e.g., short tail fibers for many myoviruses and central tail fibers or tail tip proteins for siphoviruses (2 ; see also (A)). After genome injection (3), the phage takes over the host cell, replicates, and releases the offspring by host cell lysis (4). Inside the host cell, the bacteriophage faces two lines of host defenses, first bacterial immunity systems that try to clear the infection by directly targeting the phage genome (5) and then abortive infection systems that kill the infected cell when a viral infection is sensed (6).

63 Research on phages has expanded at breathless pace over the last decade with a focus on
64 biotechnology and on clinical applications against bacterial infections (“phage therapy”) [13, 14]. Besides
65 or instead of the few traditional model phages, many researchers now employ comparably poorly described,
66 newly isolated phages that are often only used for a few studies and available only in their laboratory. The

67 consequence of this development is a rapidly growing amount of very patchy data such as, e.g., the currently
68 more than 14'000 available unique phage genomes [15] for which largely no linked phenotypic data are
69 available. Despite the value of proof-of-principle studies and a rich genome database, this lack of
70 systematic, interlinked data in combination with the diversity of bacteriophages makes it very difficult to
71 gain a mechanistic understanding of phage biology or to uncover patterns in the data that would support the
72 discovery of broad biological principles beyond individual models.

73 As an example, phage isolates for treating a specific case of bacterial infection are necessarily
74 chosen largely empirically due to the lack of systematic data about relevant phage properties. Currently,
75 the selection of native phages and their engineering for therapeutic applications primarily focus on a lytic
76 lifestyle, a broad host range, and very occasionally on biofilm- or cell wall-degrading enzymes that are
77 comparably well understood genetically and mechanistically [13, 14, 16, 17]. However, the molecular
78 mechanisms and genetic basis underlying other desired features such as resistance to different bacterial
79 immunity systems and, in general, the distribution of all these features across different groups of phages
80 have remained understudied. Given the notable incidence of treatment failure in phage therapy [18-20], a
81 better understanding of the links between phage taxonomy, genome sequence, and phenotypic properties
82 seems timely to select more effective native phages for therapeutic applications and to expand the potential
83 of phage engineering.

84 In this work we therefore present the BASEL (Bacteriophage Selection for your Laboratory)
85 collection as a reference set of 66 newly isolated lytic bacteriophages that infect the laboratory strain *E. coli*
86 K-12 and make it accessible to the scientific community. We provide a systematic phenotypic and genomic
87 characterization of these phages alongside ten classical model phages regarding host receptors, sensitivity
88 and resistance to bacterial immunity, and host range across diverse enterobacteria. Our results highlight
89 clear phenotypic patterns between and within taxonomic groups of phages that reveal strong trade-offs
90 between important bacteriophage traits. These findings greatly expand our understanding of bacteriophage
91 ecology, evolution, and their interplay with bacterial immunity systems. We therefore anticipate that our

92 work will not only establish the BASEL collection as a reference point for future studies exploring
93 fundamental bacteriophage biology but also promote a rational application of phage therapy based on an
94 improved selection and engineering of bacteriophages.

95 **Results**

96 **Composition of the BASEL collection**

97 The first aim of our study was to generate a collection of new phage isolates infecting the
98 ubiquitously used *E. coli* K-12 laboratory strain that would provide representative insight into the diversity
99 of tailed, lytic phages by covering all major groups and containing a suitable selection of minor ones.
100 Similar collections exist, e.g., for *E. coli* in form of the ECOR collection of 72 *E. coli* strains that are
101 commonly used to study how this model organism varies in certain traits or can deal with / evolves under
102 certain conditions [21, 22]. Though nothing truly comparable is available for phages, it is notable that the
103 seven T phages had originally been chosen in the early 1940s with the explicit aim of providing a reference
104 point that would enable comparative, systematic research on bacteriophages [reviewed in reference 6].
105 However, while these and the other classical model phages such as lambda have been invaluable to uncover
106 many fundamental principles of molecular biology, their number and taxonomic range are too limited to
107 serve as a representative reference even for bacteriophages infecting *E. coli*.

108 As a first step, we generated a derivative of *E. coli* K-12 without any of the native barriers that
109 might limit or bias phage isolation unfavorably. This strain, *E. coli* K-12 MG1655 Δ RM, therefore lacks
110 the O-antigen glycan barrier (see below), all restriction systems, as well as the RexAB and PifA Abi systems
111 (see *Materials and Methods* as well as S1 Text). *E. coli* K-12 Δ RM was subsequently used to isolate
112 hundreds of phages from environmental samples such as river water or compost, but mostly from the inflow
113 of different sewage treatment facilities (Fig 2A and *Materials and Methods*).

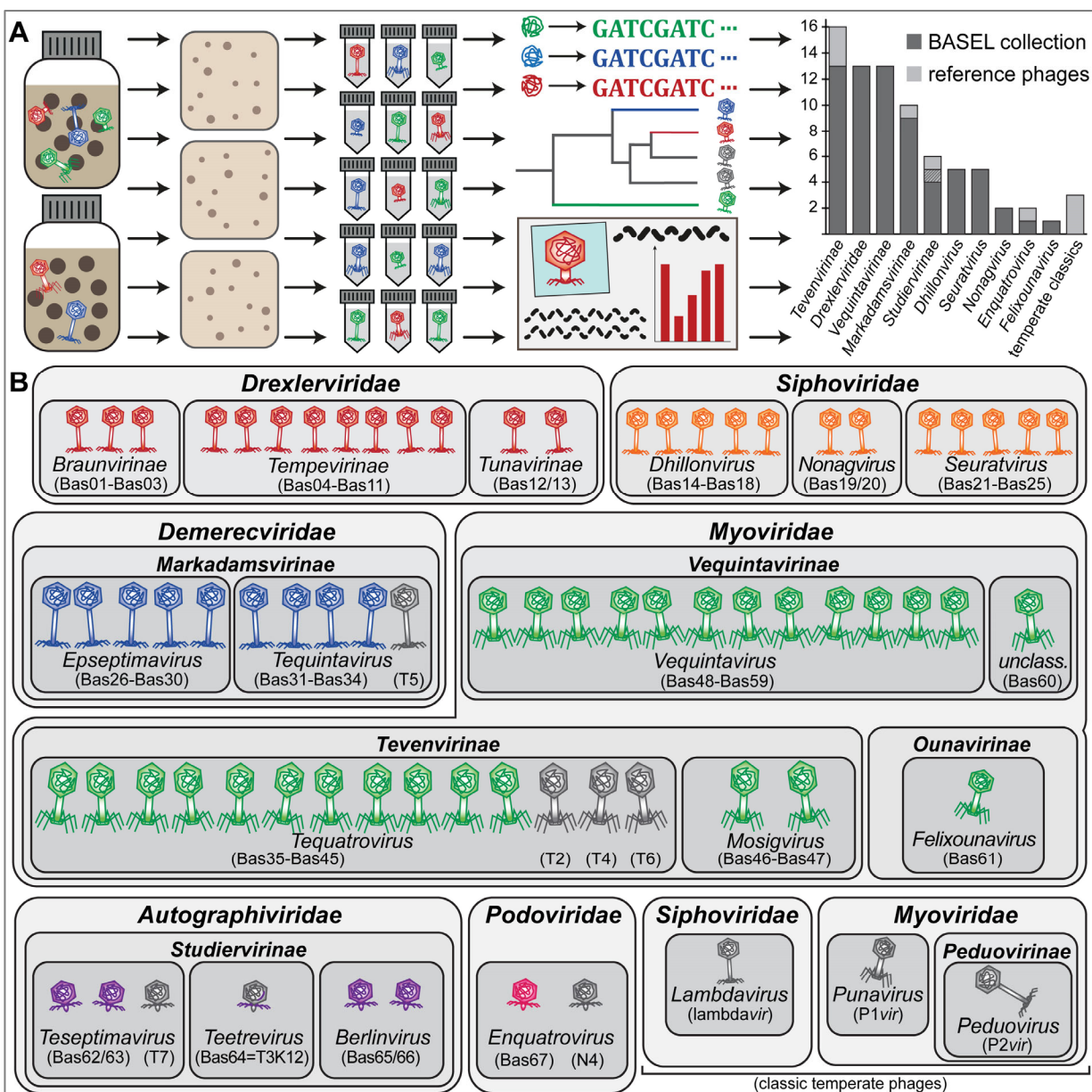


Fig 2. Overview of the BASEL collection.

(A) Illustration of the workflow of bacteriophage isolation, characterization, and selection that resulted in the BASEL collection (details in *Materials and Methods*). (B) Taxonomic overview of the bacteriophages included in the BASEL collection and their unique Bas## identifiers. Newly isolated phages are colored according to their family while well-studied reference phages are shown in grey.

114 Previous bacteriophage isolation studies had already provided deep insight into the diversity of
 115 tailed, lytic *E. coli* phages in samples ranging from sewage over diverse natural environments to infant guts
 116 or blood and urine of patients in tertiary care [23-29]. Despite the wide diversity of known *E. coli* phages
 117 [30], nearly all phage isolates reported in these studies belonged to five major groups and were either

118 myoviruses of 1) *Tevenvirinae* or 2) *Vequintavirinae* subfamilies and close relatives, 3) large siphoviruses
119 of the *Markadamsvirinae* subfamily within *Demerecviridae*, or small siphoviruses of 4) diverse
120 *Drexlerviridae* subfamilies or 5) the genera *Dhillonvirus*, *Nonagvirus*, and *Seuratvirus* of the *Siphoviridae*
121 family. Podoviruses of any kind were rarely reported, and if, then were mostly *Autographiviridae* isolated
122 using enrichment cultures that are known to greatly favor such fast-growing phages [24, 31]. This pattern
123 does not seem to be strongly biased by any given strain of *E.coli* as isolation host because a large, very
124 thorough study using diverse *E. coli* strains reported essentially the same composition of taxonomic groups
125 [23].

126 Whole-genome sequencing of around 120 different isolates from our isolation experiments largely
127 reproduced this pattern, which suggests that several intrinsic limitations of our approach did not strongly
128 affect the spectrum of phages that we sampled (S3 Text). After eliminating closely related isolates, the
129 BASEL collection was formed as a set of 66 new phage isolates (Fig 2; see also *Materials and Methods*
130 and S5 Table). We deliberately did not give full proportional weight to highly abundant groups like
131 *Tevenvirinae* so that the BASEL collection is not truly representative in a narrow quantitative sense. Instead,
132 we included as many representatives of rarely isolated groups (e.g., podoviruses) as possible to increase the
133 biological diversity of phages in our collection that could be an important asset for studying the genetics of
134 phage / host interactions or for unraveling genotype / phenotype relationships. Besides these 66 new isolates
135 (serially numbered as Bas01, Bas02, etc.; Fig 2 and S5 Table), we included a panel of ten classical model
136 phages in our genomic and phenotypic characterization and view them as an accessory part of the BASEL
137 collection. Beyond the T phages (without T1 that is a notorious laboratory contaminant [32]), we included
138 well-studied podovirus N4 and obligately lytic mutants of the three most commonly studied temperate
139 phages lambda, P1, and P2 [5, 7, 33, 34] (Fig 2; see also S5 Table).

140 **Overview: Identification of phage surface receptors**

141 The infection cycle of most tailed phages begins with host recognition by reversible adsorption to
142 a first “primary” receptor on host cells (often a “sugar motif on surface glycans) followed by irreversible

143 binding to a terminal or “secondary” receptor directly on the cell surface which results in DNA injection
144 (Fig 1B) [35]. Importantly, the adsorption to many potential hosts is blocked by long O-antigen chains on
145 the LPS and other exopolysaccharides that effectively shield the cell surface unless they can be degraded
146 or specifically serve as the phage’s primary receptor [35-38]. Tailed phages bind to primary and secondary
147 receptors using separate structures at the phage tail which display the dedicated receptor-binding
148 proteins (RBPs) in the form of tail fibers, tail spikes (smaller than fibers, often with enzymatic domains),
149 or central tail tips [comprehensively reviewed in reference 35]. Most commonly, surface glycans such as
150 the highly variable O-antigen chains or the enterobacterial common antigen (ECA) are bound as primary
151 receptors. Secondary receptors on Gram-negative hosts are near-exclusively porin-family outer
152 membrane proteins for siphoviruses and core LPS sugar structures for podoviruses, while myoviruses
153 were found to use either one of the two depending on phage subfamily or genus [35, 39, 40]. Notably, no
154 host receptor is known for the vast majority of phages that have been studied, but understanding the
155 genetic basis and molecular mechanisms underlying host recognition as the major determinant of phage
156 host range is a crucial prerequisite for host range engineering or a rational application of phage therapy
157 [41]. Since tail fibers and other host recognition modules are easily identified in phage genomes, we used
158 phage receptor specificity as a model to demonstrate the usefulness of systematic phenotypic data with
159 the BASEL collection as a key to unlock information hidden in the genome databases.

160 We therefore first experimentally determined the essential host receptor(s) of all phages in the
161 BASEL collection before analyzing the phages’ genomes for the mechanisms underlying receptor
162 specificity. Briefly, the dependence on surface proteins was assessed by plating each phage on a set of more
163 than fifty single-gene mutants (S1 Table) or whole-genome sequencing of spontaneously resistant bacterial
164 clones (see *Materials and Methods*). The role of host surface glycans was quantified with *waaG* and *waaC*
165 mutants that display different truncations of the LPS core, a *wbbL(+)* strain with restored O16-type O-

166 antigen expression, and a *wecB* mutant that is specifically deficient in production of the ECA [42-44] (Fig
 167 3A, S1 Table, and *Materials and Methods*).

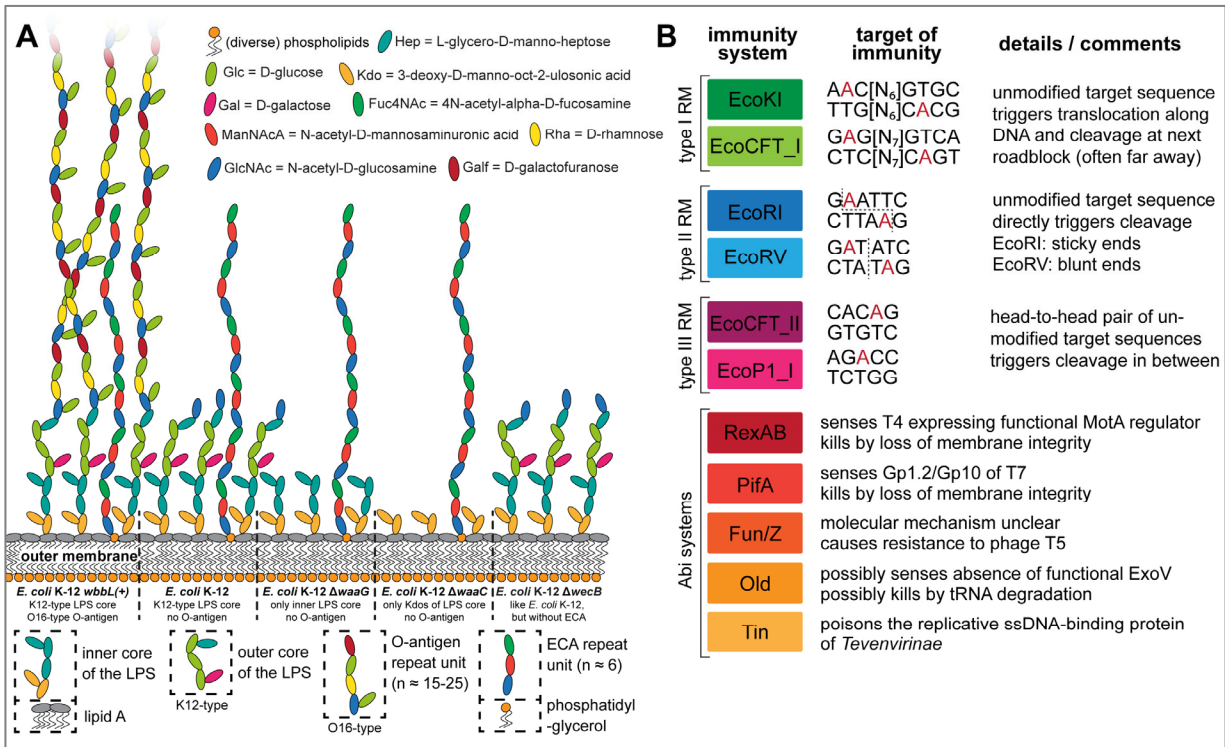


Fig 3. Overview of *E. coli* surface glycan variants and the immunity systems used in this study

(A) The surface glycans of different *E. coli* K-12 MG1655 variants are shown schematically (details in running text and *Materials and Methods*). Note that the *E. coli* K-12 MG1655 laboratory wildtype does not merely display the K12-type core LPS (classical rough LPS phenotype) but also the most proximal D-glucose of the O16-type O-antigen. (B) Key features of the six RM systems (each two of type I, type II, and type III) and the five Abi systems used for the phenotyping of this study are summarized schematically. Recognition sites of RM systems have either been determined experimentally or were predicted in REBASE (red nucleotides: methylation sites; dotted lines: cleavage sites) [47-49, 128]. The Abi systems have been characterized to very different extent but constitute the most well-understood representatives of these immunity systems of *E. coli* [10, 50].

168 Overview: Phenotyping of sensitivity / resistance to bacterial immunity systems

169 Some bacterial immunity systems are very common among different strains of a species (like
 170 certain types of RM systems for *E. coli*), while others – especially the various Abi systems – have each a
 171 very patchy distribution but are no less abundant if viewed together [11]. Each bacterial strain therefore
 172 encodes a unique repertoire of a few very common and a larger number of rarer, strain-specific immunity
 173 systems, but it is unknown how far these systems impact the isolation of phages or their efficacy in
 174 therapeutic applications. A systematic view of the potency and target range of different immunity systems

175 and how the diverse groups of phages differ in sensitivity / resistance to these systems might enable us to
176 select or engineer phages with a higher and more reliable potency for phage therapy or biotechnology. As
177 an example, previous work showed that *Tevenvirinae* or *Seuratvirus* and *Nonagvirus* phages exhibit broad
178 resistance to RM systems due to the hypermodification of cytosines or guanosines in their genomes,
179 respectively, which could be an interesting target for phage engineering [45, 46]. However, it is unknown
180 whether this mechanism of RM resistance (or any other viral anti-immunity function) actually results in a
181 measurably broader phage host range.

182 We therefore systematically quantified the sensitivity of all phages of the BASEL collection against
183 a panel of eleven immunity systems and scored their infectivity on a range of pathogenic enterobacteria that
184 are commonly used as model systems (see *Materials and Methods* and Fig 3B). Shortly, we tested six RM
185 systems by including each two type I, type II, and type III systems that differ in the molecular mechanisms
186 of DNA modification and cleavage [10, 47-49] (Fig 3B). Besides these, we included the most well-studied
187 *Abi* systems of *E. coli*, *RexAB* of the lambda prophage, *PifA* of the F-plasmid, as well as the *Old*, *Tin*, and
188 *Fun/Z* systems of the P2 prophage (Fig 3B). Previous work suggested that *RexAB* and *PifA* sense certain
189 proteins of phages T4 and T7, respectively, to trigger host cell death by membrane depolarization [10].
190 Conversely, *Old* possibly senses the inhibition of *RecBCD / ExoV* during lambda infections and might kill
191 by tRNA degradation, *Fun/Z* abolishes infections by phage T5 via an unknown mechanism, and *Tin* poisons
192 the replicative ssDNA binding protein of *Tevenvirinae* [50]. Beyond *E. coli* K-12, we quantified the
193 infectivity of the BASEL collection on uropathogenic *E. coli* (UPEC) strains UTI89 and CFT073,
194 enteroaggregative *E. coli* (EAEC) strain 55989, alternative laboratory strain *E. coli* B REL606, and
195 *Salmonella enterica* subsp. *enterica* serovar Typhimurium strains 12023s and SL1344 (see *Materials and*
196 *Methods* and S1 Table).

197 **Properties of the *Drexelviriidae* family**

198 Phages of the *Drexelviriidae* family (previously also known as T1 superfamily [30]) are small
199 siphoviruses with genome sizes of ca. 43-52 kb (Figs 4A-D). The BASEL collection contains thirteen new

200 *Drexlerviridae* phages that are broadly spread out across the various subfamilies and genera of this family
201 (Fig 4B). Though it has apparently never been directly demonstrated, it seems likely that the *Drexlerviridae*
202 use their lateral tail fibers in the same way as their larger cousins of the *Markadamsvirinae* (see below) to
203 contact specific O-antigen glycans as primary receptors without depending on this interaction for host
204 recognition [51] (Fig 4A). Consistently, the locus encoding the lateral tail fibers is very diverse among
205 *Drexlerviridae* and the proteins forming these tail fibers are only highly related at the far N-terminus of the
206 distal subunits where these are likely attached to the tail (S1B Fig). Among the *Drexlerviridae* that we
207 isolated, only JakobBernoulli (Bas07) shows robust plaque formation on *E. coli* K-12 MG1655 with
208 restored O16-type O-antigen expression, suggesting that its lateral tail fibers can use this O-antigen as
209 primary receptor (Figs 4A and 4D).

210 Just like the much larger *Markadamsvirinae* siphoviruses (see below), *Drexlerviridae* phages use
211 a small set of outer membrane porins as their secondary / final receptors for irreversible adsorption and
212 DNA injection. To the best of our knowledge, previous work had only identified the receptors of T1 and
213 IME18 (FhuA), IME347 (YncD), IME253 (FepA), and of LL5 as well as TLS (TolC) while for an additional
214 phage, RTP, no protein receptor could be identified [40, 52-54]. Using available single-gene mutants, we
215 readily determined the terminal receptor of eleven out of our thirteen *Drexlerviridae* phages as FhuA, BtuB,
216 YncD, and TolC (Figs 4B and 4C) but failed for two others, AugustePiccard (Bas01) and JeanPiccard
217 (Bas02). However, whole-genome sequencing of spontaneously resistant *E. coli* mutants showed that
218 resistance was linked to mutations in the gene coding for LptD, the LPS export channel [36], strongly
219 suggesting that this protein was the terminal receptor of these phages (Fig 5 and *Materials and Methods*).

220 Similar to the central tail fibers of *Markadamsvirinae*, the RBPs of *Drexlerviridae* are thought to
221 be displayed at the distal end of a tail tip protein related to well-studied GpJ of bacteriophage lambda [51,
222 54, 55]. The details of this host recognition module had remained elusive, though it was suggested that (like
223 for T5 and unlike for lambda) dedicated RBPs are non-covalently attached to the J-like protein and might
224 be encoded directly downstream of the *gpJ* homologs together with cognate superinfection exclusion
225 proteins [54, 55]. By comparing the genomes of all *Drexlerviridae* phages with experimentally determined
226 surface protein receptors, we were able to match specific allelic variants of this *bona fide* RBP loci to each
227 known surface receptor of this phage family (Fig 4C). Notably, for the three known phages targeting TolC
228 including DanielBernoulli (Bas08), the RBP locus is absent and apparently functionally replaced by a C-
229 terminal extension of the GpJ-like tail tip protein that probably directly mediates receptor specificity like
230 GpJ of bacteriophage lambda (Fig 4C) [56, 57]. Interestingly, similar RBP loci with homologous alleles are
231 also found at the same genomic locus in small *Siphoviridae* of *Dhillonvirus*, *Nonagvirus*, and *Seuratvirus*
232 genera (see below) where they also match known receptor specificity without exception (Figs 4-6 and S1C).
233 Pending experimental validation, we therefore conclude that these distantly related groups of small
234 siphoviruses share a common, limited repertoire of RBPs that enables receptor specificity of most
235 representatives to be predicted *in silico*. As an example, it seems clear that phage RTP targets LptD as
236 terminal receptor (Figs 4B and S1D). The poor correlation of predicted receptor specificity with the
237 phylogenetic relationships of small siphoviruses (Figs 4B, 6B, and 6D) is indicative of frequent horizontal
238 transfer of these RBP loci. This highlights the modular nature of this host recognition system which might
239 enable the targeted engineering of receptor specificity to generate “designer phages” for different
240 applications as previously shown for siphoviruses infecting *Listeria* [14, 58]. LptD would be a particularly
241 attractive target for such engineering because it is strictly essential under all conditions, highly conserved,
242 and heavily constrained due to multiple interactions that are critical for its functionality [36].

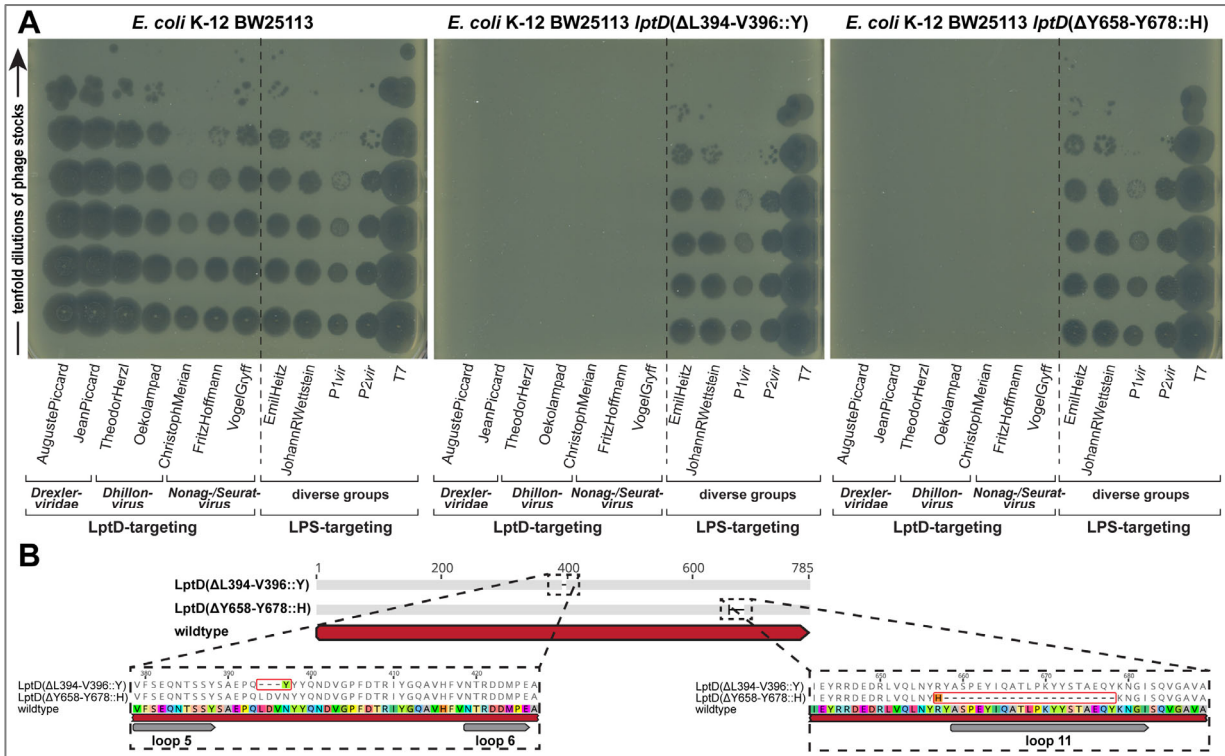


Fig 5. LptD is a commonly targeted terminal receptor of small siphoviruses

(A) Whole-genome sequencing of bacterial mutants exhibiting spontaneous resistance to seven small siphoviruses with no previously known receptor revealed different mutations or small deletions in the essential gene *lptD* that encodes the LptD LPS export channel. Top agar assays with two representative mutants in comparison to the ancestral *E. coli* K-12 BW25113 strain were performed with serial tenfold dilutions of twelve different phages (undiluted high-titer stocks at the bottom and increasingly diluted samples towards the top). Both mutants display complete resistance to the seven small siphoviruses of diverse genera within *Drexlerviridae* and *Siphoviridae* families that share the same *bona fide* RBP modules (S1C Fig) while no other phage of the BASEL collection was affected. In particular, we excluded indirect effects, e.g., via changes in the LPS composition in the *lptD* mutants, by confirming that five LPS-targeting phages of diverse families (see below) showed full infectivity on all strains.

(B) The amino acid sequence alignment of wildtype LptD with the two mutants highlighted in (A) shows that resistance to LptD-targeting phages is linked to small deletions in or adjacent to regions encoding extracellular loops as defined in previous work [147], suggesting that they abolish the RBP-receptor interaction.

243 Once inside the host cell, our results show that *Drexlerviridae* phages are highly diverse in their
 244 sensitivity or resistance to diverse bacterial immunity systems (Fig 4D). While few representatives like
 245 FritzSarasin (Bas04) or PeterMerian (Bas05) are highly resistant, most *Drexlerviridae* are very sensitive to
 246 any kind of RM systems sometimes including the type I machineries that are largely unable to target any
 247 other phage that we tested (Fig 4D). Previous work suggested that *Drexlerviridae* might employ DNA
 248 methyltransferases as a defense strategy against host restriction [24], and these phages indeed encode
 249 variable sets of N6-adenine and C5-cytosine methyltransferases. However, we found no obvious pattern

250 that would link DNA methyltransferases or any other specific genomic features to restriction resistance /
251 sensitivity. Instead, sensitivity and resistance to bacterial immunity strongly correlate with *Drexlerviridae*
252 phylogeny: While *Hanrivervirus* and *Warwickvirus* genera of *Tempevirinae* are highly resistant and
253 *Tunavirinae* show comparably intermediate sensitivity, the other phages (in particular *Braunvirinae*, but
254 also *Tlsvirus* phage DanielBernoulli (Bas08)) are highly sensitive (Figs 4B and 4D).

255 **Properties of *Siphoviridae* genera *Dhillonvirus*, *Nonagvirus*, and *Seuratvirus***

256 Phages of the *Dhillonvirus*, *Seuratvirus*, and *Nonagvirus* genera within the *Siphoviridae* family are
257 small siphoviruses that are superficially similar to *Drexlerviridae* and have genomes with characteristic
258 size ranges of 43-46 kb (*Dhillonvirus*), 56-61 kb (*Seuratvirus*), and 56-64 kb (*Nonagvirus*; see Fig 6A-E).
259 Our twelve isolates included in the BASEL collection are spread out broadly across the phylogenetic ranges
260 of these genera (Figs 6B and 6D). Similar to *Drexlerviridae* (and *Markadamsvirinae*, see below), we
261 suggest that they also recognize glycan motifs at the O-antigen as their primary receptor on different host
262 strains (Fig 6A). This notion is strongly supported by the remarkable variation exhibited by the different
263 genomes at the lateral tail fiber locus (S2A Fig), as observed previously [23, 24]. None of these phages can
264 infect *E. coli* K-12 MG1655 with restored O16-type O-antigen expression, but (like for *Drexlerviridae*)
265 some require an intact LPS core for infectivity (Figs 6C and 6F). Experimental identification of the terminal
266 receptor of all small *Siphoviridae* confirmed that receptor specificity seems to be encoded by the same
267 system of *bona fide* RBP loci downstream of *gpJ* as for the *Drexlerviridae* (Figs 4B, 6B, and 6D). Many of
268 these phages target LptD or FhuA as terminal receptors while others, unlike any *Drexlerviridae*, bind to
269 LamB (Figs 6C and 6F). Notably, three related *Nonagvirus* phages encode a distinct *bona fide* RBP module
270 that could not be matched to any known terminal receptor (S2B Fig), suggesting that these phages might
271 target a different protein.

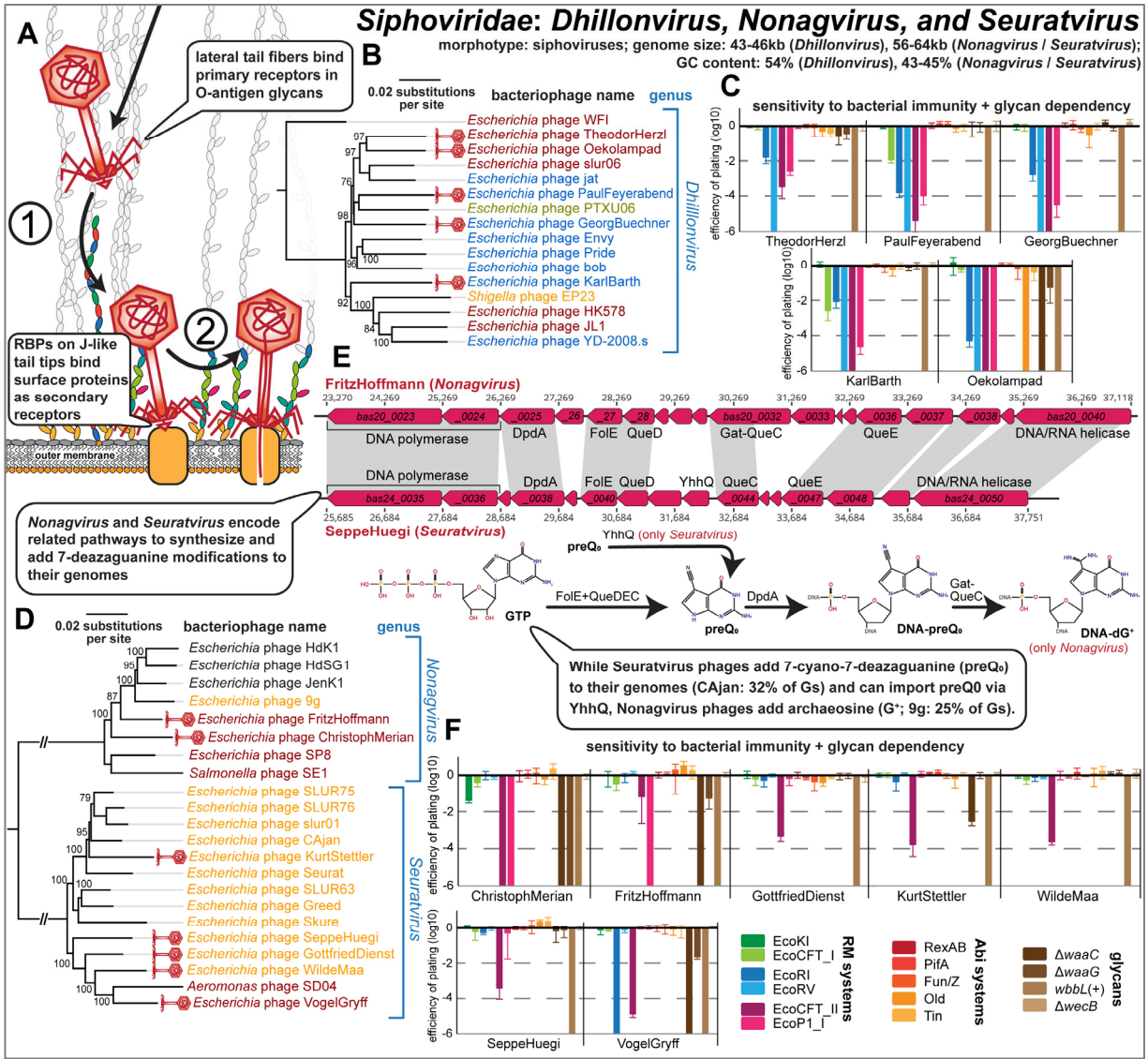


Fig 6. Overview of Siphoviridae genera Dhillonvirus, Nonagvirus, and Seuratvirus.

(A) Schematic illustration of host recognition by small siphoviruses. (B) Maximum-Likelihood phylogeny of the *Dhillonvirus* genus based on a whole-genome alignment with bootstrap support of branches shown if > 70/100. Newly isolated phages of the BASEL collection are highlighted by red phage icons and the determined or proposed terminal receptor specificity is highlighted at the phage names using the color code highlighted in Fig 4C. The phylogeny was rooted between phage WFI and all others based on a representative phylogeny including *Drexlerviridae* sequences as outgroup (S1A Fig). (C) The results of quantitative phenotyping experiments with *Dhillonvirus* phages regarding sensitivity to altered surface glycans and bacterial immunity systems are presented as efficiency of plating (EOP). (D) Maximum-Likelihood phylogeny of the *Nonagvirus* and *Seuratvirus* genera based on a whole-genome alignment with bootstrap support of branches shown if > 70/100. Newly isolated phages of the BASEL collection are highlighted by red phage icons and the determined or proposed terminal receptor specificity is highlighted at the phage names using the color code highlighted in Fig 4C. The phylogeny was rooted between the two genera. (E) *Nonagvirus* and *Seuratvirus* phages share a core 7-deazaguanosine biosynthesis pathway involving FoIE, QueD, QueE, and QueC which synthesizes dPreQ₀ that is inserted into their genomes by DpdA. In *Nonagvirus* phages, the fusion of QueC with a glutamate amidotransferase (Gat) domain to Gat-QueC results in the modification with dG⁺ instead of dPreQ₀ [45]. (F) The results of quantitative phenotyping experiments with *Nonagvirus* and *Seuratvirus* phages regarding sensitivity to altered surface glycans and bacterial immunity systems are presented as efficiency of plating (EOP). In (C) and (F), data points and error bars represent average and standard deviation of at least three independent experiments.

272 In difference to *Dhillonvirus* phages that are relatives of *Drexlerviridae* [23] (see also S1A Fig),
273 *Nonagvirus* and *Seuratvirus* phages are closely related genera with genomes that are 10-15 kb larger than
274 those of the other small siphoviruses in the BASEL collection (S5 table) [59]. This difference in genome
275 size is largely due to genes encoding their signature feature, the 7-deazaguanine modification of
276 2'-deoxyguanosine (dG) in their genomes into 2'-deoxy-7-cyano-7-deazaguanosine (dpreQ₀) for
277 *Seuratvirus* phages and into 2'-deoxyarchaosine (dG⁺) for *Nonagvirus* phages [45] (Fig 6E). These
278 modifications were shown to provide considerable (dG⁺) or at least moderate (dpreQ₀) protection against
279 restriction of genomic DNA of *Seuratvirus* phage CAjan and *Nonagvirus* phage 9g *in vitro*, although
280 chemical analyses showed that only around one third (CAjan) or one fourth (9g) of the genomic dG content
281 is modified [45] (Fig 6E). Consistently, we found that both *Nonagvirus* and *Seuratvirus* phages are
282 remarkably resistant to type I and type II RM systems in our infection experiments, particularly if compared
283 to other small siphoviruses of *Dhillonvirus* or *Drexlerviridae* groups (Figs 4D, 6C, and 6F). Among
284 *Nonagvirus* and *Seuratvirus* phages, only ChristophMerian (Bas19, EcoKI) and VogelGryff (Bas25, EcoRI)
285 show some sensitivity to these RM systems. However, all phages of these genera are highly sensitive to
286 type III RM systems (Fig 6F). This observation does not necessarily indicate a lower sensitivity of type III
287 RM systems to guanosine modifications *per se* but is likely simply a consequence of the much larger
288 number of type III RM recognition sites in their genomes (S5 Table, see also Fig 3B).

289 **Properties of *Demerecviridae*: *Markadamsvirinae***

290 Phages of the *Markadamsvirinae* subfamily of the *Demerecviridae* family (previously known as
291 T5-like phages [30]) are large siphoviruses with genomes of 101-116 kb length (Fig 7A-C). Our nine new
292 isolates in the BASEL collection (plus well-studied phage T5) are well representative of the two major
293 genera *Eseptimavirus* and *Tequintavirus* and their subclades (Fig 7B). These phages characteristically use
294 their lateral tail fibers to bind each one or a few types of O-antigen very specifically as their primary host
295 receptor, but this interaction is not essential for hosts like *E. coli* K-12 laboratory strains that don't express

296 an O-antigen barrier [51] (Fig 7A). As expected and observed previously [51, 60], the diversity of O-antigen
297 glycans is reflected in a high genetic diversity at the lateral tail fiber locus of the *Markadamsvirinae* of the
298 BASEL collection (S3A Fig). Only one of these phages, IrisVonRoten (Bas32), can infect *E. coli* K-12 with
299 restored expression of O16-type O-antigen, suggesting that it can recognize this glycan as its primary
300 receptor, but several others can infect different *E. coli* strains with smooth LPS or even *Salmonella* (see
301 below in Fig 12). Similar to what was proposed for the different small siphoviruses described above, the
302 terminal receptor specificity of T5 and relatives is determined by dedicated RBPs attached non-covalently
303 to the tip of a straight central tail fiber [51]. Compared to their smaller relatives, the repertoire of terminal
304 receptors among *Markadamsvirinae* seems limited – the vast majority target BtuB (shown for, e.g., EPS7
305 [61] and S132 [62]), and each a few others bind FhuA (T5 itself [51] and probably S131 [62]) or FepA (H8
306 [63] and probably S124 [62]). Sequence analyses of the RBP locus allowed us to predict the terminal
307 receptor of all remaining *Markadamsvirinae*, confirming that nearly all target BtuB (Fig 7B and S3B Fig).

308 It has long been known that phage T5 is largely resistant to RM systems, and this was thought to
309 be due to elusive DNA protection functions encoded in the early-injected genome region largely shared by
310 T5 and other *Markadamsvirinae* [64]. Surprisingly, we find that this resistance to restriction is a shared
311 feature only of the *Tequintavirus* genus, while their sister genus *Epseptimavirus* shows detectable yet
312 variable sensitivity in particular to the type II RM system EcoRV (Fig 7B). It seems likely that this
313 difference between the genera is due to the largely different number of EcoRV recognition sites in
314 *Epseptimavirus* genomes (70-90 sites, S5 Table) and *Tequintavirus* genomes (4-18 sites, S5 Table). This
315 observation suggests that efficient DNA ligation and RM site avoidance [65] play important roles in the
316 restriction resistance of T5 and relatives besides their putative DNA protection system. Remarkably, all
317 *Markadamsvirinae* are invariably sensitive to the Fun/Z immunity system of phage P2 which had already
318 been shown for T5 previously [50].

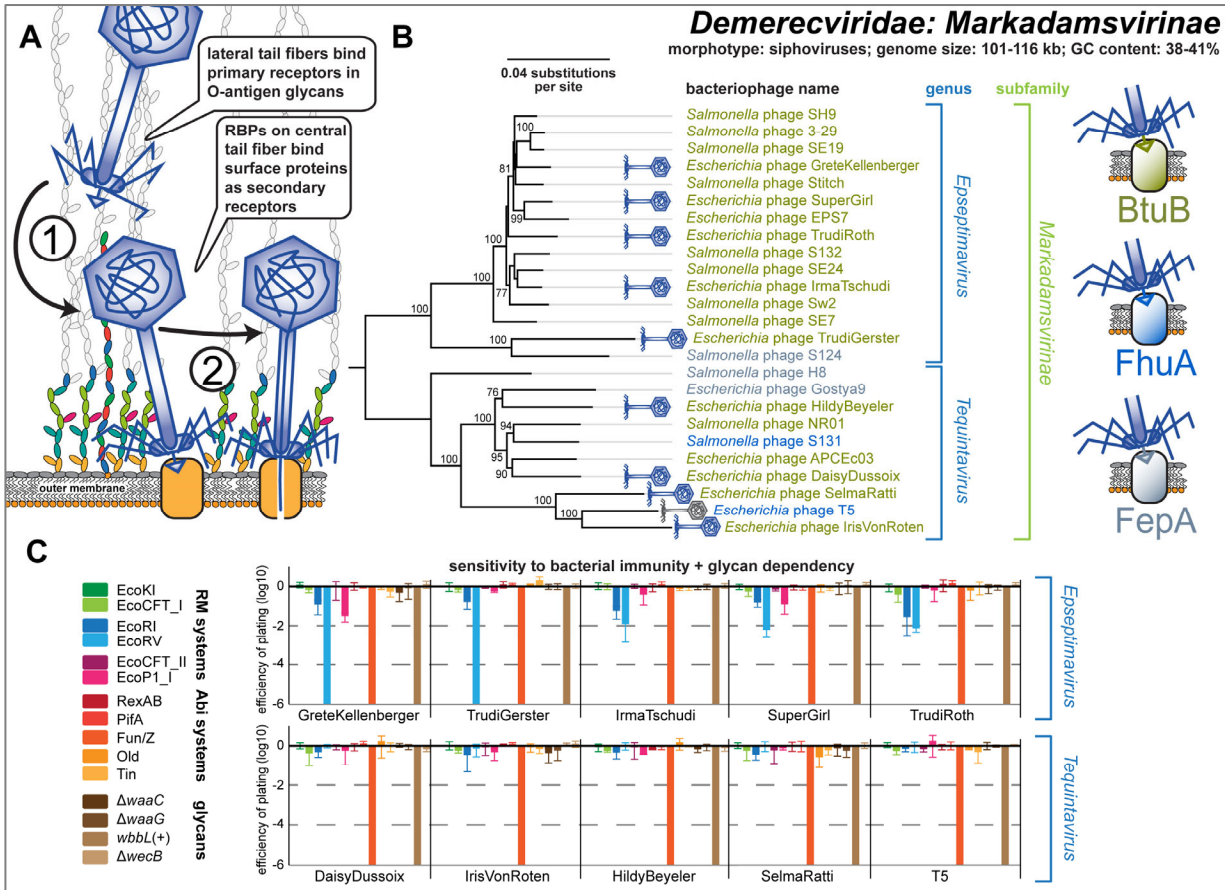


Fig 7. Overview of *Demerecviridae* subfamily *Markadamsvirinae*.

(A) Schematic illustration of host recognition by T5-like siphoviruses. (B) Maximum-Likelihood phylogeny of the *Markadamsvirinae* subfamily of *Demerecviridae* based on several core genes with bootstrap support of branches shown if > 70/100. Phages of the BASEL collection are highlighted by little phage icons and the determined or proposed terminal receptor specificity is highlighted at the phage names using the color code highlighted at the right side (same as for the small siphoviruses). The phylogeny was rooted between the *Eseptimavirus* and *Tequintavirus* genera. (C) The results of quantitative phenotyping experiments with *Markadamsvirinae* phages regarding sensitivity to altered surface glycans and bacterial immunity systems are presented as efficiency of plating (EOP). Data points and error bars represent average and standard deviation of at least three independent experiments.

319 **Properties of *Myoviridae*: *Tevenvirinae***

320 Phages of the *Tevenvirinae* subfamily within the *Myoviridae* family are large myoviruses with
 321 characteristically prolate capsids and genomes of 160-172 kb size that infect a wide variety of Gram-
 322 negative hosts [30] (Figs 8A-E). The kinked lateral tail fibers of these phages contact primary receptors on
 323 the bacterial cell surface that are usually surface proteins like OmpC, Tsx, and FadL for prototypic
 324 *Tevenvirinae* phages T4, T6, and T2, respectively, but can also be sugar motifs in the LPS like in case of
 325 T4 when OmpC is not available [66] (Fig 8A). Robust interaction with the primary receptor unpins the short

326 tail fibers from the myovirus baseplate which enables their irreversible adsorption to terminal receptors in
327 the LPS core followed by contraction of the tail sheath. Consequently, the phage tail penetrates the cell
328 envelope and the viral genome is injected via a syringe-like mechanism [35] (Fig 8A).

329 Our thirteen newly isolated *Tevenvirinae* phages in the BASEL collection mostly belong to
330 different groups of the *Tequatrovirus* genus that also contains well-studied reference phages T2, T4, and
331 T6, but two isolates were assigned to the distantly related *Mosigvirus* genus (Fig 8B). As expected, the
332 infectivity of our thirteen isolates and of T2, T4, and T6 reference phages shows strong dependence on
333 each one of a small set of *E. coli* surface proteins that have previously been described as *Tevenvirinae*
334 primary receptors, i.e., Tsx, OmpC, OmpF, OmpA, and FadL [66] (Fig 8B). Interestingly, while for some
335 of these phages the absence of the primary receptor totally abolished infectivity, others still showed
336 detectable yet greatly reduced plaque formation (S4A Fig). It seems likely that these differences are caused
337 by the ability of some *Tevenvirinae* lateral tail fibers to contact several primary receptors such as, e.g.,
338 OmpC and the truncated *E. coli* B LPS core in case of T4 [66, 67].

339 Specificity for the secondary receptor depends on the short tail fibers that, in case of T4, target the
340 lipid A – Kdo region deep in the enterobacterial LPS core [68]. Given that this region is still present in the
341 *waaC* mutant, the most deep-rough mutant of *E. coli* K-12 that is viable (Fig 3A), it is unsurprising that T4
342 and some other *Tevenvirinae* did not seem to show a dependence on the LPS core in our experiments (Fig
343 8C). However, some *Tequatrovirus* and all tested *Mosigvirus* isolates required an intact inner core of the
344 host LPS for infectivity (Fig 8C). This phenotype is correlated with an alternative allele of the short tail
345 fiber gene that varies between *Tevenvirinae* phages irrespective of their phylogenetic position (Fig 8D). We
346 therefore suggest that those phages encoding the alternative allele express a short tail fiber that targets parts
347 of the LPS core above the lipid A – Kdo region (Figs 8D and 8E; see also Fig 3A).

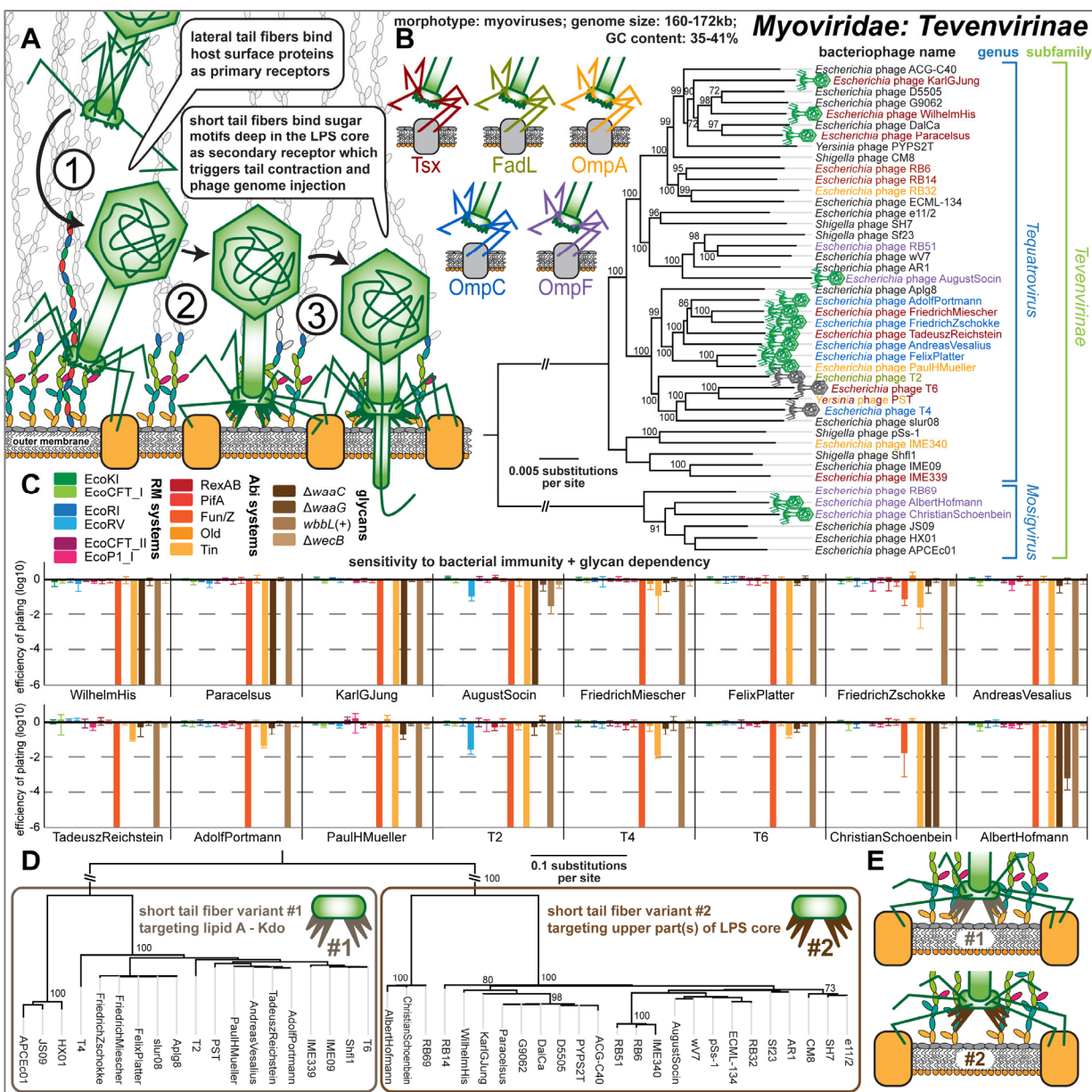


Fig 8. Overview of the *Myoviridae* subfamily *Tevenvirinae*.

(A) Schematic illustration of host recognition by T4-like myoviruses. (B) Maximum-Likelihood phylogeny of the *Tevenvirinae* subfamily of *Myoviridae* based on a curated whole-genome alignment with bootstrap support of branches shown if > 70/100. The phylogeny was rooted between the *Tequatrovirus* and *Mosigivirus* genera. Phages of the BASEL collection are highlighted by little phage icons and experimentally determined primary receptor specificity is highlighted at the phage names using the color code highlighted at the top left. Primary receptor specificity of *Tevenvirinae* depends on RBPs expressed either as a C-terminal extension of the distal half fiber (T4 and other OmpC-targeting phages) or as separate small fiber tip adhesins [66], but sequence analyses of the latter remained ambiguous. We therefore only annotated experimentally determined primary receptors (see also S4A Fig) [53, 66]. (C) The results of quantitative phenotyping experiments with *Tevenvirinae* phages regarding sensitivity to altered surface glycans and bacterial immunity systems are presented as efficiency of plating (EOP). Data points and error bars represent average and standard deviation of at least three independent experiments. (D) The Maximum-Likelihood phylogeny *Tevenvirinae* short tail fiber proteins reveals two homologous, yet clearly distinct, clusters that correlate with the absence (variant #1, like T4) or presence (variant #2) of detectable LPS core dependence as shown in (C).

(E) The results of (D) indicate that variant #1, as shown for T4, binds the deep lipid A – Kdo region of the enterobacterial LPS core, while variant #2 binds a more distal part of the (probably inner) core.

348 Besides receptor specificity, the phenotypes of our diverse *Tevenvirinae* phages were highly
349 homogeneous. The hallmark of this *Myoviridae* subfamily is a high level of resistance to DNA-targeting
350 immunity like RM systems because of cytosine hypermodifications (hydroxymethyl-glucosylated for
351 *Tequatrovirus* and hydroxymethyl-arabinosylated for *Mosigvirus*) [46, 69]. Consistently, no or only very
352 weak sensitivity to any of the six RM systems was detected for any tested *Tevenvirinae* phage (Fig 8B).
353 The weak sensitivity to EcoRV observed for AugustSocin (Bas38) and phage T2 does, unlike for
354 *Markadamsvirinae* (see above), not correlate with a higher number of recognition sites and therefore
355 possibly depends on another feature of these phages such as, e.g., differences in DNA ligase activity (S5
356 Table). Conversely, all tested *Tevenvirinae* were sensitive to the Fun/Z and Tin Abi systems (Fig 8B). Tin
357 was previously shown to specifically target the DNA replication of T-even phages [50], and we found that
358 indeed all *Tevenvirinae* but no other tested phage are sensitive to this Abi system (Fig 8B). No sensitivity
359 was observed for RexAB, the iconic Abi system targeting *rIIA/B* mutants of phage T4 [10] (S4B),
360 suggesting that this Abi system is generally unable to affect wildtype *Tevenvirinae* phages (Fig 8C).

361 **Properties of *Myoviridae*: *Vequentavirinae* and relatives**

362 Phages of the *Vequentavirinae* subfamily within the *Myoviridae* family are myoviruses with
363 genomes of 131-140 kb size that characteristically encode three different sets of lateral tail fibers [23, 70]
364 (Figs 9A-E). Besides *Vequentavirinae* of the *Vequentavirus* genus, this feature is shared by two groups of
365 phages that are closely related to these *Vequentavirinae sensu stricto*: One group forms a cluster around
366 phage phAPEC8 (recently proposed as a new genus *Phapecoctavirus* within *Myoviridae* [23]), the other
367 group is their sister clade including phage phi92 [71] that is unclassified (Fig 9B). Despite not being
368 *Vequentavirinae* by current taxonomic classification, we are covering them together due to their
369 considerable similarities and propose to classify the phi92-like phages (including PaulScherrer (Bas60)) as
370 *Nonagintaduovirus* genus within the *Vequentavirinae*.

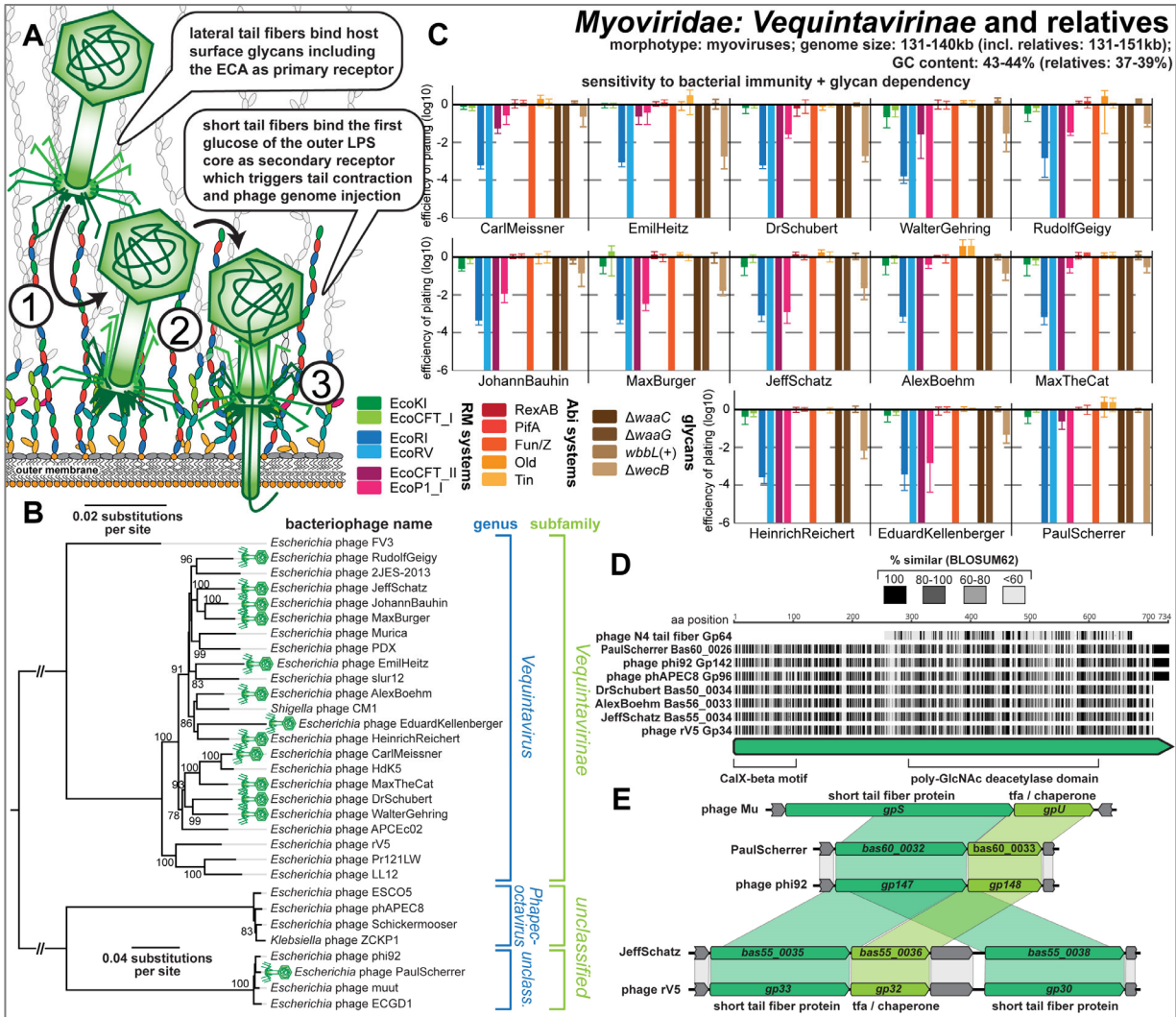


Fig 9. Overview of the *Myoviridae* subfamily *Vequintavirinae* and relatives.

(A) Schematic illustration of host recognition by rV5-like myoviruses. (B) Maximum-Likelihood phylogeny of the *Vequintavirinae* subfamily of *Myoviridae* and relatives based on a curated whole-genome alignment with bootstrap support of branches shown if > 70/100. The phylogeny was rooted between the *Vequintavirus* genus and the two closely related, unclassified groups at the bottom. Newly isolated phages of the BASEL collection are highlighted by green phage icons. (C) The results of quantitative phenotyping experiments with *Vequintavirinae* and phage PaulScherrer regarding sensitivity to altered surface glycans and bacterial immunity systems are presented as efficiency of plating (EOP). Data points and error bars represent average and standard deviation of at least three independent experiments. (D) Amino acid sequence alignment of the lateral tail fiber Gp64 of phage N4 (*Enquatrovirus*, see below) and a lateral tail fiber conserved among *Vequintavirinae* and relatives (representatives shown). The proteins share a predicted poly-GlcNAc deacetylase domain as identified by Phyre2 [136]. (E) *Vequintavirinae sensu stricto* (represented by rV5 and Jeff Schatz) encode two paralogous short tail fiber proteins and a tail fiber chaperone that are homologous to the corresponding locus in phi92-like phages incl. PaulScherrer and, ultimately, to short tail fiber GpS and chaperone GpU of Mu(+) (which targets a different glucose in the K12-type LPS core GpS [95, 96]).

371 Three different, co-expressed lateral tail fibers have been directly visualized in the cryogenic
372 electron microscopy structure of phi92, and large orthologous loci are found in all *Vequintavirinae* and

373 relatives [23, 70, 71]. The considerable repertoire of glycan-hydrolyzing protein domains in these tail fiber
374 proteins has been compared to a “nanosized Swiss army knife” and is probably responsible for the
375 exceptionally broad host range of these phages and their ability to infect even diverse capsulated strains of
376 enterobacteria [23, 52, 70, 71]. However, it is far from clear which genes code for which components of
377 the different lateral tail fibers. While three lateral tail fiber genes exhibit considerable allelic variation
378 between phage genomes and might therefore encode the distal parts of the tail fibers with the receptor-
379 binding domains, the biggest part of the lateral tail fiber locus is highly conserved including diverse proteins
380 with sugar-binding or glycan-hydrolyzing domains (S5 Fig). This observation fits well with our finding that
381 the lysis host range of all *Vequintavirinae* available to us is remarkably homogeneous and suggests that, in
382 the absence of capsules and other recognized exopolysaccharides, these phages do not vary widely in their
383 host recognition (see below in *Host range across pathogenic enterobacteria and E. coli B*). Interestingly,
384 all *Vequintavirinae* in the BASEL collection are detectably inhibited when infecting the *wecB* knockout
385 (albeit to variable degree), strongly suggesting that the ECA is a shared primary receptor (Figs 9A and 9B).
386 This phenotype and the specific lysis host range of *Vequintavirinae* are shared with podoviruses of the
387 *Enquatrovirus* family (see below). Notably, one of the conserved lateral tail fiber proteins of the
388 *Vequintavirinae* is homologous to the lateral tail fiber protein of *Enquatrovirus* phages (Fig 9D), suggesting
389 that these two groups of phages might target the ECA in a similar way.

390 The terminal receptor of *Vequintavirinae* has been unraveled genetically for phage LL12, a close
391 relative of rV5 (Fig 9B), and seems to be at the first, heptose-linked glucose of the LPS outer core which is
392 shared by all *E. coli* core LPS types [52, 72] (Fig 9A). Consistently, we found that all *Vequintavirinae* in
393 the BASEL collection are completely unable to infect the *waaC* and *waaG* mutants with core LPS defects
394 that result in the absence of this sugar (Fig 9C, see also Fig 3A). This observation would be compatible
395 with the idea that all (tested) *Vequintavirinae* and also PaulScherrer of the phi92-like phages use the same
396 secondary receptor. Indeed, the two very similar short tail fiber paralogs of *Vequintavirinae sensu stricto*
397 do not show any considerable allelic variation between genomes (S5A Fig; unlike, e.g., the *Tevenvirinae*

398 short tail fibers presented in Figs 8D and 8E) and are also closely related to the single short tail fiber protein
399 of phi92-like phages or *Phapecoetavirus* (Fig 9E).

400 Unlike large myoviruses of the *Tevenvirinae* subfamily, the *Vequintavirinae* and relatives are
401 exceptionally susceptible to type II and type III RM systems, albeit with (minor) differences in the pattern
402 of sensitivity and resistance from phage to phage (Fig 9C). We therefore see no evidence for effective
403 mechanisms of these phages to overcome RM systems like, as proposed previously, covalent DNA
404 modifications which could be introduced by the notable repertoire of sugar-related enzymes found in their
405 genomes [24]. Similarly, the *Vequintavirinae* are invariably sensitive to the Fun/Z Abi system.

406 **Properties of the *Autographiviridae* family and *Podoviridae*: *Enquatrovirus***

407 Phages of the *Autographiviridae* family and the genus *Enquatrovirus* in the *Podoviridae* family are
408 podoviruses that have been well studied in form of their representatives T3 and T7 (*Autographiviridae*
409 subfamily *Studiervirinae*) and N4 (*Enquatrovirus*). While they differ in their genome size (ca. 37-41 kb for
410 *Studiervirinae*, ca. 68-74 kb for *Enquatrovirus*) and each exhibit characteristic unique features, the overall
411 mode of infection of these podoviruses is the same: Lateral tail fibers of the virion contact bacterial surface
412 glycans at the cell surface for host recognition after which direct contact of the stubby tail with a terminal
413 receptor on the host triggers irreversible adsorption and DNA injection (Fig 10A).

414 This process has been studied in detail for the archetype of all *Autographiviridae*, phage T7, though
415 several open questions remain. The lateral tail fibers of this phage contact a receptor in rough LPS of *E.*
416 *coli* K-12 that is not fully understood, possibly because several alternative and overlapping sugar motifs in
417 the K-12 LPS core can be targeted [73-75] (Fig 10A). Conformational changes in the stubby tail tube
418 triggered by this receptor interaction then initiate the injection of the phage genome from the virion [75,
419 76]. Remarkably, at first several internal virion proteins are ejected and then fold into an extended tail that
420 spans the full bacterial cell envelope which, in a second step, enables DNA injection into the host cytosol
421 [77] (Fig 10A). Notably, our knowledge of this process does not allow the distinction between a “primary”
422 receptor for host recognition and a “secondary” terminal receptor for irreversible adsorption and DNA

423 injection. However, other *Autographiviridae* follow this classical scheme more closely and feature
424 enzymatic domains at their tail fibers or tail spikes that likely mediate attachment to surface glycans as
425 primary receptors followed by enzyme-guided movement towards the cell surface [38, 78].

426 The *Autographiviridae* are a large family of podoviruses hallmarked (and named) with reference
427 to their single-subunit T3/T7-type RNA polymerase that plays several key roles for the phage infection but
428 has also become a ubiquitous tool in biotechnology [79]. All *Autographiviridae* isolates of the BASEL
429 collection belong to several different genera within the very broad *Studiervirinae* subfamily that also
430 contains the classical T7 and T3 phages which we included as references (Fig 10B). Because phage T3
431 recognizes the peculiarly truncated R1-type LPS core of *E. coli* B (see also below) and cannot infect K-12
432 strains, we generated a T3(K12) chimera that encodes the lateral tail fiber gene of T7 similar as was reported
433 previously by others (see *Materials and Methods*) [80]. As expected, all tested *Autographiviridae* use core
434 LPS structures as host receptor and show impaired plaque formation on *waaC* and *waaG* mutants, but in
435 almost all cases some infectivity is retained even on the *waaC* mutant (Fig 10C). This suggests that, as
436 postulated for T7 [73-75], these phages are not strictly dependent on a single glycan motif but might
437 recognize a broader range target structures at the LPS core.

438 The overall pattern of restriction sensitivity and resistance is similar for all tested
439 *Autographiviridae*. While type I and type II RM systems are largely ineffective, type III RM systems show
440 remarkable potency across all phage isolates. Good part of the resistance to type II RM systems is likely
441 due to the near-complete absence of EcoRI and EcoRV recognition sites in the genomes of these phages as
442 described previously [65] (S5 Table) with the exception of ten EcoRV sites in T3(K12) which,
443 consequently, cause massive restriction (Fig 10C). The relatively few recognition sites for type I RM
444 systems do not result in considerable sensitivity for any phage, because at the *gp0.3* locus all of them either
445 encode an Ocr-type DNA mimic type I restriction inhibitor like T7 (*Teseptimavirus*) or an
446 S-adenosylmethionine (SAM) hydrolase that deprives these RM systems of their substrate like T3 (all other
447 genera) [9, 81, 82]. Notably, phages JacobBurekhardt (Bas63) and its close relative T7 are the only phages

448 tested in this work that show any sensitivity to the PifA Abi system encoded on the *E. coli* K-12 F-plasmid
 449 (Fig 10C). Previous work showed that sensitivity of T7 to PifA immunity – as opposed to T3 which is
 450 resistant – depends on the dGTPase Gp1.2 of the phage, though the major capsid protein Gp10 also seems
 451 to play some role in sensitivity [83, 84]. Consequently, we find that phages T7 and JacobBurckhardt, but
 452 not closely related *Teseptimavirus* JeanTingely (Bas62), encode a distinct variant of dGTPase Gp1.2 that
 453 likely causes their sensitivity to PifA (Fig 10D).

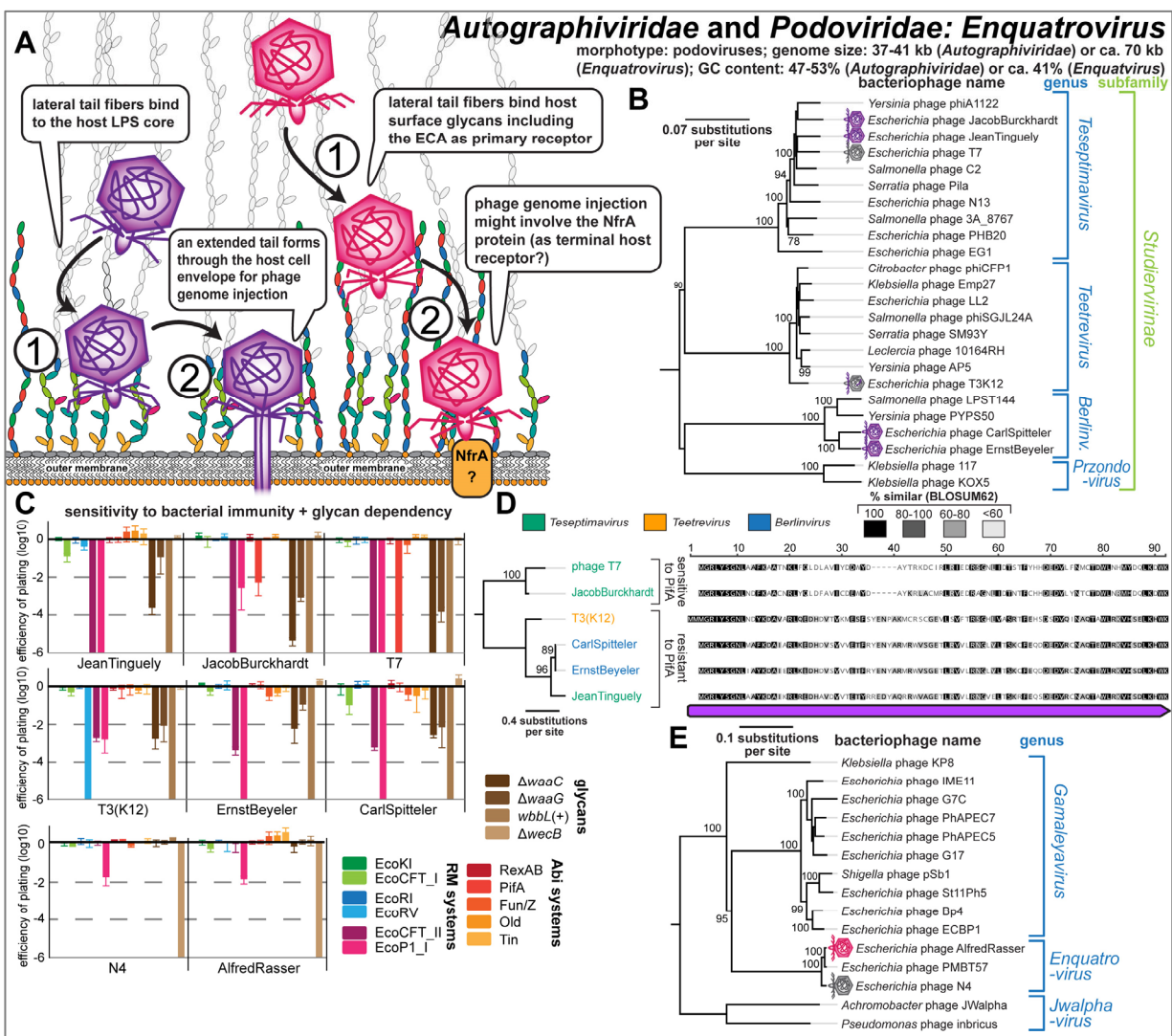


Fig 10. Overview of *Autographiviridae* phages and *Podoviridae* genus *Enquatrovirus*.

(A) Schematic illustration of host recognition by *Autographiviridae* and *Enquatrovirus* phages. (B) Maximum-Likelihood phylogeny of the *Studiervirinae* subfamily of *Autographiviridae* based on several core genes with bootstrap support of branches shown if > 70/100. The phylogeny was midpoint-rooted between the clade formed by *Teseptimavirus* and *Teetrevirus* and the other genera. Phages of the BASEL collection are highlighted by little phage icons. (C) The results of quantitative phenotyping

experiments with *Autographiviridae* regarding sensitivity to altered surface glycans and bacterial immunity systems are presented as efficiency of plating (EOP). Data points and error bars represent average and standard deviation of at least three independent experiments. **(D)** Amino acid sequence alignment and Maximum-Likelihood phylogeny of Gp1.2 orthologs in all tested *Autographiviridae* phages. Phage JeanTinguely belongs to the *Teseptimavirus* genus but encodes an allele of *gp1.2* that is closely related to those of the *Berlinvirus* genus, possibly explaining its resistance to PifA (see (C)). **(E)** Maximum-Likelihood phylogeny of the *Enquatrovirus* genus and related groups of *Podoviridae* based on several core genes with bootstrap support of branches shown if > 70/100. The phylogeny was midpoint-rooted between the distantly related *Jwalphavirus* genus and the others. Phages of the BASEL collection are highlighted by little phage icons.

454 Bacteriophage N4 is the archetype of *Enquatrovirus* phages that are hallmarked by using a large,
455 virion-encapsidated RNA polymerase for the transcription of their early genes [33], and our new
456 *Enquatrovirus* isolate AlfredRasser (Bas67) is a very close relative of N4 (Fig 10E). Based primarily on
457 genetic evidence, phage N4 is thought to initiate infections by contacting the host's ECA with its lateral tail
458 fibers [73, 85, 86] (Fig 10A). We indeed confirmed a remarkable dependence of N4 and AlfredRasser on
459 *wecB* (Fig 10C) and detected homology between the glycan deacetylase domain of the N4 lateral tail fiber
460 and a lateral tail fiber protein of *Vequintavirinae* which also seem to use the ECA as their primary receptor
461 (see above, Figs 9 and 10C). Similar to the O-antigen deacetylase tail fiber of its relative G7C (Fig 10E),
462 the enzymatic activity of the N4 tail fiber might provide a directional movement towards the cell surface
463 that is essential for the next steps of infection [38, 87] (Fig 10A). At the cell surface, the elusive outer
464 membrane porin NfrA was suggested to be the terminal receptor of phage N4 based on the findings that it
465 is required for N4 infection and interacts with the stubby tail of this phage [73, 85, 88]. To the best of our
466 knowledge, this would make phage N4 the first podovirus with an outer membrane protein as terminal
467 receptor [39, 40], though the absence of homologs to the tail extension proteins of *Autographiviridae* indeed
468 suggests a somewhat different mode of DNA injection (Fig 10A).

469 With regard to bacterial immunity, *Enquatrovirus* phages are highly resistant to any tested antiviral
470 defenses with exception to a slight sensitivity to the EcoP1_I type III RM system (Fig 10C). While their
471 resistance to tested type II RM systems is due to the absence of EcoRI or EcoRV recognition sites
472 (S5 Table), the genetic basis for their only slight sensitivity to type III RM systems is not known. We note
473 that *Enquatrovirus* phages encode an *rIIAB* locus homologous to the long-known yet poorly understood
474 *rIIAB* locus found in many large myoviruses which, in case of phage T4, provides resistance to the RexAB

475 Abi system of phage lambda [89] (S4B and S4C Figs). Both phage N4 and AlfredRasser are indifferent to
476 the presence of (O16-type) O-antigen or the tested truncations of the K-12 LPS core at the host cell surface
477 (Fig 10C), suggesting that LPS structures play no role for their infection process.

478 **Properties of *Myoviridae*: *Ounavirinae* and classical temperate phages**

479 The *Felixounavirus* genus in the *Ounavirinae* subfamily of *Myoviridae* comprises a group of
480 phages with genomes of 84-91 kb and characteristically straight lateral tail fibers of which *Salmonella*
481 phage Felix O1 has been most well studied [30, 90] (Figs 11A and 11B). Previous work aimed at the
482 isolation of *E. coli* phages differed greatly in the reported abundance of *Felixounavirus* phages, ranging
483 from no detection [23] over a moderate number of isolates in most studies [25, 91] to around one fourth of
484 all [24]. Across our phage sampling experiments we found a single *Felixounavirus* phage,
485 JohannRWettstein (Bas61), which is rather distantly related to Felix O1 within the eponymous genus (Fig
486 11B). Prototypic phage Felix O1 has been used for decades in *Salmonella* diagnostics because it lyses
487 almost every *Salmonella* strain but only very few other *Enterobacteriaceae* (reviewed in reference [90]).
488 The mechanism of its host recognition and the precise nature of its host receptor(s) have remained elusive,
489 but it is generally known to target bacterial LPS and not any kind of protein receptors [90]. While many
490 *Ounavirinae* seem to bind O-antigen glycans of smooth LPS, the isolation of multiple phages of this
491 subfamily on *E. coli* K-12 with rough LPS and on *E. coli* B with an even further truncated LPS indicate
492 that the functional expression of O-antigen is not generally required for their host recognition [24, 90, 92].
493 Phage JohannRWettstein is only slightly inhibited on *E. coli* K-12 with restored O16-type O-antigen,
494 suggesting that it can either use or bypass these glycans, and totally depends on an intact LPS core (Fig
495 11E). In addition, it is remarkably sensitive to several tested RM systems and shares sensitivity to the Fun/Z
496 Abi system with all other tested *Myoviridae* and the *Markadamsvirinae* (Fig 11E).

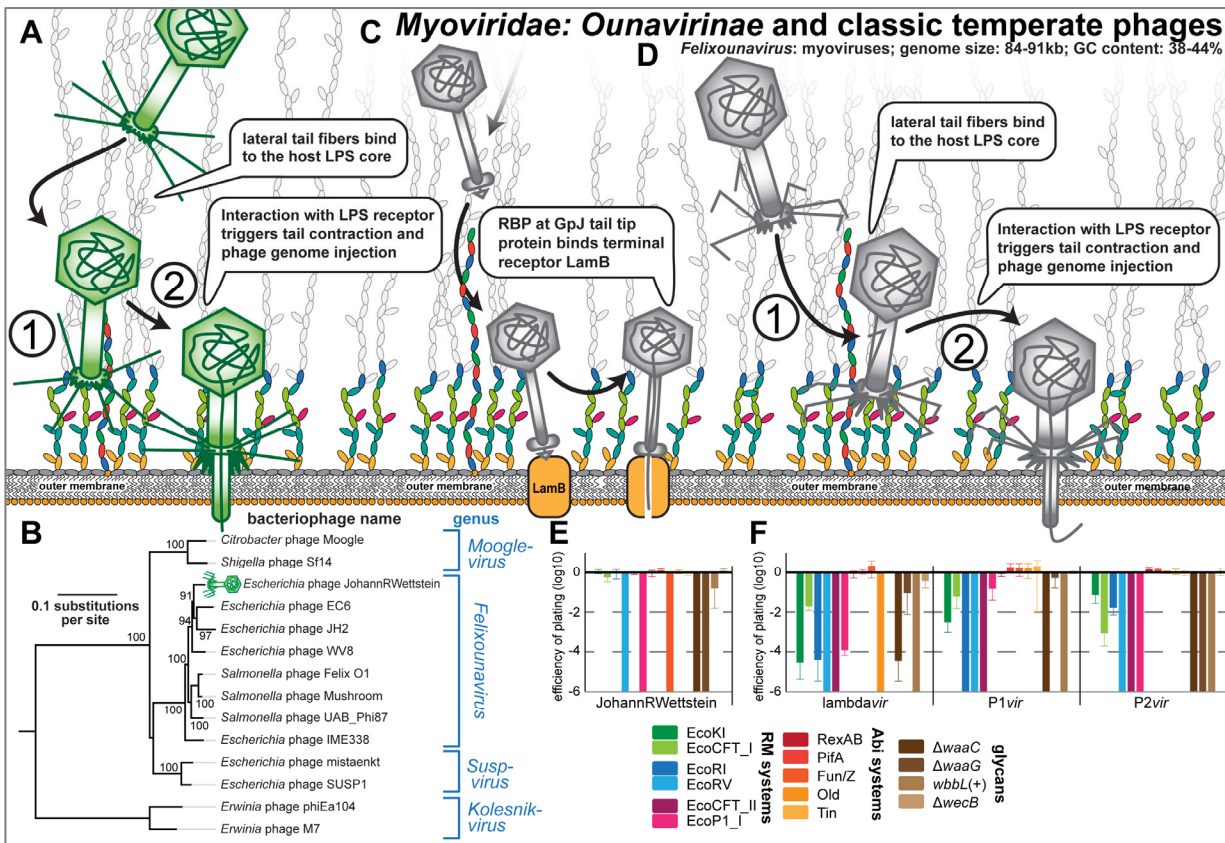


Fig 11. Overview of Myoviridae: Ounavirinae and classic temperate phages.

(A) Schematic illustration of host recognition by *Ounavirinae: Felixounavirinae* phages. Note that the illustration shows short tail fibers simply in analogy to *Tevenvirinae* or *Vequintavirinae* (Figs 8A and 9A), but any role for such structures has not been explored for Felix O1 and relatives. (B) Maximum-Likelihood phylogeny of the *Ounavirinae* subfamily of *Myoviridae* based on several core genes with bootstrap support of branches shown if > 70/100. The phylogeny was midpoint-rooted between *Kolesnikvirus* and the other genera. Our new isolate JohannRWettstein is highlighted by a green phage icon. (C,D) Schematic illustration of host recognition by classic temperate phages lambda, P1, and P2. Note the absence of lateral tail fibers due to a mutation in lambda PaPa laboratory strains [94]. (E,F) The results of quantitative phenotyping experiments with JohannRWettstein and classic temperate phages regarding sensitivity to altered surface glycans and bacterial immunity systems are presented as efficiency of plating (EOP). Data points and error bars represent average and standard deviation of at least three independent experiments.

497 Besides the lytic T phages, temperate phages lambda, P1, and P2 have been extensively studied
 498 both as model systems for fundamental biology questions as well as regarding the intricacies of their
 499 infection cycle [7, 34, 50]. Phage lambda was a prophage encoded in the original *E. coli* K-12 isolate and
 500 forms siphovirus particles that display the GpJ tail tip to contact the LamB porin as the terminal receptor
 501 for DNA injection [7, 93], while the lateral tail fibers (thought to contact OmpA as primary receptor) are
 502 missing in most laboratory strains of this phage due to a mutation [7, 94] (Fig 11C). We reproduced the
 503 dependence of our lambdavirus variant on LamB and, as reported previously, found that an intact inner core

504 of the LPS was required for infectivity [73 and literature cited therein] (Fig 11F and S5 Table). Myoviruses
505 P1 and P2 were both shown to require a rough LPS phenotype to contact their receptors in the LPS core,
506 but the exact identity of these receptors has not been unraveled [40, 50, 73, 95]. While the molecular details
507 of the infection process after adsorption have not been well studied for P1, previous work showed that an
508 interaction of the P2 lateral tail fibers with the LPS core of K-12 strains triggers penetration of the outer
509 membrane by the tail tip [40, 50, 96] (Fig 11D). Consistently, our results confirm that mutations
510 compromising the integrity of the K-12 core LPS abolished bacterial sensitivity to P1_{vir} and P2_{vir} [50, 73,
511 95] (Fig 11F). The quantification of these phages' sensitivity to different immunity systems revealed that
512 they are remarkably sensitive to all tested RM systems (Fig 11F), a property only shared with a few
513 *Drexlerviridae* (Fig 4D). As expected from the considerably lower number of restriction sites, the
514 sensitivity was less pronounced for type I RM systems (Fig 11F and S5 Table). Phage lambda was
515 additionally specifically sensitive to the Old Abi system of the P2 prophage (Fig 11F), as shown previously
516 [50].

517 **Host range across pathogenic enterobacteria and laboratory wildtype *E. coli* B**

518 The host range of bacteriophages has repeatedly been highlighted as a critical feature for phage
519 therapy because broad infectivity can enable phages to be used against different strains of the same pathogen
520 without repeated sensitivity testing “analogous to the use of broad-spectrum antibiotics” [16]. Intuitively,
521 across strains of the same host species the infectivity of phages depends on their ability to successfully bind
522 the variable surface structures of host cells and to overpower or evade strain-specific bacterial immunity
523 [16, 97]. While simple qualitative tests assessing the lysis host range primarily inform about host
524 recognition alone, the more laborious detection of robust plaque formation as a sign of full infectivity is the
525 gold standard of host range determination [16, 97]. We therefore challenged a panel of commonly used
526 pathogenic enterobacterial strains with the BASEL collection and recorded the phages' lysis host range as
527 well as plaque formation separately to gain insight into their host recognition and the ability to overcome
528 immunity barriers inside host cells (Fig 12; see *Materials and Methods*).

529

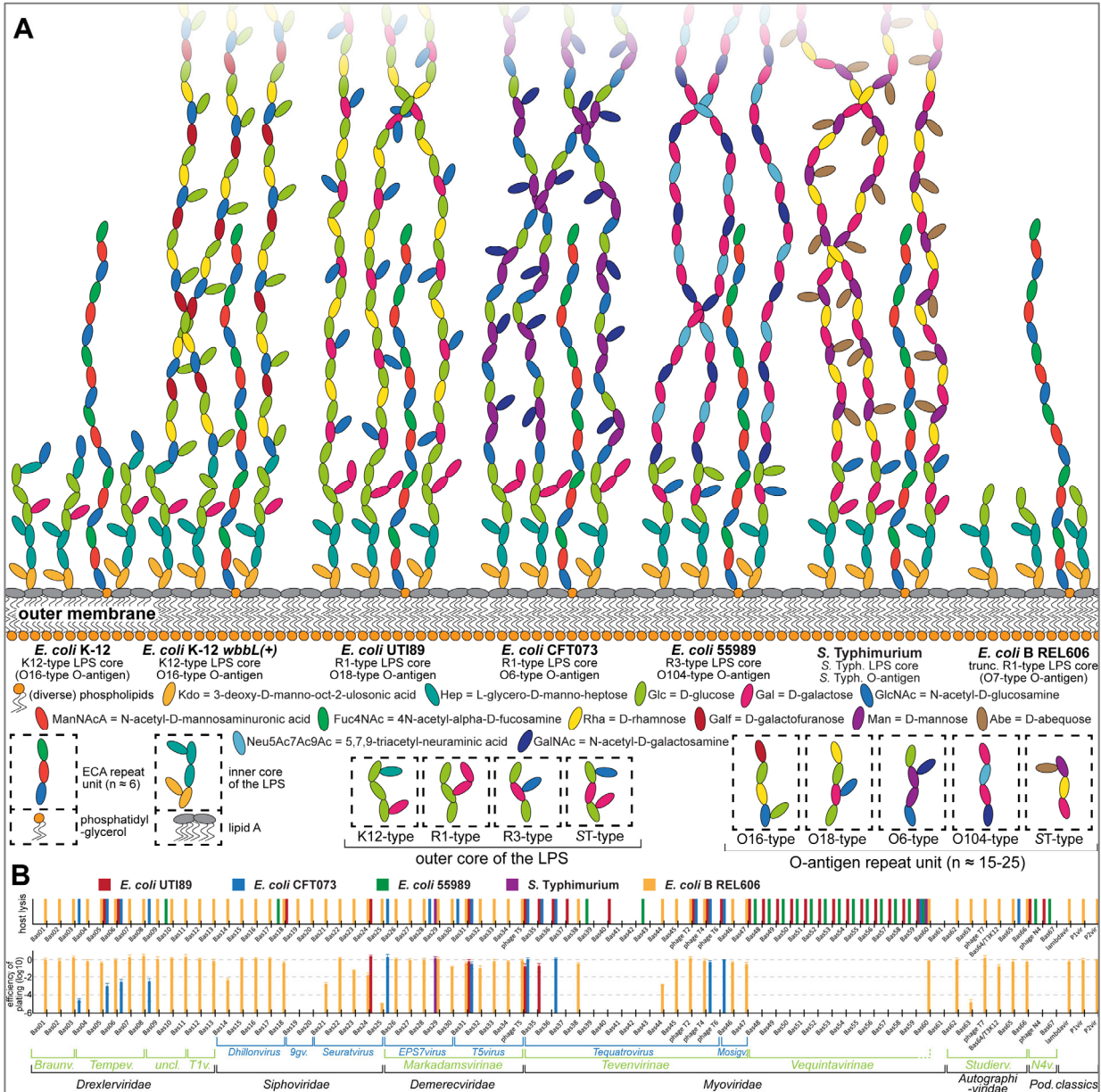


Fig 12. Host range of phages in the BASEL collection

(A) Surface glycans of the enterobacterial strains used in this work (see *Materials and Methods* for details on how the illustration of glycan chains was composed). (B) The ability of all phages in the BASEL collection to infect different enterobacteria was studied qualitatively (lysis host range; top) and, more stringently, based on the ability to form plaques (bottom). Top: The observation of lysis zones with high-titer lysate ($>10^9$ pfu/ml) in at least three independent experiments is indicated by colored bars. Bottom: The infectivity of BASEL collection phages on diverse enterobacterial hosts was quantified as efficiency of plating (EOP). Data points and error bars represent average and standard deviation of at least three independent experiments. Since the data obtained with *Salmonella* Typhimurium 12023s and SL1344 were indistinguishable, we only show the results of one representative strain (*S. Typhimurium* 12023s).

530 As expected from previous work, *Vequintavirinae* phages showed an outstanding lysis host range
531 [23, 25, 70, 71] and invariably infected *E. coli* UTI89, *E. coli* 55989, and *E. coli* K-12 with restored O16-
532 type O-antigen (Figs 9C and 12B). The diversity of infected hosts suggests that *Vequintavirinae* can readily
533 bypass the O-antigen barrier, but the homogeneity of their lysis host ranges is clearly at odds with the
534 polyvalent nature of their virions that display several different lateral tail fibers and variable RBPs [70, 71]
535 (S5 Fig). Notably, we showed that *Enquatrovirus* phages share the exact same host range and an
536 insensitivity to the O-antigen barrier with *Vequintavirinae* (Figs 10C and 12B), possibly because these
537 phages target the highly conserved ECA as primary receptor using a homologous tail fiber (Fig 9D).
538 Recognition of the ECA molecules among smooth LPS (Fig 12A) might enable *Vequintavirinae* and
539 *Enquatrovirus* to bypass the O-antigen barrier and move to the cell surface along this glycan chain, possibly
540 using the deacetylase domain of their shared tail fiber as previously described for *Salmonella* phage P22
541 and the N4 relative G7C [38, 87] (Fig 10E). If true, the *Vequintavirinae* would be effectively monovalent
542 on the tested hosts and might primarily use their “nanosized Swiss army knife” of tail fibers to bind and
543 overcome capsules or other more specialized exopolysaccharides [70, 71]. Given the remarkable lysis host
544 range of *Vequintavirinae* and *Enquatrovirus*, it would be valuable to explore the molecular basis of their
545 host recognition in future studies in order to use this knowledge for phage host range engineering [14].

546 A decently broad lysis host range was also observed for *Tevenvirinae* phages (Fig 12B), in line
547 with previous work [23], though more scattered and far less remarkable than for the *Vequintavirinae*. For
548 both groups of phages it is astonishing how poorly their broad host recognition is reflected by actual plaque
549 formation (Fig 12B). Despite robust “lysis-from-without” in some cases [98], no reliable plaque formation
550 on any other host than *E. coli* K-12 was observed for *Vequintavirinae*, and the range of plaque formation
551 of *Tevenvirinae* was also severely contracted relative to the lysis host range (Fig 12B).

552 Besides *Vequintavirinae* and *Enquatrovirus* that can apparently bypass the O-antigen barrier, we
553 find that the lysis host range of around a third of the tested phages (24 / 61) included at least one host strain
554 with smooth LPS, while the O16-type O-antigen of *E. coli* K-12 blocked infections by all but five of these

555 phages scattered across the different taxonomic groups (5 / 61; Fig 12; see also Figs 4 and 6-11). These
556 results confirm an important role of the O-antigen as a formidable barrier to bacteriophage infection that
557 can only be overcome by specific recognition with tail fibers to breach it, e.g., via enzymatic activities [35].
558 Notably, less than half of the phages that could lyse any strain besides the *E. coli* K-12 Δ RM isolation host
559 showed robust plaque formation on that strain (Fig 12B), probably due to different layers of bacterial
560 immunity. In comparison to *Vequintavirinae* and *Tevenvirinae*, it is surprising how the lysis host range of
561 *Markadamsvirinae* is almost exactly reflected in their range of plaque formation (Fig 12B). One of these
562 phages, SuperGirl (Bas29) is the only phage in the BASEL collection that shows robust plaque formation
563 on *Salmonella* Typhimurium (Fig 12B).

564 The *E. coli* B lineage comprises a number of laboratory strains including REL606 that have, like
565 *E. coli* K-12, lost O-antigen expression and even part of its R1-type LPS core during domestication but are
566 significant as the original hosts of the T phages [5, 99]. In line with the barrier function of the O-antigen
567 (see above), the vast majority of phages in the BASEL collection can at least lyse this strain with the notable
568 exception of *Vequintavirinae* and *Enquatrovirus* (Fig 12B). We can only speculate about the molecular
569 basis of this observation, but maybe the *Vequintavirinae* are unable to use the truncated core LPS of this
570 strain for their infections (Figs 12A and 12B; compare Fig 9C). If inherited from earlier *E. coli* B strains, it
571 seems likely that this total resistance to *Vequintavirinae* is the reason why the T phages contain no
572 representative of this group despite their abundance. Similarly, the observation that phage T5 with its FhuA
573 receptor (Fig 7B) is a rather unusual member of the *Markadamsvirinae* can be explained by the loss of *btuB*
574 in older variants of *E. coli* B, but this mutation reverted in an ancestor of *E. coli* B REL606 [100].
575 Consequently, this modern *E. coli* B strain is sensitive to the various BtuB-targeting *Markadamsvirinae*
576 (Fig 12B). Similarly, *E. coli* B strains lack expression of *ompC* and the REL606 strain additionally lacks
577 functional *tsx* that both encode common primary receptors of the *Tevenvirinae* (Fig 8B) [66, 100]. Though
578 phage T4 itself can use the *E. coli* B LPS core as a primary receptor when OmpC is absent [67], the inability
579 of several other *Tevenvirinae* to infect *E. coli* B REL606 corresponds well to the dependency on OmpC and

580 Tsx as primary receptors (Figs 8B, 12B, and S4A). A number of additional phages of, e.g., the *Nonagvirus*
581 genus can lyse but not form plaques on *E. coli* B REL606 (Fig 12B). Based on previous work, we suggest
582 that this phenotype is caused by immunity systems encoded in the specific repertoire of cryptic prophages
583 of *E. coli* B strains that differ considerably between *E. coli* B and K-12 strains and are known to harbor
584 active immunity systems [100].

585 **Discussion**

586 **Remarkable patterns of bacteriophage receptor specificity**

587 Our results regarding the terminal receptor specificity of different groups of siphoviruses inherently
588 present the question why all these phages target less than ten of the more than 150 outer membrane proteins
589 of *E. coli* K-12 of which around two dozen are porins [39, 40, 101] (Figs 4C and 7B). Similarly,
590 *Tevenvirinae* use only five different outer membrane proteins as primary receptors (Fig 8B) [39, 40].
591 Previous work suggested that this bias might be linked to the abundance of the targeted proteins, both via
592 a preference for particularly numerous proteins (favoring phage adsorption) or very scarce ones (avoid
593 competition among phages) [102]. However, we feel that this stark bias in phage preference might be largely
594 driven by functional constraints. Notably, the large siphoviruses of *Markadamsvirinae* bind exactly a subset
595 of those terminal receptors targeted by the small siphoviruses despite using non-homologous RBPs, while
596 there is no overlap between these proteins and the primary receptors of the *Tevenvirinae* [39, 40] (Figs 4-8).
597 It seems therefore likely that the receptors targeted by siphoviruses need to have certain properties, e.g.,
598 favoring DNA injection, that greatly limit the repertoire of suitable candidates. We envision that future
599 studies might unravel the molecular mechanisms of how siphoviruses recognize and use outer membrane
600 proteins as terminal receptors on Gram-negative hosts similar to, e.g., how it has been studied for
601 myoviruses and podoviruses that directly puncture the outer membrane [68, 77].

602 Many open questions remain regarding the host recognition and receptor specificity of *E. coli*
603 phages that could be tackled with a combination of systematic phenotypic and genomic analyses. Why do
604 some small siphoviruses in *Drexelviridae* and *Siphoviridae* but none of the larger ones of *Demereciviridae*:
605 *Markadamsvirinae* strongly depend on an intact LPS core, seemingly independent of primary receptor
606 usage or terminal receptor specificity (Figs 4D, 6C, 6F, and 7B)? Is it possible to perform analyses like we
607 did it for the RBPs of siphoviruses or *Tevenvirinae* for the much more variable lateral tail fibers (S1B, S2A,
608 and S3A Figs) that probably bind to the around 200 O-antigen types of *E. coli* [103]? And is there a
609 genetically encoded specificity for the inner membrane channels used by siphoviruses (like ManYZ by
610 phage lambda or PtsG for HK97 [7]) similar to the mix-and-match of RBPs and outer membrane proteins?
611 Addressing these questions in future studies would not only greatly expand our knowledge regarding the
612 molecular basis of bacteriophage ecology and evolution, but would also help making use of this knowledge
613 to optimize the application of phages in biotechnology and for therapeutic applications, e.g., for “phage
614 steering” [14, 104].

615 **Bacteriophage sensitivity and resistance to host immunity**

616 Our systematic analysis of the sensitivity and resistance profiles across the different taxonomic of
617 phages of the BASEL collection revealed several strong patterns that are informative about underlying
618 molecular mechanisms. While some groups of phages like *Tevenvirinae* or *Nonagvirus* and *Seuratvirus*
619 genera are highly homogeneous in their profiles of sensitivity or resistance (Figs 6F and 8C) – probably
620 largely driven by conserved DNA modifications – others are more heterogeneous but never showed merely
621 random differences. For example, the two genera of *Markadamsvirinae* differ systematically in their
622 resistance to EcoRV (Fig 7C), likely due to vastly different numbers of recognition sites (S5 Table). Specific
623 deviations of single phages from these patterns are sometimes readily explained like, e.g., the PifA
624 sensitivity of T7 and JacobBurckhardt (due to their *gpl.2* allele, Figs 10C and 10D) or the EcoRV sensitivity
625 of T3 (as the only podovirus failing in RM site avoidance regarding EcoRV; S5 Table and Fig 10C).
626 Notably, podoviruses generally show a remarkable lack of recognition sites of type I and type II RM systems

627 (S5 Table) which makes them phenotypically resistant [65], but this evolutionary strategy does not seem to
628 be effective for type III RM systems (Fig 11C), possibly due to the abundance of their (shorter) recognition
629 sequences (Fig 3B and S5 Table). Overall, we observed that phages with bigger genomes such as
630 *Tevenvirinae*, *Vequintavirinae*, and *Markadamsvirinae* are broadly targeted by Abi systems, while smaller
631 siphoviruses or podoviruses are either not or only sparingly targeted (Figs 4 and 6-11, see also S3 Text).
632 Temperate phages in general seem to be highly sensitive to any kind of host immunity (Fig 11F), possibly
633 because their evolution is less driven by selection to overcome host defenses but rather by optimizing the
634 lysogens' fitness, e.g., by providing additional bacterial immunity systems [8, 9].

635 Regarding the immunity systems themselves, we confirmed the intuitive expectation that the
636 potency of RM systems is linked to the number of recognition sites in each phage genome unless they are
637 masked by DNA modifications. Consequently, large phages with many recognition sites (like
638 *Vequintavirinae*) are exceptionally sensitive to RM systems (Fig 8C), while type I RM systems perform
639 very poorly against most phages because their long recognition sites are rare (Fig 3B and S5 Table; see also
640 Figs 4 and 6-11). For several groups of phages like *Markadamsvirinae* and *Tevenvirinae*, the EcoRV system
641 is the only RM system with significant impact (Figs 7C and 8C). We suggest that this is due to the blunt-
642 cutting activity of EcoRV that is much more difficult to seal for DNA repair than the sticky ends introduced
643 by the other tested RM systems (Fig 3B), though phage DNA ligases are known to differ in their efficiency
644 on different kinds of DNA breaks [105].

645 One surprising result of our phenotyping was the remarkably poor target range of the most well-
646 studied Abi systems of *E. coli* K-12, RexAB and PifA, that each affected only two or three phages (Figs 4
647 and 6-11). We do not think that this finding is an artifact of, e.g., the genetic constructs that we used,
648 because both systems protected its host very well against the phages that they were known to target [12]:
649 An *rIIAB* mutant of T4 was highly sensitive to RexAB (S4B Fig), and phage T7 was unable to infect a host
650 with PifA (Fig 10C). In stark difference to RexAB and PifA, the three Abi systems of phage P2 protected
651 each against a considerable number of phages, especially Fun/Z that inhibited all *Tevenvirinae*,

652 *Vequintavirinae*, and *Markadamsvirinae* plus the *Felixounavirus* JohannRWettstein (Figs 4 and 6-11).
653 Despite this remarkable potency, the molecular mechanism of Fun/Z immunity has remained unknown [50].
654 A common first step to unraveling the activities of an Abi system is the analysis of insensitive phage escape
655 mutants which can be particularly insightful if they were isolated from several very different phages [106].
656 It seems clear that the BASEL collection as a well-assorted set of very diverse phages could be an effective
657 tool for this purpose and also in general for a first phenotypic profiling of novel immunity systems that are
658 commonly tested against much smaller, less well-defined sets of phages [106, 107].

659 Though the technicalities of our immunity phenotyping are subject to a few minor caveats (see
660 *Materials and Methods* and S3 Text), our results demonstrate how the BASEL collection can be used to
661 explore the biology of bacterial immunity systems and the underlying molecular mechanisms. Several
662 important open questions remain: What is the evolutionarily or mechanistic reason for the stark differences
663 in Abi system target range? To which extent do the different layers of bacterial immunity limit
664 bacteriophage host range? Why are some groups of phages like the *Tevenvirinae* so strongly targeted by
665 seemingly unrelated Abi systems and other groups of phages apparently not at all? And how well would it
666 be possible, based on systematic phenotypic data of the BASEL collection or extensions thereof, to predict
667 the sensitivity of newly isolated phages to diverse immunity systems just based on their genome sequences?

668 **Trade-offs between phage traits limit their effective host range**

669 Our results show very clearly that seemingly advantageous phage traits such as the broad host
670 recognition of *Vequintavirinae* or the remarkable resistance of *Tevenvirinae* to RM systems do not confer
671 these phages a particularly large effective host range (Figs 8C and 12B). This observation can be explained
672 by strong trade-offs between different phage fitness traits as proposed already in earlier work [108]. Unlike
673 the hypothetical “Darwinian Demon” that would maximize all fitness traits simultaneously and dominate
674 its ecosystem alone [109], the limits imposed by these trade-offs instead drive the adaptation of different
675 phage groups towards specific niches that enable their long-term coexistence [108]. In marine
676 environments, the coexistence of a few specialized, highly successful phage groups was proposed to be

677 stable in space and time because extinction of individual phages would usually result in their replacement
678 by relatives from the same, highly adapted group [110]. This “royal family model” could also explain why
679 the same groups of *E. coli* phages sampled in our work have already been found again and again in previous
680 studies that sampled diverse other environments [23-29] (Fig 2).

681 With our data we can at least shed light on the molecular basis of the proximal causes of the
682 trade-offs between phage fitness traits that limit very broad effective host ranges in the selected example:
683 *Vequintavirinae* phages are highly sensitive to various RM systems (Fig 9C), while the *Tevenvirinae* appear
684 to be a major target of different Abi systems and have to evade a variety of those already only to infect
685 regular *E. coli* K-12 (Figs 8C, S4B, and S4C; see also S3 Text) [9, 10, 12]. The deeper evolutionary or
686 mechanistic basis of our observations is not clear – as an example, phages of *Nonagvirus* and *Seuratvirus*
687 genera with genomes that are far less than half the size of *Vequintavirinae* afford full pathways for
688 guanosine modifications that protect them reasonably well from RM systems (Figs 6E and 6F). It is not
689 intuitive why natural selection has not resulted in similarly effective mechanisms for the *Vequintavirinae*,
690 particularly because their promiscuity in host adsorption should bring them into very frequent contact with
691 the diverse RM systems that form a major pillar of *E. coli* immunity [11, 49]. A good illustration for this
692 paradox is phage PaulScherrer (Bas60), a phi92-like relative of the *Vequintavirinae* (Fig 9B), that is the
693 only phage in the BASEL collection lysing all tested host strains but without robust plaque formation on
694 any strain besides *E. coli* K-12 (Fig 12B).

695 The observed trade-offs between desired phage traits suggest that newly isolated phages might
696 greatly profit from improvements by experimental evolution or genetic engineering to help them escape
697 these constraints at least long enough for applications like phage therapy [14]. Such improvements seem to
698 be principally feasible without immediate loss of fitness because, e.g., phage FriedrichZschokke (Bas41)
699 of the *Tevenvirinae* displays only weak sensitivity to the Tin and Fun/Z Abi systems that are highly potent
700 against its relatives (Fig 8C). However, targeted improvements of phage properties directly depend on
701 fundamental knowledge of the molecular mechanisms underlying receptor specificity, the phages’ anti-

702 immunity systems, and their host counterparts that are frequently unavailable [14, 41]. Future studies
703 targeting the fundamental biology of phage-host interactions could therefore be directly helpful for such
704 applications, and for *E. coli* phages the BASEL collection might be a suitable tool for such research.

705 A different way to rationalize the paradox highlighted above is that the observed trade-offs might
706 be less pronounced in natural environments, e.g., when bacteria are starved, stressed, in biofilms, or in some
707 other physiological state not well reflected by our laboratory experiments. Consistently, the insufficiency
708 of regular phage phenotyping using standard laboratory growth conditions has already been recognized
709 previously, but only limited data comparing, e.g., different host physiologies are available [16, 111]. Further
710 studies exploring how phage infectivity, host range, and sensitivity to immunity systems change under
711 different growth conditions would therefore be important to better understand the challenges for successful
712 phage therapy and, more generally, the ecology and evolution of phages in natural environments.

713 **Concluding remarks**

714 A recent landmark study systematically explored the genetic profile of host requirements for several
715 *E. coli* phages and uncovered multiple unexpected and exciting twists of phage biology such as the
716 dependence of phage N4 on high levels of the second messenger cyclic di-GMP [73]. Our current study
717 based on the BASEL collection represents a complementary approach to explore the biology of *E. coli*
718 phages not with elaborate genome-wide screens on the host side but rather by combining phenotypic and
719 genomic analyses of a well-assorted set of bacteriophages. With this strategy we achieved significant
720 advances in bacteriophage biology regarding the recognition of host receptors, the sensitivity or resistance
721 of phages to host immunity, and how these factors come together to determine bacteriophage host range.
722 Our work therefore establishes the BASEL collection as a powerful tool to explore new aspects of
723 bacteriophage biology by unraveling links between phage phenotypes and their genome sequences.
724 Furthermore, our extensive characterization of the most abundant lineages of *E. coli* phages also provides
725 a useful field guide for teaching and outreach activities analogous to the successful SEA-PHAGES initiative

726 [112] and the diverse student and high school projects that have enabled our study (see *Acknowledgments*
727 and S5 Table).

728 **Materials and Methods**

729 **Preparation of culture media and solutions**

730 Lysogeny Broth (LB) was prepared by dissolving 10 g/l tryptone, 5 g/l yeast extract, and 10 g/l
731 sodium chloride in Milli-Q H₂O and sterilized by autoclaving. LB agar plates were prepared by
732 supplementing LB medium with agar at 1.5% w/v before autoclaving. The M9RICH culture medium was
733 conceived as a variant of regular M9 medium [113] supplemented with trace elements and 10% v/v LB
734 medium prepared without NaCl to promote the growth of diverse enterobacterial strains. It was prepared
735 from sterilized components by mixing (for 50 ml) 33.75 ml Milli-Q H₂O, 10 ml 5x M9 salts solution, 5 ml
736 LB medium without NaCl, 500 µl 40% w/v D-glucose solution, 100 µl 1 M MgSO₄, and 5 µl 1 M CaCl₂
737 using sterile technique. Unless indicated otherwise, all components were sterilized by filtration (0.22 µm).

738 Phosphate-buffered saline (PBS) was prepared as a solution containing 8 g/l NaCl, 0.2 g/l KCl,
739 1.44 g/l NA₂HPO₄·2H₂O, and 0.24 g/l KH₂PO₄ with the pH adjusted to 7.4 using 10 M NaOH and sterilized
740 by autoclaving. SM buffer was prepared as 0.1 M NaCl, 10 mM MgSO₄, and 0.05 M Tris (pH 7.5) using
741 sterile technique.

742 **Bacterial handling and culturing**

743 *Escherichia coli* and *Salmonella* Typhimurium strains were routinely cultured in LB medium at
744 37°C in glass culture tubes or Erlenmeyer flasks with agitation at 170rpm. For all phenotyping assays, the
745 bacteria were instead grown in M9RICH which supports robust growth of all strains to high cell densities.
746 LB agar plates were routinely used as solid medium. Selection for genetic modifications or plasmid
747 maintenance was performed with ampicillin at 50 µg/ml, kanamycin at 25 µg/ml, and zeocin at 50 µg/ml.

748

749 **Bacteriophage handling and culturing**

750 Bacteriophages were generally cultured using the double-agar overlay method [114] with a top agar
751 prepared as LB agar with only 0.5% w/v agar supplemented with 20 mM MgSO₄ and 5 mM CaCl₂. Top
752 agar plates were incubated at 37°C and plaques were counted as soon as they were identified by visual
753 inspection. However, the plates were always incubated for at least 24 hours to record also slow-growing
754 plaques. We routinely used the improvements of classical phage techniques published by Kauffman and
755 Polz [115].

756 High-titer stocks of bacteriophages were generated using the plate overlay method. Briefly, top
757 agar plates were set up to grow almost confluent plaques of a given phage and then covered with 12 ml of
758 SM buffer. After careful agitation for 24 hours at 4°C, the suspension on each plate was pipetted off and
759 centrifuged at 8'000g for 10 minutes. Supernatants were sterilized with few drops of chloroform and stored
760 in the dark at 4°C. For archiving, bacteriophages were stored as virocells at -80°C [116]

761 **Bacterial strains and strain construction**

762 All bacterial strains used in this work are listed in S1 Table, all oligonucleotide primers in S2 Table,
763 and all plasmids in S3 Table.

764 ***Escherichia coli* K-12 MG1655 ΔRM**

765 The standard laboratory strain *E. coli* K-12 MG1655 (CGSC #6300) was engineered into a more
766 permissive host for bacteriophage isolation by knocking out the EcoKI type I restriction-modification
767 system (encoded by *hsdRMS*) and the McrA, Mrr, and McrBC type IV restriction systems using lambda red
768 recombineering [117] (see Text S1 and our previous work for more technical details [118]). The resulting
769 strain lacks all known *E. coli* K-12 restriction systems and was therefore called *E. coli* K-12 ΔRM. To
770 enable isolation of bacteriophages with tropism for the sex pilus of the F-plasmid conjugation system, we
771 supplied *E. coli* K-12 MG1655 ΔRM with a variant of the F-plasmid in which the *pifA* immunity gene
772 (which might otherwise have interfered with bacteriophage isolation) had been replaced with a zeocin

773 resistance cassette by one-step recombineering (see S1 Text for details). The strain was additionally
774 transformed with plasmid pBR322_Δ*Ptet* of reference [119] as an empty vector control for experiments
775 with plasmid-encoded immunity systems (see below).

776 ***Escherichia coli* K-12 MG1655 ΔARM mutants with altered surface glycans**

777 To test the effect of altered surface glycans of bacteriophage infection, we generated derivatives of
778 *E. coli* K-12 MG1655 ΔARM in which genes linked to specific glycans were knocked out. The *waaC* and
779 *waaG* genes of the LPS core biosynthesis pathway were knocked out to generate mutants displaying a deep-
780 rough or extremely deep-rough phenotype (Fig 3A). Expression of the O16-type O-antigen of *E. coli* K-12
781 was restored by precisely removing the IS5 element disrupting *wbbL* [44] (Fig 3A). These mutants were
782 generated by two-step recombineering (see details in S1 Text and a list of all strains in S1 Table). A strain
783 specifically lacking the enterobacterial common antigen (ECA) was obtained by flipping out the kanamycin
784 resistance cassette of the *wecB* mutant of the KEIO collection using plasmid pCP20 [117, 120]. This strain
785 is deficient in WecB, the enzyme synthesizing UDP-ManNAcA (UDP-N-acetyl-D-mannosaminuronic
786 acid), which is specifically required for the synthesis of the ECA but no other known glycan of *E. coli* K-12
787 [43].

788 ***Escherichia coli* K-12 BW25113 *btuB* and *tolC* knockout mutants**

789 *btuB* and *tolC* knockout mutants isogenic with the KEIO collection were generated to use these
790 strains lacking known bacteriophage receptors for qualitative top agar assays (see below). Details of the
791 strain construction are provided in S1 Text.

792 **Other enterobacterial strains used for bacteriophage phenotyping**

793 *E. coli* B REL606 is a commonly used laboratory strain with a parallel history of domestication to
794 *E. coli* K-12 MG1655 [99]. *E. coli* UTI89 (ST95, O18:K1:H7) and *E. coli* CFT073 (ST73, O6:K2:H1; we
795 used the variant with restored *rpoS* described previously [121]) are commonly used as model strains for
796 uropathogenic *E. coli* (UPEC) and belong to phylogroup B2 [122]. *E. coli* 55989 (phylogroup B1, ST678,

797 O104:H4) is commonly used as a model strain for enteroaggregative *E. coli* (EAEC) and closely related
798 the Shiga toxin-producing *E. coli* which caused the 2011 outbreak in Germany [123, 124]. *Salmonella*
799 *enterica* subsp. *enterica* serovar Typhimurium strains 12023s (also known as ATCC 14028) and SL1344
800 are both commonly used in laboratory experiments but exhibit phylogenetic and biological differences
801 [125].

802 **Plasmid construction**

803 Plasmid vectors were generally cloned following the method of Gibson et al. (“Gibson Assembly”)
804 [126] in which two or more linear fragments (usually PCR products) are ligated directionally guided by
805 short 25 bp overlaps. Initially, some plasmids were also constructed using classical restriction-based
806 molecular cloning. Briefly, a PCR-amplified insert and the vector backbone were each cut with appropriate
807 restriction enzymes (New England Biolabs). After dephosphorylation of the backbone (using FastAP
808 dephosphorylase; Thermo Scientific), insert and backbone were ligated using T4 DNA ligase (Thermo
809 Scientific). Local editing of plasmid sequences was performed by PCR with partially overlapping primers
810 as described by Liu and Naismith (127). *E. coli* strain EC100 *pir*(+) was used as host for all clonings. The
811 successful construction of every plasmid was confirmed by Sanger Sequencing. A list of all plasmids used
812 in this study is found in S3 Table and their construction is summarized in S4 Table. The sequences of all
813 oligonucleotide primers used in this study are listed in S2 Table.

814 For the series of plasmids encoding the eleven different bacterial immunity systems studied in this
815 work (see Fig 3B), we used the EcoRI and EcoRV constructs of Pleška, Qian et al. [119] as templates and,
816 consequently, the corresponding empty vector pBR322_Δ*Ptet* as general cloning backbone and
817 experimental control. The different immunity systems were generally cloned together with their own
818 transcriptional promoter region. However, the *rexAB* genes are transcribed together with the cI repressor of
819 the lambda prophage [7]. We therefore cloned them directly downstream of the *Ptet* promoter of the
820 pBR322 backbone and obtained a functional construct (validated in S4B Fig). The EcoKI, EcoRI, EcoRV,
821 and EcoP1_I RM systems have been studied intensively in previous work [47-49]. Besides the type IA RM

822 system EcoKI we also cloned EcoCFT_I that is nearly identical to the well-characterized type IB RM
823 system EcoAI but encoded in the genome of *E. coli* CFT073 that was available to us [47, 128]. Similarly,
824 the EcoCFT_II system was identified as a type III RM system in the *E. coli* CFT073 genome using REBASE
825 [49, 128]. Due to problems with toxicity, some immunity systems were cloned not into pBR322_Δ*Ptet* but
826 rather into a similar plasmid carrying a low-copy SC101 origin of replication (pAH186SC101e [121], see
827 S3 and S4 Tables as well as the considerations in S3 Text). Since we failed to obtain any functional construct
828 for the ectopic expression of *pifA* (as evidenced by lack of immunity against T7 infection), we instead
829 replaced the F(*pifA::zeoR*) plasmid in *E. coli* K-12 MG1655 ΔRM with a wildtype F plasmid that had
830 merely been tagged with kanamycin resistance and encodes a functional *pifA* (pAH200e).

831 **Bacteriophage isolation**

832 **Basic procedure**

833 Bacteriophages were isolated from various different samples between July 2019 and November
834 2020 using *E. coli* K-12 MG1655 ΔRM as the host (see S5 Table for details) using a protocol similar to
835 common procedures in the field [16]. Phage isolation was generally performed without an enrichment step
836 to avoid biasing the isolation towards fast-growing phages (but see below).

837 For aqueous samples we directly used 50 ml, while samples with major solid components (like soil
838 or compost) were agitated overnight at 4°C in 50 ml of PBS to release viral particles. Subsequently, all
839 samples were centrifuged at 8'000 g for 15 minutes to spin down particles larger than viruses. The
840 supernatants were sterilized treated with 5% v/v chloroform which safely inactivates any bacteria as well
841 as enveloped viruses but will generally leave most *Caudovirales* intact [16]. Subsequently, viral particles
842 were precipitated by adding 1 ml of a 2 M ZnCl₂ solution per 50 ml of sample, mixing shortly by inversion,
843 and incubating the suspension at 37°C without agitation for 15 minutes [129]. After precipitation, the
844 samples were centrifuged again at 8'000 g for 15 minutes and the supernatant was discarded. The pellets
845 were carefully resuspended in each 500 μl of SM buffer by agitation at 4°C for 15 minutes. Subsequently,
846 the suspensions were cleared quickly using a tabletop spinner and mixed with 500 μl of bacterial overnight

847 culture (resuspended in fresh LB medium to induce resuscitation). After incubation at room temperature
848 for 15 minutes to promote phage adsorption, each mixture was added to 9 ml of pre-warmed top agar and
849 poured onto a pre-warmed square LB agar plate (ca. 12 cm x 12 cm). After solidification, the plates were
850 incubated at 37°C for up to 24 hours.

851 **Isolation of bacteriophage clones**

852 Bacteriophages were visible as plaques forming in the dense bacterial growth of the top agar. For
853 isolation of bacteriophage clones, they were picked from clearly separated plaques of diverse morphologies
854 with sterile toothpicks and propagated at least three times via single plaques on top agars of the isolation
855 host strain *E. coli* K-12 MG1655 Δ RM. To avoid isolating temperate phages or phages that are poorly
856 adapted to *E. coli* hosts, we only picked clear plaques (indicative of lytic phages) and discarded isolates
857 that showed poor plaque formation [16].

858 **Isolation of *Autographiviridae* using enrichment cultures**

859 The direct plating procedure outlined above never resulted in the isolation of phages belonging to
860 the *Autographiviridae* like iconic T phages T3 and T7. Given that these phages are known for fast
861 replication and high burst sizes [130], we therefore performed a series of enrichment culture isolation
862 experiments to obtain phages forming the characteristically large, fast-growing plaques of
863 *Autographiviridae*. For this purpose, we prepared M9 medium using a 5x M9 salts solution and chloroform-
864 sterilized sewage plant inflow instead of water (i.e., containing ca. 40 ml of sewage plant inflow per 50 ml
865 of medium) and supplemented it with 0.4% w/v D-glucose as carbon source. 50 ml cultures were set up by
866 inoculating these media with each 1 ml of an *E. coli* K-12 MG1655 Δ RM overnight culture and agitated
867 the cultures at 37°C for 24 hours. Subsequently, the cultures were centrifuged at 8'000 g for 15 minutes
868 and each 50 μ l of supernatant was plated with the *E. coli* K-12 MG1655 Δ RM isolation strain in a top agar
869 on one square LB agar plate. After incubation at 37°C for three or four hours, the first *Autographiviridae*
870 plaques characteristically appeared (before most other plaques) and were picked and propagated as

871 described above. Using this procedure, we isolated four different new *Autographiviridae* isolates (see S5
872 Table and Fig 10B).

873 **Composition of the BASEL collection**

874 Bacteriophages were mostly isolated and characterized from randomly picked plaques in direct
875 selection experiments, but we later adjusted the procedure to specifically isolate *Autographiviridae* which
876 were the only major group of phages previously shown to infect *E. coli* K-12 missing from our collection
877 (see above). After every set of 10-20 phages that had been isolated, we performed whole-genome
878 sequencing and preliminary phylogenetic analyses to keep an overview of the growing collection (see
879 below). In total, more than 120 different bacteriophages were sequenced and analyzed of which we selected
880 66 tailed, lytic phage isolates to compose the BASEL collection (see Fig 2 and S5 Table for details). Phages
881 closely related to other isolates were deliberately excluded unless they displayed obvious phenotypic
882 differences such as, e.g., a different host receptor. In addition to the 66 newly isolated bacteriophages, ten
883 classical model phages were included for genomic and phenotypic characterization, and we view these
884 phages as an accessory part of the BASEL collection. These ten phages were six of the seven T phages
885 (excluding T1 because it is a notorious laboratory contaminant [32]), phage N4, and obligately lytic mutants
886 of the three well-studied temperate phages lambda, P1, and P2 [5, 7, 33, 34] (Fig 2; see also S5 Table). To
887 generate the T3(K12) chimera, the 3' end of *gp17* lateral tail fiber gene of phage T7 was cloned into low-
888 copy plasmid pUA139 with flanking regions exhibiting high sequence similarity to the phage T3 genome
889 (generating pUA139_T7(*gp17*), see S4 Table). Phage T3 was grown on *E. coli* B REL606 transformed with
890 this plasmid and then plated on *E. coli* K-12 MG1655 Δ RM to isolate recombinant clones. Successful
891 exchange of the parental T3 *gp17* allele with the variant of phage T7 was confirmed by Sanger Sequencing.

892 **Qualitative top agar assays**

893 The lysis host range of isolated bacteriophages on different enterobacterial hosts and their ability
894 to infect strains of a set of KEIO collection mutants lacking each one surface protein (or isogenic mutants
895 that were generated in this study, see S1 Table and S1 Text) were tested by qualitative top agar assays. For

896 this purpose, top agars were prepared for each bacterial strain on LB agar plates. For by overlaying them
897 with top agar supplemented with a suitable bacterial inoculum. For regular round Petri dishes (ca. 9.4 cm
898 diameter) we used 3 ml of top agar supplemented with 100 μ l of bacterial overnight culture, while for larger
899 square Petri dishes (ca. 12 cm x 12 cm) we used 9 ml of top agar supplemented with 200 μ l of overnight
900 culture. After solidification, each 2.5 μ l of undiluted high-titer stocks of all tested bacteriophages ($>10^9$
901 pfu/ml) were spotted onto the top agar plates and dried into the top agar before incubation at 37°C for at
902 least 24 hours. If lysis zones on any enterobacterial host besides our *E. coli* K-12 Δ RM reference strain
903 were observed, we quantified phage infectivity in efficiency of plating assays (see below). Whenever a
904 phage failed to show lysis on a mutant strain lacking a well-known phage receptor, we interpreted this result
905 as indicating that the phage infecting depends on this factor as host receptor.

906 **Efficiency of Plating assays**

907 The infectivity of a given bacteriophage on a given host was quantified by determining the
908 efficiency of plating (EOP), i.e., by quantitatively comparing its plaque formation on a certain experimental
909 host to plaque formation on reference strain *E. coli* K-12 MG1655 Δ RM carrying F(*pifA::zeoR*) and
910 pBR322_ Δ Ptet [131]. Experimental host strains were identical to the reference strain with the difference that
911 they either carried plasmids encoding a certain bacterial immunity system (S3 Table) or had a chromosomal
912 modification changing surface glycan expression (Fig 3A and S1 Table).

913 For quantitative phenotyping, top agars were prepared for each bacterial strain on LB agar plates
914 by overlaying them with top agar (LB agar containing only 0.5% agar and additionally 20 mM MgSO₄ as
915 well as 5 mM CaCl₂; stored at 60°C) supplemented with a suitable bacterial inoculum. For regular round
916 Petri dishes (ca. 9.4 cm diameter) we used 3 ml of top agar supplemented with 100 μ l of bacterial overnight
917 culture, while for larger square Petri dishes (ca. 12 cm x 12 cm) we used 9 ml of top agar supplemented
918 with 200 μ l of overnight culture. While the top agars were solidifying, serial dilutions of bacteriophage
919 stocks (previously grown on *E. coli* K-12 MG1655 Δ RM to erase any EcoKI methylation) were prepared
920 in sterile phosphate-buffered saline (PBS). Subsequently, each 2.5 μ l of all serial dilutions were spotted on

921 all top agar plates and dried into the top agar before incubation at 37°C for at least 24 hours. Plaque
922 formation was recorded repeatedly throughout this time (starting after 3 hours of incubation for fast-
923 growing phages). The EOP of a given phage on a certain host was determined by calculating the ratio of
924 plaques obtained on this host over the number of plaques obtained on the reference strain *E. coli* K-12
925 MG1655 Δ RM carrying F(*pifA::zeoR*) and pBR322_ Δ Ptet [131].

926 When no plaque formation could be unambiguously recorded by visual inspection, the EOP was
927 determined to be below detection limit even if the top agar showed lysis from without (i.e., lysis zones
928 caused by bacterial cell death without phage infection at an efficiency high enough to form plaques [98]).
929 However, for all non-K12 strains of *E. coli* as well as *Salmonella* Typhimurium we determined the lysis
930 host range (i.e., the range of hosts on which lysis zones were observed) besides the numerical determination
931 of EOP (see above). Occasionally, we found that certain phage / host pairs were on the edge between merely
932 strong lysis from without and very poor plaque formation. Whenever in doubt, we recorded the result
933 conservatively as an EOP below detection limit (e.g., for phage FriedrichMiescher on *E. coli* 55989,
934 *Enquatrovirus* phages and EmilHeitz on *E. coli* UTI89, and all *Vequentavirinae* on the host expressing the
935 Fun/Z Abi system).

936 **Bacteriophage genome sequencing and assembly**

937 Genomic DNA of bacteriophages was prepared from high-titer stocks using the Norgen Biotek
938 Phage DNA Isolation Kit according to the manufacturer's guidelines and sequenced at the Microbial
939 Genome Sequencing Center (MiGS) using the Illumina NextSeq 550 platform. Trimmed sequencing reads
940 were assembled using the Geneious Assembler implemented in Geneious Prime 2021.0.1 with a coverage
941 of typically 50-100x (S5 Table). Usually, circular contigs (indicating a complete assembly due to the fusion
942 of characteristically repeated sequence at the genome ends [132]) were easily obtained using the "Medium
943 Sensitivity / Fast" setting. Consistently incomplete assemblies or local ambiguities were solved by PCR
944 amplification using the high-fidelity polymerase Phusion (NEB) followed by Sanger Sequencing. For
945 annotation and further analyses, sequences were linearized with the 5' end set either to the first position of

946 the small terminase subunit gene or the first position of the operon containing the small terminase subunit
947 gene.

948 **Bacteriophage genome annotation**

949 A preliminary, automated annotation of the genes in all genomes was generated using MultiPhate
950 [133] and then manually refined. For this purpose, whole-genome alignments of all new isolates within a
951 given group of phages and well-studied and / or well-annotated references were generated using
952 progressiveMauve [134] implemented in Geneious 2021.0.1 and used to inform the annotation based on
953 identified orthologs. *Bona fide* protein-coding genes without clear functional annotation were translated
954 and analyzed using the blastp tool on the NCBI server (<https://blast.ncbi.nlm.nih.gov/Blast.cgi>), the
955 InterPro protein domain signature database [135], as well as the Phyre2 fold recognition server [136;
956 <http://www.sbg.bio.ic.ac.uk/~phyre2/html/page.cgi?id=index>]. tRNA genes were predicted using tRNA-
957 ScanSE in the [137; <http://lowelab.ucsc.edu/tRNAscan-SE/>] and spanins were annotated with help of the
958 SpaninDataBase tool [138]. While endolysin genes were easily recognized by homology to lysozyme-like
959 proteins and other peptidoglycan hydrolases, holins were more difficult to identify when no holins were
960 annotated in closely related bacteriophage genomes. In these cases, we analyzed all small proteins (<250
961 amino acids) for the presence of transmembrane helices – a prerequisite for the functionality of known
962 holins [139] – and studied their possible relationships to previously described holins using blastp and
963 InterPro. In most but not all cases, *bona fide* holins encoded close to endolysin and / or spanin genes could
964 be identified. The annotation of our genomes in a comparative genomics setup made it easily possible to
965 identify the boundaries of introns associated with putative homing endonucleases and to precisely identify
966 inteins (see also S5 Table). The annotated genome sequences of all 66 newly isolated phages as well as
967 T3(K12) have been submitted to the NCBI GenBank database under accession numbers listed in S5 Table.

968 **Bacteriophage naming and taxonomy**

969 Newly isolated bacteriophages were named according to rules and conventions in the field and
970 classified in line with the rules of the International Committee on the Taxonomy of Viruses (ICTV) [79,

971 140] (S5 Table). As a first step of taxonomic classification, phages were roughly sorted by family and genus
972 based on whole-genome blastn searches against the non-redundant nucleotide collection database
973 [<https://blast.ncbi.nlm.nih.gov/Blast.cgi>; see also reference 141]. For each such broad taxonomic group, we
974 selected a set of reference sequences from NCBI GenBank that would cover the diversity of this group and
975 that always included all members which had already previously been studied intensively. Subsequently, we
976 generated whole-genome alignments of these sets of sequences using progressiveMauve implemented in
977 Geneious Prime 2021.0.1 [134]. These alignments or merely regions encoding highly conserved marker
978 genes such as the terminase subunits, portal protein gene, major capsid protein gene, or other suitable loci
979 were then used to generate Maximum-Likelihood phylogenies to unravel the evolutionary relationships
980 between the different bacteriophage isolates and database references (see S2 Text for details). Care was
981 taken to avoid genome regions that are recognizably infested with homing endonucleases or that showed
982 obvious signs of having recently moved by horizontal gene transfer (e.g., an abrupt shift in the local
983 sequence identity to the different other genomes in the alignment). Clusters of phage isolates observed in
984 these phylogenies generally correlated very well with established taxonomy as inferred from NCBI
985 taxonomy (<https://www.ncbi.nlm.nih.gov/taxonomy>), the ICTV [<https://talk.ictvonline.org/taxonomy/>;
986 reference 142], and other reports in the literature [30]. To classify our phage isolates on the species level,
987 we generated pairwise whole-genome alignments using progressiveMauve implemented in Geneious Prime
988 2021.0.1 [134] with genomes of related phages as identified in our phylogenies. From these alignments, the
989 nucleotide sequence identity was determined as the query coverage multiplied by the identity of aligned
990 segments [24]. When the genomes were largely syntenic and showed >95% nucleotide sequence identity,
991 we classified our isolates as the same species as their close relative [141], at least if this phage has been
992 assigned to a species by the ICTV [142].

993 **Sequence alignments and phylogenetic analyses**

994 The NCBI GenBank accession numbers of all previously published genomes used in this study are
995 listed in S6 Table. Sequence alignments of different sets of homologous genes were generated using

996 MAFFT v7.450 implemented in Geneious Prime 2021.0.1 [143]. Whenever required, poor or missing
997 annotations in bacteriophage genomes downloaded from NCBI GenBank were supplemented using the
998 ORF finder tool of Geneious Prime 2021.0.1 guided by orthologous sequence parts of related genomes.
999 Alignments were set up using default settings typically with the fast FFT-NS-2 algorithm and 200PAM/k=2
1000 or BLOSUM62 scoring matrices for nucleotide and amino acid sequences, respectively. Subsequently,
1001 alignments were curated manually to improve poorly aligned sequence stretches and to mask non-
1002 homologous parts.

1003 For phylogenetic analyses, sequence alignments of orthologous stretches from different genomes
1004 (genes, proteins, or whole genome) were used to calculate Maximum-Likelihood phylogenies with PhyML
1005 3.3.20180621 implemented in Geneious Prime 2021.0.1 [144]. Phylogenies were calculated with the
1006 HYK85 substitution model for nucleotide sequences and with the LG substitution model for amino acid
1007 sequences. For the inference of phylogenetic relationships between phage genomes, we sometimes used
1008 curated whole-genome alignments, but the infestation with homing endonucleases and the associated gene
1009 conversion made this approach impossible for all larger genomes. Instead, we typically used curated
1010 sequence alignments of several conserved core genes (on nucleotide or amino acid level, depending on the
1011 distance between the genomes) as the basis for Maximum-Likelihood phylogenies. The detailed procedures
1012 for each phylogeny shown in this article are described in S2 Text.

1013 **LPS structures of enterobacterial strains**

1014 *Escherichia* K-12 MG1655 (serogroup A) codes for a K12-type LPS core and an O16-type O-
1015 antigen, but functional expression of the O-antigen was lost during laboratory adaptation due to inactivation
1016 of *wbbL* by an IS5 insertion so that only a single terminal GlcNAc is attached to the LPS core [44, 72]. *E.*
1017 *coli* strains UTI89 (serogroup B2), CFT073 (serogroup B2), and 55989 (serogroup B1) express O-antigens
1018 of the O18, O6, and O104 types, respectively [122, 123]. Their core LPS types were determined to be R1
1019 (UTI89 and CFT073) and R3 (55989) by BLAST searches with diagnostic marker genes similar to the
1020 PCR-based approach described previously [72]. For the illustration in Fig 12A, the structures of LPS

1021 cores and linked O-antigen polysaccharides were drawn as described in the literature with typical O-antigen
1022 chain lengths of 15 - 25 repeat units [72, 103, 145]. For the O18-type of O-antigen polysaccharides, different
1023 subtypes with slight differences in the repeat unit have been described [103], but to the best of our
1024 knowledge it has remained elusive which subtype is expressed by *E. coli* UTI89. In Fig 12A we therefore
1025 chose an O18A type as exemplary O-antigen polysaccharide for *E. coli* UTI89. Similar to the laboratory
1026 adaptation of *E. coli* K-12 MG1655, strains of the *E. coli* B lineage like *E. coli* B REL606 lack O-antigen
1027 expression due to an IS1 insertion in *wbbD* but have an additional truncation in their R1-type LPS core due
1028 to a second IS1 insertion in *waaT* that leaves only two glucoses in the outer core (Fig 12A) [67, 99].
1029 *Salmonella enterica* subsp. *enterica* serovar Typhimurium strains 12023s (also known as ATCC 14028)
1030 and SL1344 share the common *S. Typhimurium* LPS core and *Salmonella* serogroup B / O4 O-antigen [42,
1031 146] (Fig 12A).

1032 **Bacterial genome sequencing and analyses to identify host receptors**

1033 While top agar assays with *E. coli* mutants carrying defined deletions in genes coding for different
1034 surface proteins or genes involved in the LPS core biosynthesis readily identified the host receptor of most
1035 bacteriophages (see above), few small siphoviruses of the *Drexlerviridae* family and the *Dhillonvirus*,
1036 *Nonagvirus*, and *Seuratvirus* genera of the *Siphoviridae* family could not be assigned to any surface protein
1037 as secondary receptor. This was the case for phages AugustePiccard (Bas01) and JeanPiccard (Bas02) of
1038 *Drexlerviridae*, TheodorHerzl (Bas14) and Oekolampad (Bas18) of *Dhillonvirus*, ChristophMerian (Bas19)
1039 and FritzHoffmann (Bas20) of *Nonagvirus*, and VogelGryff (Bas25) of *Seuratvirus*. However, as
1040 siphoviruses infecting Gram-negative bacteria it seemed highly likely that these phages would use an outer
1041 membrane porin as their secondary receptor [40]. We therefore isolated resistant mutants of *E. coli* K-12
1042 BW25113 by plating bacteria on LB agar plates which had been densely covered with high-titer lysates of
1043 each of these bacteriophages. While verifying that the resistance of isolated bacterial clones was specific to
1044 the phage on which they had been isolated, we found that many clones were fully resistant specifically but

1045 without exception to all these small siphoviruses with yet no known host receptor, suggesting that they all
1046 targeted the same receptor.

1047 For multiple of these phage-resistant clones, genomic DNA was prepared using the GenElute
1048 Bacterial Genomic DNA Kit (Sigma-Aldrich) according to the manufacturer's guidelines and sequenced at
1049 the Microbial Genome Sequencing Center (MiGS) using the Illumina NextSeq 550 platform. Sequencing
1050 reads were assembled to the *E. coli* K-12 MG1655 reference genome (NCBI GenBank accession
1051 U000096.3) using Geneious Prime 2021.0.1 with a coverage of typically 100-200x to identify the mutations
1052 underlying their phage resistance. These analyses uncovered a diversity of in-frame deletions in *lptD* for
1053 the different mutant clones (Fig 5).

1054 **Quantification and statistical analysis**

1055 Quantitative data sets were analyzed by calculating mean and standard deviation of at least three
1056 independent biological replicates for each experiment. Detailed information about replicates and statistical
1057 analyses for each experiment is provided in the figure legends.

1058 **Acknowledgments**

1059 The authors are grateful to Prof. Urs Jenal, Prof. Marek Basler, Prof. Martin Loessner, and Dr. Julie
1060 Sollier for valuable input and critical reading of the manuscript. Dr. Christian Beisel is acknowledged for
1061 advice regarding DNA sequencing. The authors are deeply indebted to Prof. Urs Jenal and Prof. Christoph
1062 Dehio for sharing multiple different *E. coli* strains and plasmids (S1 and S3 Tables). Furthermore, the
1063 authors thank high school students participating in the Biozentrum Summer Science Academy 2019, Julia
1064 Harms, and Dr. Thomas Schubert for assistance with the isolation of multiple bacteriophages described in
1065 this study (S5 Table). *Salmonella* Typhimurium strains 12023s and SL1344 were obtained from Prof. Dirk
1066 Bumann and Prof. Mederic Diard, respectively, while *E. coli* B REL606 was obtained from Dr. Jenna
1067 Gallie. Phage P2_{vir} was generously shared by Dr. Nicolas Wenner and Prof. Jay Hinton. The Coli Genetic

1068 Stock Center (CGSC) and the Deutsche Sammlung von Mikroorganismen und Zellkulturen (DSMZ) are
1069 acknowledged for sharing different strains of *E. coli* or different bacteriophages, respectively (S1 and S5
1070 Tables). The authors are grateful to ARA Basel, ARA Canius (Lenzerheide), and ARA Limeco (Dietikon)
1071 for providing samples of sewage plant inflow and to Universitätsspital Basel for hospital sewage.

1072 **References**

- 1073 1. Mahmoudabadi G, Phillips R. A comprehensive and quantitative exploration of thousands of viral
1074 genomes. *Elife*. 2018;7. doi: 10.7554/eLife.31955. PubMed PMID: 29624169; PubMed Central PMCID:
1075 PMCPMC5908442.
- 1076 2. Dion MB, Oechslin F, Moineau S. Phage diversity, genomics and phylogeny. *Nat Rev Microbiol*.
1077 2020;18(3):125-38. Epub 2020/02/06. doi: 10.1038/s41579-019-0311-5. PubMed PMID: 32015529.
- 1078 3. Cobian Güemes AG, Youle M, Cantu VA, Felts B, Nulton J, Rohwer F. Viruses as Winners in the
1079 Game of Life. *Annu Rev Virol*. 2016;3(1):197-214. Epub 2016/10/16. doi: 10.1146/annurev-virology-
1080 100114-054952. PubMed PMID: 27741409.
- 1081 4. Keen EC. A century of phage research: bacteriophages and the shaping of modern biology.
1082 *Bioessays*. 2015;37(1):6-9. doi: 10.1002/bies.201400152. PubMed PMID: 25521633; PubMed Central
1083 PMCID: PMCPMC4418462.
- 1084 5. Demerec M, Fano U. Bacteriophage-Resistant Mutants in *Escherichia Coli*. *Genetics*.
1085 1945;30(2):119-36. Epub 1945/03/01. PubMed PMID: 17247150; PubMed Central PMCID:
1086 PMCPMC1209279.
- 1087 6. Abedon ST. The murky origin of Snow White and her T-even dwarfs. *Genetics*. 2000;155(2):481-6.
1088 Epub 2000/06/03. PubMed PMID: 10835374; PubMed Central PMCID: PMCPMC1461100.
- 1089 7. Casjens SR, Hendrix RW. Bacteriophage lambda: Early pioneer and still relevant. *Virology*.
1090 2015;479-480:310-30. doi: 10.1016/j.virol.2015.02.010. PubMed PMID: 25742714; PubMed Central
1091 PMCID: PMCPMC4424060.
- 1092 8. Howard-Varona C, Hargreaves KR, Abedon ST, Sullivan MB. Lysogeny in nature: mechanisms,
1093 impact and ecology of temperate phages. *ISME J*. 2017;11(7):1511-20. doi: 10.1038/ismej.2017.16.
1094 PubMed PMID: 28291233; PubMed Central PMCID: PMCPMC5520141.
- 1095 9. Hampton HG, Watson BNJ, Fineran PC. The arms race between bacteria and their phage foes.
1096 *Nature*. 2020;577(7790):327-36. Epub 2020/01/17. doi: 10.1038/s41586-019-1894-8. PubMed PMID:
1097 31942051.
- 1098 10. Dy RL, Richter C, Salmond GP, Fineran PC. Remarkable Mechanisms in Microbes to Resist Phage
1099 Infections. *Annu Rev Virol*. 2014;1(1):307-31. doi: 10.1146/annurev-virology-031413-085500. PubMed
1100 PMID: 26958724.
- 1101 11. Bernheim A, Sorek R. The pan-immune system of bacteria: antiviral defence as a community
1102 resource. *Nat Rev Microbiol*. 2020;18(2):113-9. Epub 2019/11/07. doi: 10.1038/s41579-019-0278-2.
1103 PubMed PMID: 31695182.
- 1104 12. Lopatina A, Tal N, Sorek R. Abortive Infection: Bacterial Suicide as an Antiviral Immune Strategy.
1105 *Annu Rev Virol*. 2020;7(1):371-84. Epub 2020/06/20. doi: 10.1146/annurev-virology-011620-040628.
1106 PubMed PMID: 32559405.

- 1107 13. Schmidt C. Phage therapy's latest makeover. *Nat Biotechnol.* 2019;37(6):581-6. Epub 2019/05/10.
1108 doi: 10.1038/s41587-019-0133-z. PubMed PMID: 31068679.
- 1109 14. Kilcher S, Loessner MJ. Engineering Bacteriophages as Versatile Biologics. *Trends Microbiol.*
1110 2019;27(4):355-67. Epub 2018/10/17. doi: 10.1016/j.tim.2018.09.006. PubMed PMID: 30322741.
- 1111 15. Millard A. Phage Genomes - Dec2020 2020 [16.02.2021]. Available from:
1112 <http://millardlab.org/bioinformatics/bacteriophage-genomes/phage-genomes-dec2020/>.
- 1113 16. Hyman P. Phages for Phage Therapy: Isolation, Characterization, and Host Range Breadth.
1114 Pharmaceuticals (Basel). 2019;12(1). Epub 2019/03/14. doi: 10.3390/ph12010035. PubMed PMID:
1115 30862020; PubMed Central PMCID: PMC6469166.
- 1116 17. Gordillo Altamirano FL, Barr JJ. Phage Therapy in the Postantibiotic Era. *Clin Microbiol Rev.*
1117 2019;32(2). Epub 2019/01/18. doi: 10.1128/CMR.00066-18. PubMed PMID: 30651225; PubMed Central
1118 PMCID: PMC6431132.
- 1119 18. Kortright KE, Chan BK, Koff JL, Turner PE. Phage Therapy: A Renewed Approach to Combat
1120 Antibiotic-Resistant Bacteria. *Cell Host Microbe.* 2019;25(2):219-32. Epub 2019/02/15. doi:
1121 10.1016/j.chom.2019.01.014. PubMed PMID: 30763536.
- 1122 19. Aslam S, Lampley E, Wooten D, Karris M, Benson C, Strathdee S, et al. Lessons Learned From the
1123 First 10 Consecutive Cases of Intravenous Bacteriophage Therapy to Treat Multidrug-Resistant Bacterial
1124 Infections at a Single Center in the United States. *Open Forum Infect Dis.* 2020;7(9):ofaa389. Epub
1125 2020/10/03. doi: 10.1093/ofid/ofaa389. PubMed PMID: 33005701; PubMed Central PMCID:
1126 PMC67519779.
- 1127 20. Pires DP, Costa AR, Pinto G, Meneses L, Azeredo J. Current challenges and future opportunities of
1128 phage therapy. *FEMS Microbiol Rev.* 2020;44(6):684-700. Epub 2020/05/31. doi:
1129 10.1093/femsre/fuaa017. PubMed PMID: 32472938.
- 1130 21. Ochman H, Selander RK. Standard reference strains of *Escherichia coli* from natural populations.
1131 *J Bacteriol.* 1984;157(2):690-3. PubMed PMID: 6363394; PubMed Central PMCID: PMC6215307.
- 1132 22. Tenaillon O, Skurnik D, Picard B, Denamur E. The population genetics of commensal *Escherichia*
1133 *coli*. *Nat Rev Microbiol.* 2010;8(3):207-17. doi: 10.1038/nrmicro2298. PubMed PMID: 20157339.
- 1134 23. Korf IHE, Meier-Kolthoff JP, Adriaenssens EM, Kropinski AM, Nimtz M, Rohde M, et al. Still
1135 Something to Discover: Novel Insights into *Escherichia coli* Phage Diversity and Taxonomy. *Viruses.*
1136 2019;11(5). doi: 10.3390/v11050454. PubMed PMID: 31109012; PubMed Central PMCID:
1137 PMC6563267.
- 1138 24. Olsen NS, Forero-Junco L, Kot W, Hansen LH. Exploring the Remarkable Diversity of Culturable
1139 *Escherichia coli* Phages in the Danish Wastewater Environment. *Viruses.* 2020;12(9). Epub 2020/09/10.
1140 doi: 10.3390/v12090986. PubMed PMID: 32899836; PubMed Central PMCID: PMC67552041.
- 1141 25. Mathieu A, Dion M, Deng L, Tremblay D, Moncaut E, Shah SA, et al. Virulent coliphages in 1-year-
1142 old children fecal samples are fewer, but more infectious than temperate coliphages. *Nat Commun.*
1143 2020;11(1):378. Epub 2020/01/19. doi: 10.1038/s41467-019-14042-z. PubMed PMID: 31953385; PubMed
1144 Central PMCID: PMC6969025.
- 1145 26. Sørensen PE, Van Den Broeck W, Kiil K, Jasinskyte D, Moodley A, Garmyn A, et al. New insights
1146 into the biodiversity of coliphages in the intestine of poultry. *Sci Rep.* 2020;10(1):15220. Epub 2020/09/18.
1147 doi: 10.1038/s41598-020-72177-2. PubMed PMID: 32939020; PubMed Central PMCID:
1148 PMC67494930.
- 1149 27. Michniewski S, Redgwell T, Grigonyte A, Rihtman B, Aguilo-Ferretjans M, Christie-Oleza J, et al.
1150 Riding the wave of genomics to investigate aquatic coliphage diversity and activity. *Environ Microbiol.*
1151 2019;21(6):2112-28. Epub 2019/03/19. doi: 10.1111/1462-2920.14590. PubMed PMID: 30884081;
1152 PubMed Central PMCID: PMC6563131.

- 1153 28. Smith R, O'Hara M, Hobman JL, Millard AD. Draft Genome Sequences of 14 *Escherichia coli* Phages
1154 Isolated from Cattle Slurry. *Genome Announc.* 2015;3(6). Epub 2016/01/02. doi:
1155 10.1128/genomeA.01364-15. PubMed PMID: 26722010; PubMed Central PMCID: PMC698387.
- 1156 29. Pacifico C, Hilbert M, Sofka D, Dinhopf N, Pap IJ, Aspöck C, et al. Natural Occurrence of *Escherichia*
1157 *coli*-Infecting Bacteriophages in Clinical Samples. *Front Microbiol.* 2019;10:2484. Epub 2019/11/19. doi:
1158 10.3389/fmicb.2019.02484. PubMed PMID: 31736918; PubMed Central PMCID: PMC6834657.
- 1159 30. Grose JH, Casjens SR. Understanding the enormous diversity of bacteriophages: the tailed phages
1160 that infect the bacterial family *Enterobacteriaceae*. *Virology.* 2014;468-470:421-43. Epub 2014/09/23. doi:
1161 10.1016/j.virol.2014.08.024. PubMed PMID: 25240328; PubMed Central PMCID: PMC4301999.
- 1162 31. Olsen NS, Hendriksen NB, Hansen LH, Kot W. A New High-Throughput Screening Method for
1163 Phages: Enabling Crude Isolation and Fast Identification of Diverse Phages with Therapeutic Potential.
1164 *PHAGE.* 2020;1(3):137-48. doi: 10.1089/phage.2020.0016.
- 1165 32. Drexler H. Bacteriophage T1. In: Calendar R, editor. *The Bacteriophages*. Boston, MA: Springer US;
1166 1988. p. 235-58.
- 1167 33. Wittmann J, Turner D, Millard AD, Mahadevan P, Kropinski AM, Adriaenssens EM. From Orphan
1168 Phage to a Proposed New Family-the Diversity of N4-Like Viruses. *Antibiotics (Basel).* 2020;9(10). Epub
1169 2020/10/04. doi: 10.3390/antibiotics9100663. PubMed PMID: 33008130; PubMed Central PMCID:
1170 PMC67650795.
- 1171 34. Bertani G. Lysogeny at mid-twentieth century: P1, P2, and other experimental systems. *J Bacteriol.*
1172 2004;186(3):595-600. Epub 2004/01/20. doi: 10.1128/jb.186.3.595-600.2004. PubMed PMID: 14729683;
1173 PubMed Central PMCID: PMC321500.
- 1174 35. Nobrega FL, Vlot M, de Jonge PA, Dreesens LL, Beaumont HJE, Lavigne R, et al. Targeting
1175 mechanisms of tailed bacteriophages. *Nat Rev Microbiol.* 2018;16(12):760-73. Epub 2018/08/15. doi:
1176 10.1038/s41579-018-0070-8. PubMed PMID: 30104690.
- 1177 36. Henderson JC, Zimmerman SM, Crofts AA, Boll JM, Kuhns LG, Herrera CM, et al. The Power of
1178 Asymmetry: Architecture and Assembly of the Gram-Negative Outer Membrane Lipid Bilayer. *Annu Rev*
1179 *Microbiol.* 2016;70:255-78. Epub 2016/07/01. doi: 10.1146/annurev-micro-102215-095308. PubMed
1180 PMID: 27359214.
- 1181 37. Letarov AV, Kulikov EE. Adsorption of Bacteriophages on Bacterial Cells. *Biochemistry (Mosc).*
1182 2017;82(13):1632-58. Epub 2018/03/11. doi: 10.1134/S0006297917130053. PubMed PMID: 29523063.
- 1183 38. Broecker NK, Barbirz S. Not a barrier but a key: How bacteriophages exploit host's O-antigen as an
1184 essential receptor to initiate infection. *Mol Microbiol.* 2017;105(3):353-7. Epub 2017/06/16. doi:
1185 10.1111/mmi.13729. PubMed PMID: 28618013.
- 1186 39. Bertozzi Silva J, Storms Z, Sauvageau D. Host receptors for bacteriophage adsorption. *FEMS*
1187 *Microbiol Lett.* 2016;363(4). Epub 2016/01/13. doi: 10.1093/femsle/fnw002. PubMed PMID: 26755501.
- 1188 40. Hantke K. Compilation of *Escherichia coli* K-12 outer membrane phage receptors - their function
1189 and some historical remarks. *FEMS Microbiol Lett.* 2020;367(2). Epub 2020/02/06. doi:
1190 10.1093/femsle/fnaa013. PubMed PMID: 32009155.
- 1191 41. Gordillo Altamirano FL, Barr JJ. Unlocking the next generation of phage therapy: the key is in the
1192 receptors. *Curr Opin Biotechnol.* 2020;68:115-23. Epub 2020/11/18. doi: 10.1016/j.copbio.2020.10.002.
1193 PubMed PMID: 33202354.
- 1194 42. Bertani B, Ruiz N. Function and Biogenesis of Lipopolysaccharides. *EcoSal Plus.* 2018;8(1). Epub
1195 2018/08/02. doi: 10.1128/ecosalplus.ESP-0001-2018. PubMed PMID: 30066669; PubMed Central PMCID:
1196 PMC6091223.
- 1197 43. Rai AK, Mitchell AM. Enterobacterial Common Antigen: Synthesis and Function of an Enigmatic
1198 Molecule. *mBio.* 2020;11(4). Epub 2020/08/14. doi: 10.1128/mBio.01914-20. PubMed PMID: 32788387;
1199 PubMed Central PMCID: PMC67439462.

- 1200 44. Liu D, Reeves PR. *Escherichia coli* K12 regains its O antigen. *Microbiology*. 1994;140 (Pt 1):49-57.
1201 doi: 10.1099/13500872-140-1-49. PubMed PMID: 7512872.
- 1202 45. Hutinet G, Kot W, Cui L, Hillebrand R, Balamkundu S, Gnanakalai S, et al. 7-Deazaguanine
1203 modifications protect phage DNA from host restriction systems. *Nat Commun*. 2019;10(1):5442. Epub
1204 2019/12/01. doi: 10.1038/s41467-019-13384-y. PubMed PMID: 31784519; PubMed Central PMCID:
1205 PMCPMC6884629.
- 1206 46. Weigele P, Raleigh EA. Biosynthesis and Function of Modified Bases in Bacteria and Their Viruses.
1207 *Chem Rev*. 2016;116(20):12655-87. Epub 2016/06/21. doi: 10.1021/acs.chemrev.6b00114. PubMed
1208 PMID: 27319741.
- 1209 47. Loenen WA, Dryden DT, Raleigh EA, Wilson GG. Type I restriction enzymes and their relatives.
1210 *Nucleic Acids Res*. 2014;42(1):20-44. Epub 2013/09/27. doi: 10.1093/nar/gkt847. PubMed PMID:
1211 24068554; PubMed Central PMCID: PMCPMC3874165.
- 1212 48. Pingoud A, Wilson GG, Wende W. Type II restriction endonucleases--a historical perspective and
1213 more. *Nucleic Acids Res*. 2014;42(12):7489-527. Epub 2014/06/01. doi: 10.1093/nar/gku447. PubMed
1214 PMID: 24878924; PubMed Central PMCID: PMCPMC4081073.
- 1215 49. Rao DN, Dryden DT, Bheemanaik S. Type III restriction-modification enzymes: a historical
1216 perspective. *Nucleic Acids Res*. 2014;42(1):45-55. Epub 2013/07/19. doi: 10.1093/nar/gkt616. PubMed
1217 PMID: 23863841; PubMed Central PMCID: PMCPMC3874151.
- 1218 50. Christie GE, Calendar R. Bacteriophage P2. *Bacteriophage*. 2016;6(1):e1145782. Epub
1219 2016/05/05. doi: 10.1080/21597081.2016.1145782. PubMed PMID: 27144088; PubMed Central PMCID:
1220 PMCPMC4836473.
- 1221 51. Goulet A, Spinelli S, Mahony J, Cambillau C. Conserved and Diverse Traits of Adhesion Devices
1222 from *Siphoviridae* Recognizing Proteinaceous or Saccharidic Receptors. *Viruses*. 2020;12(5). Epub
1223 2020/05/10. doi: 10.3390/v12050512. PubMed PMID: 32384698; PubMed Central PMCID:
1224 PMCPMC7291167.
- 1225 52. Piya D, Lessor L, Koehler B, Stonecipher A, Cahill J, Gill JJ. Genome-wide screens reveal *Escherichia*
1226 *coli* genes required for growth of T1-like phage LL5 and V5-like phage LL12. *Sci Rep*. 2020;10(1):8058. Epub
1227 2020/05/18. doi: 10.1038/s41598-020-64981-7. PubMed PMID: 32415154; PubMed Central PMCID:
1228 PMCPMC7229145.
- 1229 53. Li P, Lin H, Mi Z, Xing S, Tong Y, Wang J. Screening of Polyvalent Phage-Resistant *Escherichia coli*
1230 Strains Based on Phage Receptor Analysis. *Front Microbiol*. 2019;10:850. Epub 2019/05/21. doi:
1231 10.3389/fmicb.2019.00850. PubMed PMID: 31105661; PubMed Central PMCID: PMCPMC6499177.
- 1232 54. Wietzorrek A, Schwarz H, Herrmann C, Braun V. The genome of the novel phage Rtp, with a
1233 rosette-like tail tip, is homologous to the genome of phage T1. *J Bacteriol*. 2006;188(4):1419-36. Epub
1234 2006/02/03. doi: 10.1128/JB.188.4.1419-1436.2006. PubMed PMID: 16452425; PubMed Central PMCID:
1235 PMCPMC1367250.
- 1236 55. Hamdi S, Rousseau GM, Labrie SJ, Tremblay DM, Kourda RS, Ben Slama K, et al. Characterization
1237 of two polyvalent phages infecting *Enterobacteriaceae*. *Sci Rep*. 2017;7:40349. Epub 2017/01/17. doi:
1238 10.1038/srep40349. PubMed PMID: 28091598; PubMed Central PMCID: PMCPMC5238451.
- 1239 56. Wang J, Hofnung M, Charbit A. The C-terminal portion of the tail fiber protein of bacteriophage
1240 lambda is responsible for binding to LamB, its receptor at the surface of *Escherichia coli* K-12. *J Bacteriol*.
1241 2000;182(2):508-12. Epub 2000/01/12. doi: 10.1128/jb.182.2.508-512.2000. PubMed PMID: 10629200;
1242 PubMed Central PMCID: PMCPMC94303.
- 1243 57. Meyer JR, Dobias DT, Weitz JS, Barrick JE, Quick RT, Lenski RE. Repeatability and contingency in
1244 the evolution of a key innovation in phage lambda. *Science*. 2012;335(6067):428-32. Epub 2012/01/28.
1245 doi: 10.1126/science.1214449. PubMed PMID: 22282803; PubMed Central PMCID: PMCPMC3306806.

- 1246 58. Dunne M, Rupf B, Tala M, Qabrati X, Ernst P, Shen Y, et al. Reprogramming Bacteriophage Host
1247 Range through Structure-Guided Design of Chimeric Receptor Binding Proteins. *Cell Rep.* 2019;29(5):1336-
1248 50 e4. Epub 2019/10/31. doi: 10.1016/j.celrep.2019.09.062. PubMed PMID: 31665644.
- 1249 59. Sazinas P, Redgwell T, Rihtman B, Grigonyte A, Michniewski S, Scanlan DJ, et al. Comparative
1250 Genomics of Bacteriophage of the Genus *Seuratvirus*. *Genome Biol Evol.* 2018;10(1):72-6. Epub
1251 2017/12/23. doi: 10.1093/gbe/evx275. PubMed PMID: 29272407; PubMed Central PMCID:
1252 PMC5758909.
- 1253 60. Golomidova AK, Kulikov EE, Prokhorov NS, Guerrero-Ferreira Rcapital Es C, Knirel YA, Kostryukova
1254 ES, et al. Branched Lateral Tail Fiber Organization in T5-Like Bacteriophages DT57C and DT571/2 is
1255 Revealed by Genetic and Functional Analysis. *Viruses.* 2016;8(1). Epub 2016/01/26. doi:
1256 10.3390/v8010026. PubMed PMID: 26805872; PubMed Central PMCID: PMC4728585.
- 1257 61. Hong J, Kim KP, Heu S, Lee SJ, Adhya S, Ryu S. Identification of host receptor and receptor-binding
1258 module of a newly sequenced T5-like phage EPS7. *FEMS Microbiol Lett.* 2008;289(2):202-9. Epub
1259 2008/11/26. doi: 10.1111/j.1574-6968.2008.01397.x. PubMed PMID: 19025561.
- 1260 62. Gencay YE, Gambino M, Prussing TF, Brondsted L. The genera of bacteriophages and their
1261 receptors are the major determinants of host range. *Environ Microbiol.* 2019;21(6):2095-111. Epub
1262 2019/03/20. doi: 10.1111/1462-2920.14597. PubMed PMID: 30888719.
- 1263 63. Rabsch W, Ma L, Wiley G, Najar FZ, Kaserer W, Schuerch DW, et al. FepA- and TonB-dependent
1264 bacteriophage H8: receptor binding and genomic sequence. *J Bacteriol.* 2007;189(15):5658-74. Epub
1265 2007/05/29. doi: 10.1128/JB.00437-07. PubMed PMID: 17526714; PubMed Central PMCID:
1266 PMC1951831.
- 1267 64. Davison J. Pre-early functions of bacteriophage T5 and its relatives. *Bacteriophage.*
1268 2015;5(4):e1086500. Epub 2016/02/24. doi: 10.1080/21597081.2015.1086500. PubMed PMID:
1269 26904381; PubMed Central PMCID: PMC4743489.
- 1270 65. Rusinov IS, Ershova AS, Karyagina AS, Spirin SA, Alexeevski AV. Avoidance of recognition sites of
1271 restriction-modification systems is a widespread but not universal anti-restriction strategy of prokaryotic
1272 viruses. *BMC Genomics.* 2018;19(1):885. Epub 2018/12/12. doi: 10.1186/s12864-018-5324-3. PubMed
1273 PMID: 30526500; PubMed Central PMCID: PMC6286503.
- 1274 66. Trojet SN, Caumont-Sarcos A, Perrody E, Comeau AM, Krisch HM. The gp38 adhesins of the T4
1275 superfamily: a complex modular determinant of the phage's host specificity. *Genome Biol Evol.*
1276 2011;3:674-86. Epub 2011/07/13. doi: 10.1093/gbe/evr059. PubMed PMID: 21746838; PubMed Central
1277 PMCID: PMC3157838.
- 1278 67. Washizaki A, Yonesaki T, Otsuka Y. Characterization of the interactions between *Escherichia coli*
1279 receptors, LPS and OmpC, and bacteriophage T4 long tail fibers. *Microbiologyopen.* 2016;5(6):1003-15.
1280 Epub 2016/06/09. doi: 10.1002/mbo3.384. PubMed PMID: 27273222; PubMed Central PMCID:
1281 PMC5221442.
- 1282 68. Hu B, Margolin W, Molineux IJ, Liu J. Structural remodeling of bacteriophage T4 and host
1283 membranes during infection initiation. *Proc Natl Acad Sci U S A.* 2015;112(35):E4919-28. Epub
1284 2015/08/19. doi: 10.1073/pnas.1501064112. PubMed PMID: 26283379; PubMed Central PMCID:
1285 PMC4568249.
- 1286 69. Thomas JA, Orwenyo J, Wang LX, Black LW. The Odd "RB" Phage-Identification of Arabinosylation
1287 as a New Epigenetic Modification of DNA in T4-Like Phage RB69. *Viruses.* 2018;10(6). Epub 2018/06/13.
1288 doi: 10.3390/v10060313. PubMed PMID: 29890699; PubMed Central PMCID: PMC6024577.
- 1289 70. Kropinski AM, Waddell T, Meng J, Franklin K, Ackermann HW, Ahmed R, et al. The host-range,
1290 genomics and proteomics of *Escherichia coli* O157:H7 bacteriophage rV5. *Virology.* 2013;10:76. Epub
1291 2013/03/19. doi: 10.1186/1743-422X-10-76. PubMed PMID: 23497209; PubMed Central PMCID:
1292 PMC3606486.

- 1293 71. Schwarzer D, Buettner FF, Browning C, Nazarov S, Rabsch W, Bethe A, et al. A multivalent
1294 adsorption apparatus explains the broad host range of phage phi92: a comprehensive genomic and
1295 structural analysis. *J Virol.* 2012;86(19):10384-98. Epub 2012/07/13. doi: 10.1128/JVI.00801-12. PubMed
1296 PMID: 22787233; PubMed Central PMCID: PMCPMC3457257.
- 1297 72. Amor K, Heinrichs DE, Fridrich E, Ziebell K, Johnson RP, Whitfield C. Distribution of core
1298 oligosaccharide types in lipopolysaccharides from *Escherichia coli*. *Infect Immun.* 2000;68(3):1116-24.
1299 Epub 2000/02/26. doi: 10.1128/iai.68.3.1116-1124.2000. PubMed PMID: 10678915; PubMed Central
1300 PMCID: PMCPMC97256.
- 1301 73. Mutalik VK, Adler BA, Rishi HS, Piya D, Zhong C, Koskella B, et al. High-throughput mapping of the
1302 phage resistance landscape in *E. coli*. *PLoS Biol.* 2020;18(10):e3000877. Epub 2020/10/14. doi:
1303 10.1371/journal.pbio.3000877. PubMed PMID: 33048924; PubMed Central PMCID: PMCPMC7553319
1304 following competing interests: VKM, AMD, and APA consult for and hold equity in Felix Biotechnology,
1305 Inc.
- 1306 74. Qimron U, Marintcheva B, Tabor S, Richardson CC. Genomewide screens for *Escherichia coli* genes
1307 affecting growth of T7 bacteriophage. *Proc Natl Acad Sci U S A.* 2006;103(50):19039-44. Epub 2006/12/01.
1308 doi: 10.1073/pnas.0609428103. PubMed PMID: 17135349; PubMed Central PMCID: PMCPMC1748173.
- 1309 75. Gonzalez-Garcia VA, Pulido-Cid M, Garcia-Doval C, Bocanegra R, van Raaij MJ, Martin-Benito J, et
1310 al. Conformational changes leading to T7 DNA delivery upon interaction with the bacterial receptor. *J Biol*
1311 *Chem.* 2015;290(16):10038-44. Epub 2015/02/24. doi: 10.1074/jbc.M114.614222. PubMed PMID:
1312 25697363; PubMed Central PMCID: PMCPMC4400320.
- 1313 76. Cuervo A, Fabrega-Ferrer M, Machon C, Conesa JJ, Fernandez FJ, Perez-Luque R, et al. Structures
1314 of T7 bacteriophage portal and tail suggest a viral DNA retention and ejection mechanism. *Nat Commun.*
1315 2019;10(1):3746. Epub 2019/08/23. doi: 10.1038/s41467-019-11705-9. PubMed PMID: 31431626;
1316 PubMed Central PMCID: PMCPMC6702177.
- 1317 77. Hu B, Margolin W, Molineux IJ, Liu J. The bacteriophage t7 virion undergoes extensive structural
1318 remodeling during infection. *Science.* 2013;339(6119):576-9. Epub 2013/01/12. doi:
1319 10.1126/science.1231887. PubMed PMID: 23306440; PubMed Central PMCID: PMCPMC3873743.
- 1320 78. Scholl D, Merrill C. The genome of bacteriophage K1F, a T7-like phage that has acquired the ability
1321 to replicate on K1 strains of *Escherichia coli*. *J Bacteriol.* 2005;187(24):8499-503. Epub 2005/12/03. doi:
1322 10.1128/JB.187.24.8499-8503.2005. PubMed PMID: 16321955; PubMed Central PMCID:
1323 PMCPMC1317022.
- 1324 79. Adriaenssens EM, Sullivan MB, Knezevic P, van Zyl LJ, Sarkar BL, Dutilh BE, et al. Taxonomy of
1325 prokaryotic viruses: 2018-2019 update from the ICTV Bacterial and Archaeal Viruses Subcommittee. *Arch*
1326 *Virol.* 2020;165(5):1253-60. Epub 2020/03/13. doi: 10.1007/s00705-020-04577-8. PubMed PMID:
1327 32162068.
- 1328 80. Ando H, Lemire S, Pires DP, Lu TK. Engineering Modular Viral Scaffolds for Targeted Bacterial
1329 Population Editing. *Cell Syst.* 2015;1(3):187-96. Epub 2016/03/15. doi: 10.1016/j.cels.2015.08.013.
1330 PubMed PMID: 26973885; PubMed Central PMCID: PMCPMC4785837.
- 1331 81. Studier FW, Movva NR. SAMase gene of bacteriophage T3 is responsible for overcoming host
1332 restriction. *J Virol.* 1976;19(1):136-45. Epub 1976/07/01. doi: 10.1128/JVI.19.1.136-145.1976. PubMed
1333 PMID: 781304; PubMed Central PMCID: PMCPMC354840.
- 1334 82. Bandyopadhyay PK, Studier FW, Hamilton DL, Yuan R. Inhibition of the type I restriction-
1335 modification enzymes EcoB and EcoK by the gene 0.3 protein of bacteriophage T7. *J Mol Biol.*
1336 1985;182(4):567-78. Epub 1985/04/20. doi: 10.1016/0022-2836(85)90242-6. PubMed PMID: 2989534.
- 1337 83. Schmitt CK, Molineux IJ. Expression of gene 1.2 and gene 10 of bacteriophage T7 is lethal to F
1338 plasmid-containing *Escherichia coli*. *J Bacteriol.* 1991;173(4):1536-43. Epub 1991/02/01. doi:
1339 10.1128/jb.173.4.1536-1543.1991. PubMed PMID: 1995595; PubMed Central PMCID: PMCPMC207293.

- 1340 84. Molineux IJ, Spence JL. Virus-plasmid interactions: mutants of bacteriophage T3 that abortively
1341 infect plasmid F-containing (F+) strains of *Escherichia coli*. Proc Natl Acad Sci U S A. 1984;81(5):1465-9.
1342 Epub 1984/03/01. doi: 10.1073/pnas.81.5.1465. PubMed PMID: 6324192; PubMed Central PMCID:
1343 PMCPMC344857.
- 1344 85. Kiino DR, Rothman-Denes LB. Genetic analysis of bacteriophage N4 adsorption. J Bacteriol.
1345 1989;171(9):4595-602. Epub 1989/09/01. doi: 10.1128/jb.171.9.4595-4602.1989. PubMed PMID:
1346 2670887; PubMed Central PMCID: PMCPMC210256.
- 1347 86. Kiino DR, Licudine R, Wilt K, Yang DH, Rothman-Denes LB. A cytoplasmic protein, NfrC, is required
1348 for bacteriophage N4 adsorption. J Bacteriol. 1993;175(21):7074-80. Epub 1993/11/01. doi:
1349 10.1128/jb.175.21.7074-7080.1993. PubMed PMID: 8226648; PubMed Central PMCID: PMCPMC206835.
- 1350 87. Prokhorov NS, Riccio C, Zdorovenko EL, Shneider MM, Browning C, Knirel YA, et al. Function of
1351 bacteriophage G7C esterase tailspike in host cell adsorption. Mol Microbiol. 2017;105(3):385-98. Epub
1352 2017/05/18. doi: 10.1111/mmi.13710. PubMed PMID: 28513100.
- 1353 88. McPartland J, Rothman-Denes LB. The tail sheath of bacteriophage N4 interacts with the
1354 *Escherichia coli* receptor. J Bacteriol. 2009;191(2):525-32. Epub 2008/11/18. doi: 10.1128/JB.01423-08.
1355 PubMed PMID: 19011026; PubMed Central PMCID: PMCPMC2620810.
- 1356 89. Shinedling S, Parma D, Gold L. Wild-type bacteriophage T4 is restricted by the lambda rex genes.
1357 J Virol. 1987;61(12):3790-4. Epub 1987/12/01. doi: 10.1128/JVI.61.12.3790-3794.1987. PubMed PMID:
1358 2960831; PubMed Central PMCID: PMCPMC255994.
- 1359 90. Whichard JM, Weigt LA, Borris DJ, Li LL, Zhang Q, Kapur V, et al. Complete genomic sequence of
1360 bacteriophage felix o1. Viruses. 2010;2(3):710-30. Epub 2010/03/01. doi: 10.3390/v2030710. PubMed
1361 PMID: 21994654; PubMed Central PMCID: PMCPMC3185647.
- 1362 91. Kaczorowska J, Casey E, Neve H, Franz C, Noben JP, Lugli GA, et al. A Quest of Great Importance-
1363 Developing a Broad Spectrum *Escherichia coli* Phage Collection. Viruses. 2019;11(10). Epub 2019/09/29.
1364 doi: 10.3390/v11100899. PubMed PMID: 31561510; PubMed Central PMCID: PMCPMC6832132.
- 1365 92. Simoliunas E, Vilkaityte M, Kaliniene L, Zajanckauskaite A, Kaupinis A, Staniulis J, et al. Incomplete
1366 LPS Core-Specific Felix01-Like Virus vB_EcoM_VpaE1. Viruses. 2015;7(12):6163-81. Epub 2015/12/04. doi:
1367 10.3390/v7122932. PubMed PMID: 26633460; PubMed Central PMCID: PMCPMC4690856.
- 1368 93. Blattner FR, Plunkett G, 3rd, Bloch CA, Perna NT, Burland V, Riley M, et al. The complete genome
1369 sequence of *Escherichia coli* K-12. Science. 1997;277(5331):1453-62. Epub 1997/09/05. doi:
1370 10.1126/science.277.5331.1453. PubMed PMID: 9278503.
- 1371 94. Hendrix RW, Duda RL. Bacteriophage lambda PaPa: not the mother of all lambda phages. Science.
1372 1992;258(5085):1145-8. doi: 10.1126/science.1439823. PubMed PMID: 1439823.
- 1373 95. Sandulache R, Prehm P, Kamp D. Cell wall receptor for bacteriophage Mu G(+). J Bacteriol.
1374 1984;160(1):299-303. Epub 1984/10/01. doi: 10.1128/JB.160.1.299-303.1984. PubMed PMID: 6384194;
1375 PubMed Central PMCID: PMCPMC214716.
- 1376 96. North OI, Sakai K, Yamashita E, Nakagawa A, Iwazaki T, Buttner CR, et al. Phage tail fibre assembly
1377 proteins employ a modular structure to drive the correct folding of diverse fibres. Nat Microbiol.
1378 2019;4(10):1645-53. Epub 2019/06/19. doi: 10.1038/s41564-019-0477-7. PubMed PMID: 31209305.
- 1379 97. Hyman P, Abedon ST. Bacteriophage host range and bacterial resistance. Adv Appl Microbiol.
1380 2010;70:217-48. Epub 2010/04/03. doi: 10.1016/s0065-2164(10)70007-1. PubMed PMID: 20359459.
- 1381 98. Abedon ST. Lysis from without. Bacteriophage. 2011;1(1):46-9. doi: 10.4161/bact.1.1.13980.
1382 PubMed PMID: 21687534; PubMed Central PMCID: PMCPMC3109453.
- 1383 99. Jeong H, Barbe V, Lee CH, Vallenet D, Yu DS, Choi SH, et al. Genome sequences of *Escherichia coli*
1384 B strains REL606 and BL21(DE3). J Mol Biol. 2009;394(4):644-52. Epub 2009/09/30. doi:
1385 10.1016/j.jmb.2009.09.052. PubMed PMID: 19786035.

- 1386 100. Studier FW, Daegelen P, Lenski RE, Maslov S, Kim JF. Understanding the differences between
1387 genome sequences of *Escherichia coli* B strains REL606 and BL21(DE3) and comparison of the *E. coli* B and
1388 K-12 genomes. *J Mol Biol.* 2009;394(4):653-80. doi: 10.1016/j.jmb.2009.09.021. PubMed PMID:
1389 19765592.
- 1390 101. Sueki A, Stein F, Savitski MM, Selkrig J, Typas A. Systematic Localization of *Escherichia coli*
1391 Membrane Proteins. *mSystems.* 2020;5(2). Epub 2020/03/05. doi: 10.1128/mSystems.00808-19. PubMed
1392 PMID: 32127419; PubMed Central PMCID: PMC7055658.
- 1393 102. Kortright KE, Chan BK, Turner PE. High-throughput discovery of phage receptors using transposon
1394 insertion sequencing of bacteria. *Proc Natl Acad Sci U S A.* 2020;117(31):18670-9. Epub 2020/07/18. doi:
1395 10.1073/pnas.2001888117. PubMed PMID: 32675236; PubMed Central PMCID: PMC7414163.
- 1396 103. Liu B, Furevi A, Perepelov AV, Guo X, Cao H, Wang Q, et al. Structure and genetics of *Escherichia*
1397 *coli* O antigens. *FEMS Microbiol Rev.* 2020;44(6):655-83. Epub 2019/11/30. doi: 10.1093/femsre/fuz028.
1398 PubMed PMID: 31778182; PubMed Central PMCID: PMC7685785.
- 1399 104. Gurney J, Brown SP, Kaltz O, Hochberg ME. Steering Phages to Combat Bacterial Pathogens.
1400 *Trends Microbiol.* 2020;28(2):85-94. Epub 2019/11/21. doi: 10.1016/j.tim.2019.10.007. PubMed PMID:
1401 31744662; PubMed Central PMCID: PMC76980653.
- 1402 105. Bauer RJ, Zhelkovsky A, Bilotti K, Crowell LE, Evans TC, Jr., McReynolds LA, et al. Comparative
1403 analysis of the end-joining activity of several DNA ligases. *PLoS One.* 2017;12(12):e0190062. Epub
1404 2017/12/29. doi: 10.1371/journal.pone.0190062. PubMed PMID: 29284038; PubMed Central PMCID:
1405 PMC75746248.
- 1406 106. Millman A, Bernheim A, Stokar-Avihail A, Fedorenko T, Voichek M, Leavitt A, et al. Bacterial
1407 Retrons Function In Anti-Phage Defense. *Cell.* 2020;183(6):1551-61 e12. Epub 2020/11/07. doi:
1408 10.1016/j.cell.2020.09.065. PubMed PMID: 33157039.
- 1409 107. Doron S, Melamed S, Ofir G, Leavitt A, Lopatina A, Keren M, et al. Systematic discovery of
1410 antiphage defense systems in the microbial pangenome. *Science.* 2018;359(6379). Epub 2018/01/27. doi:
1411 10.1126/science.aar4120. PubMed PMID: 29371424; PubMed Central PMCID: PMC6387622.
- 1412 108. Keen EC. Tradeoffs in bacteriophage life histories. *Bacteriophage.* 2014;4(1):e28365. Epub
1413 2014/03/13. doi: 10.4161/bact.28365. PubMed PMID: 24616839; PubMed Central PMCID:
1414 PMC3942329.
- 1415 109. Law R. Optimal Life Histories Under Age-Specific Predation. *The American Naturalist.*
1416 1979;114(3):399-417.
- 1417 110. Breitbart M, Bonnain C, Malki K, Sawaya NA. Phage puppet masters of the marine microbial realm.
1418 *Nat Microbiol.* 2018;3(7):754-66. Epub 2018/06/06. doi: 10.1038/s41564-018-0166-y. PubMed PMID:
1419 29867096.
- 1420 111. Mizuno CM, Luong T, Cederstrom R, Krupovic M, Debarbieux L, Roach DR. Isolation and
1421 Characterization of Bacteriophages That Infect *Citrobacter rodentium*, a Model Pathogen for Intestinal
1422 Diseases. *Viruses.* 2020;12(7). Epub 2020/07/12. doi: 10.3390/v12070737. PubMed PMID: 32650458;
1423 PubMed Central PMCID: PMC7412075.
- 1424 112. Jordan TC, Burnett SH, Carson S, Caruso SM, Clase K, DeJong RJ, et al. A broadly implementable
1425 research course in phage discovery and genomics for first-year undergraduate students. *mBio.*
1426 2014;5(1):e01051-13. Epub 2014/02/06. doi: 10.1128/mBio.01051-13. PubMed PMID: 24496795;
1427 PubMed Central PMCID: PMC3950523.
- 1428 113. M9 minimal medium (standard). *Cold Spring Harbor Protocols.* 2010;2010(8):pdb.rec12295. doi:
1429 10.1101/pdb.rec12295.
- 1430 114. Kropinski AM, Mazzocco A, Waddell TE, Lingohr E, Johnson RP. Enumeration of bacteriophages by
1431 double agar overlay plaque assay. *Methods Mol Biol.* 2009;501:69-76. doi: 10.1007/978-1-60327-164-6_7.
1432 PubMed PMID: 19066811.

- 1433 115. Kauffman KM, Polz MF. Streamlining standard bacteriophage methods for higher throughput.
1434 MethodsX. 2018;5:159-72. Epub 2019/01/10. doi: 10.1016/j.mex.2018.01.007. PubMed PMID: 30622914;
1435 PubMed Central PMCID: PMC6318102.
- 1436 116. Golec P, Dabrowski K, Hejnowicz MS, Gozdek A, Los JM, Wegrzyn G, et al. A reliable method for
1437 storage of tailed phages. J Microbiol Methods. 2011;84(3):486-9. Epub 2011/01/25. doi:
1438 10.1016/j.mimet.2011.01.007. PubMed PMID: 21256885.
- 1439 117. Datsenko KA, Wanner BL. One-step inactivation of chromosomal genes in *Escherichia coli* K-12
1440 using PCR products. Proc Natl Acad Sci USA. 2000;97(12):6640-5. doi: 10.1073/pnas.120163297. PubMed
1441 PMID: 10829079; PubMed Central PMCID: PMC18686.
- 1442 118. Harms A, Fino C, Sørensen MA, Semsey S, Gerdes K. Prophages and Growth Dynamics Confound
1443 Experimental Results with Antibiotic-Tolerant Persister Cells. MBio. 2017;8(6). doi: 10.1128/mBio.01964-
1444 17. PubMed PMID: 29233898; PubMed Central PMCID: PMC5727415.
- 1445 119. Pleska M, Qian L, Okura R, Bergmiller T, Wakamoto Y, Kussell E, et al. Bacterial Autoimmunity Due
1446 to a Restriction-Modification System. Curr Biol. 2016;26(3):404-9. Epub 2016/01/26. doi:
1447 10.1016/j.cub.2015.12.041. PubMed PMID: 26804559.
- 1448 120. Baba T, Ara T, Hasegawa M, Takai Y, Okumura Y, Baba M, et al. Construction of *Escherichia coli* K-
1449 12 in-frame, single-gene knockout mutants: the Keio collection. Mol Syst Biol. 2006;2:2006 0008. doi:
1450 10.1038/msb4100050. PubMed PMID: 16738554; PubMed Central PMCID: PMC1681482.
- 1451 121. Fino C, Vestergaard M, Ingmer H, Pierrel F, Gerdes K, Harms A. PasT of *Escherichia coli* sustains
1452 antibiotic tolerance and aerobic respiration as a bacterial homolog of mitochondrial Coq10.
1453 Microbiologyopen. 2020;9(8):e1064. Epub 2020/06/20. doi: 10.1002/mbo3.1064. PubMed PMID:
1454 32558363; PubMed Central PMCID: PMC67424257.
- 1455 122. Wiles TJ, Kulesus RR, Mulvey MA. Origins and virulence mechanisms of uropathogenic *Escherichia*
1456 *coli*. Exp Mol Pathol. 2008;85(1):11-9. Epub 2008/05/17. doi: 10.1016/j.yexmp.2008.03.007. PubMed
1457 PMID: 18482721; PubMed Central PMCID: PMC2595135.
- 1458 123. Grad YH, Godfrey P, Cerquiera GC, Mariani-Kurkdjian P, Gouali M, Bingen E, et al. Comparative
1459 genomics of recent Shiga toxin-producing *Escherichia coli* O104:H4: short-term evolution of an emerging
1460 pathogen. mBio. 2013;4(1):e00452-12. Epub 2013/01/24. doi: 10.1128/mBio.00452-12. PubMed PMID:
1461 23341549; PubMed Central PMCID: PMC3551546.
- 1462 124. Bernier C, Gounon P, Le Bouguenec C. Identification of an aggregative adhesion fimbria (AAF) type
1463 III-encoding operon in enteroaggregative *Escherichia coli* as a sensitive probe for detecting the AAF-
1464 encoding operon family. Infect Immun. 2002;70(8):4302-11. Epub 2002/07/16. doi:
1465 10.1128/iai.70.8.4302-4311.2002. PubMed PMID: 12117939; PubMed Central PMCID: PMC128174.
- 1466 125. Branchu P, Bawn M, Kingsley RA. Genome Variation and Molecular Epidemiology of *Salmonella*
1467 *enterica* Serovar Typhimurium Pathovariants. Infect Immun. 2018;86(8). Epub 2018/05/23. doi:
1468 10.1128/IAI.00079-18. PubMed PMID: 29784861; PubMed Central PMCID: PMC6056856.
- 1469 126. Gibson DG, Young L, Chuang RY, Venter JC, Hutchison CA, 3rd, Smith HO. Enzymatic assembly of
1470 DNA molecules up to several hundred kilobases. Nat Methods. 2009;6(5):343-5. Epub 2009/04/14. doi:
1471 10.1038/nmeth.1318. PubMed PMID: 19363495.
- 1472 127. Liu H, Naismith JH. An efficient one-step site-directed deletion, insertion, single and multiple-site
1473 plasmid mutagenesis protocol. BMC Biotechnol. 2008;8:91. doi: 10.1186/1472-6750-8-91. PubMed PMID:
1474 19055817; PubMed Central PMCID: PMC2629768.
- 1475 128. Roberts RJ, Vincze T, Posfai J, Macelis D. REBASE--a database for DNA restriction and modification:
1476 enzymes, genes and genomes. Nucleic Acids Res. 2015;43(Database issue):D298-9. Epub 2014/11/08. doi:
1477 10.1093/nar/gku1046. PubMed PMID: 25378308; PubMed Central PMCID: PMC4383893.
- 1478 129. Czajkowski R, Ozymko Z, Lojkowska E. Application of zinc chloride precipitation method for rapid
1479 isolation and concentration of infectious *Pectobacterium* spp. and *Dickeya* spp. lytic bacteriophages from

- 1480 surface water and plant and soil extracts. *Folia Microbiol* (Praha). 2016;61(1):29-33. Epub 2015/06/24.
1481 doi: 10.1007/s12223-015-0411-1. PubMed PMID: 26099750; PubMed Central PMCID: PMCPMC4691450.
- 1482 130. You L, Suthers PF, Yin J. Effects of *Escherichia coli* physiology on growth of phage T7 *in vivo* and *in*
1483 *silico*. *J Bacteriol*. 2002;184(7):1888-94. Epub 2002/03/13. doi: 10.1128/jb.184.7.1888-1894.2002.
1484 PubMed PMID: 11889095; PubMed Central PMCID: PMCPMC134924.
- 1485 131. Abedon ST, Katsaounis TI. Basic Phage Mathematics. *Methods Mol Biol*. 2018;1681:3-30. Epub
1486 2017/11/15. doi: 10.1007/978-1-4939-7343-9_1. PubMed PMID: 29134583.
- 1487 132. Garneau JR, Depardieu F, Fortier LC, Bikard D, Monot M. PhageTerm: a tool for fast and accurate
1488 determination of phage termini and packaging mechanism using next-generation sequencing data. *Sci*
1489 *Rep*. 2017;7(1):8292. Epub 2017/08/16. doi: 10.1038/s41598-017-07910-5. PubMed PMID: 28811656;
1490 PubMed Central PMCID: PMCPMC5557969.
- 1491 133. Ecale Zhou CL, Malfatti S, Kimbrel J, Philipson C, McNair K, Hamilton T, et al. multiPhATE:
1492 bioinformatics pipeline for functional annotation of phage isolates. *Bioinformatics*. 2019;35(21):4402-4.
1493 Epub 2019/05/16. doi: 10.1093/bioinformatics/btz258. PubMed PMID: 31086982; PubMed Central
1494 PMCID: PMCPMC6821344.
- 1495 134. Darling AE, Mau B, Perna NT. progressiveMauve: multiple genome alignment with gene gain, loss
1496 and rearrangement. *PLoS One*. 2010;5(6):e11147. Epub 2010/07/02. doi: 10.1371/journal.pone.0011147.
1497 PubMed PMID: 20593022; PubMed Central PMCID: PMCPMC2892488.
- 1498 135. Mitchell AL, Attwood TK, Babbitt PC, Blum M, Bork P, Bridge A, et al. InterPro in 2019: improving
1499 coverage, classification and access to protein sequence annotations. *Nucleic Acids Res*.
1500 2019;47(D1):D351-D60. Epub 2018/11/07. doi: 10.1093/nar/gky1100. PubMed PMID: 30398656; PubMed
1501 Central PMCID: PMCPMC6323941.
- 1502 136. Kelley LA, Mezulis S, Yates CM, Wass MN, Sternberg MJ. The Phyre2 web portal for protein
1503 modeling, prediction and analysis. *Nat Protoc*. 2015;10(6):845-58. doi: 10.1038/nprot.2015.053. PubMed
1504 PMID: 25950237; PubMed Central PMCID: PMCPMC5298202.
- 1505 137. Chan PP, Lowe TM. tRNAscan-SE: Searching for tRNA Genes in Genomic Sequences. *Methods Mol*
1506 *Biol*. 2019;1962:1-14. Epub 2019/04/26. doi: 10.1007/978-1-4939-9173-0_1. PubMed PMID: 31020551;
1507 PubMed Central PMCID: PMCPMC6768409.
- 1508 138. Kongari R, Rajaure M, Cahill J, Rasche E, Mijalis E, Berry J, et al. Phage spanins: diversity,
1509 topological dynamics and gene convergence. *BMC Bioinformatics*. 2018;19(1):326. Epub 2018/09/17. doi:
1510 10.1186/s12859-018-2342-8. PubMed PMID: 30219026; PubMed Central PMCID: PMCPMC6139136.
- 1511 139. Cahill J, Young R. Phage Lysis: Multiple Genes for Multiple Barriers. *Adv Virus Res*. 2019;103:33-
1512 70. Epub 2019/01/13. doi: 10.1016/bs.aivir.2018.09.003. PubMed PMID: 30635077; PubMed Central
1513 PMCID: PMCPMC6733033.
- 1514 140. Adriaenssens E, Brister JR. How to Name and Classify Your Phage: An Informal Guide. *Viruses*.
1515 2017;9(4). doi: 10.3390/v9040070. PubMed PMID: 28368359; PubMed Central PMCID: PMCPMC5408676.
- 1516 141. Tolstoy I, Kropinski AM, Brister JR. Bacteriophage Taxonomy: An Evolving Discipline. *Methods Mol*
1517 *Biol*. 2018;1693:57-71. Epub 2017/11/10. doi: 10.1007/978-1-4939-7395-8_6. PubMed PMID: 29119432.
- 1518 142. Lefkowitz EJ, Dempsey DM, Hendrickson RC, Orton RJ, Siddell SG, Smith DB. Virus taxonomy: the
1519 database of the International Committee on Taxonomy of Viruses (ICTV). *Nucleic Acids Res*.
1520 2018;46(D1):D708-D17. Epub 2017/10/19. doi: 10.1093/nar/gkx932. PubMed PMID: 29040670; PubMed
1521 Central PMCID: PMCPMC5753373.
- 1522 143. Katoh K, Standley DM. MAFFT multiple sequence alignment software version 7: improvements in
1523 performance and usability. *Mol Biol Evol*. 2013;30(4):772-80. Epub 2013/01/19. doi:
1524 10.1093/molbev/mst010. PubMed PMID: 23329690; PubMed Central PMCID: PMCPMC3603318.

- 1525 144. Guindon S, Dufayard JF, Lefort V, Anisimova M, Hordijk W, Gascuel O. New algorithms and
1526 methods to estimate maximum-likelihood phylogenies: assessing the performance of PhyML 3.0. *Syst Biol*.
1527 2010;59(3):307-21. Epub 2010/06/09. doi: 10.1093/sysbio/syq010. PubMed PMID: 20525638.
- 1528 145. Heinrichs DE, Yethon JA, Whitfield C. Molecular basis for structural diversity in the core regions of
1529 the lipopolysaccharides of *Escherichia coli* and *Salmonella enterica*. *Mol Microbiol*. 1998;30(2):221-32.
1530 Epub 1998/10/29. doi: 10.1046/j.1365-2958.1998.01063.x. PubMed PMID: 9791168.
- 1531 146. Micoli F, Ravenscroft N, Cescutti P, Stefanetti G, Londero S, Rondini S, et al. Structural analysis of
1532 O-polysaccharide chains extracted from different *Salmonella* Typhimurium strains. *Carbohydr Res*.
1533 2014;385:1-8. Epub 2014/01/05. doi: 10.1016/j.carres.2013.12.003. PubMed PMID: 24384528.
- 1534 147. Storek KM, Chan J, Vij R, Chiang N, Lin Z, Bevers J, 3rd, et al. Massive antibody discovery used to
1535 probe structure-function relationships of the essential outer membrane protein LptD. *Elife*. 2019;8. Epub
1536 2019/06/27. doi: 10.7554/eLife.46258. PubMed PMID: 31237236; PubMed Central PMCID:
1537 PMC6592684.
- 1538 148. Eriksson JM, Haggard-Ljungquist E. The multifunctional bacteriophage P2 cox protein requires
1539 oligomerization for biological activity. *J Bacteriol*. 2000;182(23):6714-23. Epub 2000/11/14. doi:
1540 10.1128/jb.182.23.6714-6723.2000. PubMed PMID: 11073917; PubMed Central PMCID:
1541 PMC111415.
- 1542 149. Silhavy TJ. Gene fusions. *J Bacteriol*. 2000;182(21):5935-8. Epub 2000/10/13. doi:
1543 10.1128/jb.182.21.5935-5938.2000. PubMed PMID: 11029410; PubMed Central PMCID: PMC94724.
- 1544 150. Crick FH, Barnett L, Brenner S, Watts-Tobin RJ. General nature of the genetic code for proteins.
1545 *Nature*. 1961;192:1227-32. Epub 1961/12/30. doi: 10.1038/1921227a0. PubMed PMID: 13882203.
- 1546 151. Benzer S, Champe SP. A change from nonsense to sense in the genetic code. *Proc Natl Acad Sci U*
1547 *S A*. 1962;48:1114-21. Epub 1962/07/15. doi: 10.1073/pnas.48.7.1114. PubMed PMID: 13867417;
1548 PubMed Central PMCID: PMC220916.
- 1549

1550 **Figures**

1551 **Fig 1. The three morphotypes of *Caudovirales* and two lines of defense in bacterial** 1552 **immunity.**

1553 (A) The virions of tailed phages or *Caudovirales* can be assigned to three general morphotypes
1554 including myoviruses (contractile tail), siphoviruses (long and flexible, non-contractile tail), and
1555 podoviruses (short and stubby tail). (B) The life cycle of a typical lytic phage begins with reversible
1556 attachment to a so-called primary receptor on the bacterial cell surface (1), usually via lateral tail fibers at
1557 the virion. Subsequently, irreversible attachment to secondary or terminal receptors usually depends on
1558 structures at the end of the tail, e.g., short tail fibers for many myoviruses and central tail fibers or tail tip
1559 proteins for siphoviruses (2 ; see also (A)). After genome injection (3), the phage takes over the host cell,
1560 replicates, and releases the offspring by host cell lysis (4). Inside the host cell, the bacteriophage faces two
1561 lines of host defenses, first bacterial immunity systems that try to clear the infection by directly targeting
1562 the phage genome (5) and then abortive infection systems that kill the infected cell when a viral infection
1563 is sensed (6).

1564 **Fig 2. Overview of the BASEL collection.**

1565 (A) Illustration of the workflow of bacteriophage isolation, characterization, and selection that
1566 resulted in the BASEL collection (details in *Materials and Methods*). (B) Taxonomic overview of the
1567 bacteriophages included in the BASEL collection and their unique Bas### identifiers. Newly isolated phages
1568 are colored according to their family while well-studied reference phages are shown in grey.

1569 **Fig 3. Overview of *E. coli* surface glycan variants and the immunity systems used in** 1570 **this study**

1571 (A) The surface glycans of different *E. coli* K-12 MG1655 variants are shown schematically (details
1572 in running text and *Materials and Methods*). Note that the *E. coli* K-12 MG1655 laboratory wildtype does
1573 not merely display the K12-type core LPS (classical rough LPS phenotype) but also the most proximal

1574 D-glucose of the O16-type O-antigen. **(B)** Key features of the six RM systems (each two of type I, type II,
1575 and type III) and the five Abi systems used for the phenotyping of this study are summarized schematically.
1576 Recognition sites of RM systems have either been determined experimentally or were predicted in REBASE
1577 (red nucleotides: methylation sites; dotted lines: cleavage sites) [47-49, 128]. The Abi systems have been
1578 characterized to very different extent but constitute the most well-understood representatives of these
1579 immunity systems of *E. coli* [10, 50].

1580 **Fig 4. Overview of *Drexlerviridae* phages.**

1581 **(A)** Schematic illustration of host recognition by *Drexlerviridae*. **(B)** Maximum-Likelihood
1582 phylogeny of *Drexlerviridae* based on several core genes with bootstrap support of branches shown if >
1583 70/100. Newly isolated phages of the BASEL collection are highlighted by red phage icons and the
1584 determined or proposed terminal receptor specificity is highlighted at the phage names using the color code
1585 highlighted in (C). The phylogeny was rooted based on a representative phylogeny including *Dhillonvirus*
1586 sequences as outgroup (S1A Fig). **(C)** On the left, the seven identified receptors of small siphoviruses are
1587 shown with a color code that is also used to annotate demonstrated or predicted receptor specificity in the
1588 phylogenies of Fig 4B and Figs 6A + 6C). On the right, we show representative *bona fide* RBP loci that
1589 seem to encode the receptor specificity of these small siphoviruses (with the same color code). Note that
1590 the loci linked to each receptor are very similar while the genetic arrangement differs considerably between
1591 loci linked to different terminal host receptors (see also S1C Fig). **(D)** The results of quantitative
1592 phenotyping experiments with *Drexlerviridae* phages regarding sensitivity to altered surface glycans and
1593 bacterial immunity systems are presented as efficiency of plating (EOP). Data points and error bars
1594 represent average and standard deviation of at least three independent experiments.

1595 **Fig 5. LptD is a commonly targeted terminal receptor of small siphoviruses**

1596 **(A)** Whole-genome sequencing of bacterial mutants exhibiting spontaneous resistance to seven
1597 small siphoviruses with no previously known receptor revealed different mutations or small deletions in the
1598 essential gene *lptD* that encodes the LptD LPS export channel. Top agar assays with two representative

1599 mutants in comparison to the ancestral *E. coli* K-12 BW25113 strain were performed with serial tenfold
1600 dilutions of twelve different phages (undiluted high-titer stocks at the bottom and increasingly diluted
1601 samples towards the top). Both mutants display complete resistance to the seven small siphoviruses of
1602 diverse genera within *Drexlerviridae* and *Siphoviridae* families that share the same *bona fide* RBP modules
1603 (S1C Fig) while no other phage of the BASEL collection was affected. In particular, we excluded indirect
1604 effects, e.g., via changes in the LPS composition in the *lptD* mutants, by confirming that five LPS-targeting
1605 phages of diverse families (see below) showed full infectivity on all strains. **(B)** The amino acid sequence
1606 alignment of wildtype LptD with the two mutants highlighted in (A) shows that resistance to LptD-targeting
1607 phages is linked to small deletions in or adjacent to regions encoding extracellular loops as defined in
1608 previous work [147], suggesting that they abolish the RBP-receptor interaction.

1609 **Fig 6. Overview of *Siphoviridae* genera *Dhillonvirus*, *Nonagvirus*, and *Seuratvirus*.**

1610 **(A)** Schematic illustration of host recognition by small siphoviruses. **(B)** Maximum-Likelihood
1611 phylogeny of the *Dhillonvirus* genus based on a whole-genome alignment with bootstrap support of
1612 branches shown if > 70/100. Newly isolated phages of the BASEL collection are highlighted by red phage
1613 icons and the determined or proposed terminal receptor specificity is highlighted at the phage names using
1614 the color code highlighted in Fig 4C. The phylogeny was rooted between phage WFI and all others based
1615 on a representative phylogeny including *Drexlerviridae* sequences as outgroup (S1A Fig). **(C)** The results
1616 of quantitative phenotyping experiments with *Dhillonvirus* phages regarding sensitivity to altered surface
1617 glycans and bacterial immunity systems are presented as efficiency of plating (EOP). **(D)** Maximum-
1618 Likelihood phylogeny of the *Nonagvirus* and *Seuratvirus* genera based on a whole-genome alignment with
1619 bootstrap support of branches shown if > 70/100. Newly isolated phages of the BASEL collection are
1620 highlighted by red phage icons and the determined or proposed terminal receptor specificity is highlighted
1621 at the phage names using the color code highlighted in Fig 4C. The phylogeny was rooted between the two
1622 genera. **(E)** *Nonagvirus* and *Seuratvirus* phages share a core 7-deazaguanosine biosynthesis pathway
1623 involving FolE, QueD, QueE, and QueC which synthesizes dPreQ₀ that is inserted into their genomes by

1624 DpdA. In *Nonagvirus* phages, the fusion of QueC with a glutamate amidotransferase (Gat) domain to Gat-
1625 QueC results in the modification with dG⁺ instead of dPreQ₀ [45]. **(F)** The results of quantitative
1626 phenotyping experiments with *Nonagvirus* and *Seuratvirus* phages regarding sensitivity to altered surface
1627 glycans and bacterial immunity systems are presented as efficiency of plating (EOP). In (C) and (F), data
1628 points and error bars represent average and standard deviation of at least three independent experiments.

1629 **Fig 7. Overview of *Demerecviridae* subfamily *Markadamsvirinae*.**

1630 **(A)** Schematic illustration of host recognition by T5-like siphoviruses. **(B)** Maximum-Likelihood
1631 phylogeny of the *Markadamsvirinae* subfamily of *Demerecviridae* based on several core genes with
1632 bootstrap support of branches shown if > 70/100. Phages of the BASEL collection are highlighted by little
1633 phage icons and the determined or proposed terminal receptor specificity is highlighted at the phage names
1634 using the color code highlighted at the right side (same as for the small siphoviruses). The phylogeny was
1635 rooted between the *Epseptimavirus* and *Tequintavirus* genera. **(C)** The results of quantitative phenotyping
1636 experiments with *Markadamsvirinae* phages regarding sensitivity to altered surface glycans and bacterial
1637 immunity systems are presented as efficiency of plating (EOP). Data points and error bars represent average
1638 and standard deviation of at least three independent experiments.

1639 **Fig 8. Overview of the *Myoviridae* subfamily *Tevenvirinae*.**

1640 **(A)** Schematic illustration of host recognition by T4-like myoviruses. **(B)** Maximum-Likelihood
1641 phylogeny of the *Tevenvirinae* subfamily of *Myoviridae* based on a curated whole-genome alignment with
1642 bootstrap support of branches shown if > 70/100. The phylogeny was rooted between the *Tequatrovirus*
1643 and *Mosigvirus* genera. Phages of the BASEL collection are highlighted by little phage icons and
1644 experimentally determined primary receptor specificity is highlighted at the phage names using the color
1645 code highlighted at the top left. Primary receptor specificity of *Tevenvirinae* depends on RBPs expressed
1646 either as a C-terminal extension of the distal half fiber (T4 and other OmpC-targeting phages) or as separate
1647 small fiber tip adhesins [66], but sequence analyses of the latter remained ambiguous. We therefore only
1648 annotated experimentally determined primary receptors (see also S4A Fig) [53, 66]. **(C)** The results of

1649 quantitative phenotyping experiments with *Tevenvirinae* phages regarding sensitivity to altered surface
1650 glycans and bacterial immunity systems are presented as efficiency of plating (EOP). Data points and error
1651 bars represent average and standard deviation of at least three independent experiments. **(D)** The Maximum-
1652 Likelihood phylogeny *Tevenvirinae* short tail fiber proteins reveals two homologous, yet clearly distinct,
1653 clusters that correlate with the absence (variant #1, like T4) or presence (variant #2) of detectable LPS core
1654 dependence as shown in (C). **(E)** The results of (D) indicate that variant #1, as shown for T4, binds the deep
1655 lipid A – Kdo region of the enterobacterial LPS core, while variant #2 binds a more distal part of the
1656 (probably inner) core.

1657 **Fig 9. Overview of the *Myoviridae* subfamily *Vequintavirinae* and relatives.**

1658 **(A)** Schematic illustration of host recognition by rV5-like myoviruses. **(B)** Maximum-Likelihood
1659 phylogeny of the *Vequintavirinae* subfamily of *Myoviridae* and relatives based on a curated whole-genome
1660 alignment with bootstrap support of branches shown if > 70/100. The phylogeny was rooted between the
1661 *Vequintavirus* genus and the two closely related, unclassified groups at the bottom. Newly isolated phages
1662 of the BASEL collection are highlighted by green phage icons. **(C)** The results of quantitative phenotyping
1663 experiments with *Vequintavirinae* and phage PaulScherrer regarding sensitivity to altered surface glycans
1664 and bacterial immunity systems are presented as efficiency of plating (EOP). Data points and error bars
1665 represent average and standard deviation of at least three independent experiments. **(D)** Amino acid
1666 sequence alignment of the lateral tail fiber Gp64 of phage N4 (*Enquatrovirus*, see below) and a lateral tail
1667 fiber conserved among *Vequintavirinae* and relatives (representatives shown). The proteins share a
1668 predicted poly-GlcNAc deacetylase domain as identified by Phyre2 [136]. **(E)** *Vequintavirinae sensu*
1669 *stricto* (represented by rV5 and Jeff Schatz) encode two paralogous short tail fiber proteins and a tail fiber
1670 chaperone that are homologous to the corresponding locus in phi92-like phages incl. PaulScherrer and,
1671 ultimately, to short tail fiber GpS and chaperone GpU of Mu(+) (which targets a different glucose in the
1672 K12-type LPS core GpS [95, 96]).

1673

1674 **Fig 10. Overview of *Autographiviridae* phages and *Podoviridae* genus *Enquatrovirus*.**

1675 (A) Schematic illustration of host recognition by *Autographiviridae* and *Enquatrovirus* phages.
1676 (B) Maximum-Likelihood phylogeny of the *Studiervirinae* subfamily of *Autographiviridae* based on
1677 several core genes with bootstrap support of branches shown if $> 70/100$. The phylogeny was midpoint-
1678 rooted between the clade formed by *Teseptimavirus* and *Teetrevirus* and the other genera. Phages of the
1679 BASEL collection are highlighted by little phage icons. (C) The results of quantitative phenotyping
1680 experiments with *Autographiviridae* regarding sensitivity to altered surface glycans and bacterial immunity
1681 systems are presented as efficiency of plating (EOP). Data points and error bars represent average and
1682 standard deviation of at least three independent experiments. (D) Amino acid sequence alignment and
1683 Maximum-Likelihood phylogeny of Gp1.2 orthologs in all tested *Autographiviridae* phages. Phage
1684 JeanTinguely belongs to the *Teseptimavirus* genus but encodes an allele of *gp1.2* that is closely related to
1685 those of the *Berlinvirus* genus, possibly explaining its resistance to PifA (see (C)). (E) Maximum-
1686 Likelihood phylogeny of the *Enquatrovirus* genus and related groups of *Podoviridae* based on several core
1687 genes with bootstrap support of branches shown if $> 70/100$. The phylogeny was midpoint-rooted between
1688 the distantly related *Jwalphavirus* genus and the others. Phages of the BASEL collection are highlighted
1689 by little phage icons.

1690 **Fig 11. Overview of *Myoviridae*: *Ounavirinae* and classic temperate phages.**

1691 (A) Schematic illustration of host recognition by *Ounavirinae*: *Felixounavirus* phages. Note that
1692 the illustration shows short tail fibers simply in analogy to *Tevenvirinae* or *Vequintavirinae* (Figs 8A and
1693 9A), but any role for such structures has not been explored for Felix O1 and relatives. (B) Maximum-
1694 Likelihood phylogeny of the *Ounavirinae* subfamily of *Myoviridae* based on several core genes with
1695 bootstrap support of branches shown if $> 70/100$. The phylogeny was midpoint-rooted between
1696 *Kolesnikvirus* and the other genera. Our new isolate JohannRWettstein is highlighted by a green phage icon.
1697 (C,D) Schematic illustration of host recognition by classic temperate phages lambda, P1, and P2. Note the
1698 absence of lateral tail fibers due to a mutation in lambda PaPa laboratory strains [94]. (E,F) The results of

1699 quantitative phenotyping experiments with JohannRWettstein and classic temperate phages regarding
1700 sensitivity to altered surface glycans and bacterial immunity systems are presented as efficiency of plating
1701 (EOP). Data points and error bars represent average and standard deviation of at least three independent
1702 experiments.

1703 **Fig 12. Host range of phages in the BASEL collection**

1704 (A) Surface glycans of the enterobacterial strains used in this work (see *Materials and Methods* for
1705 details on how the illustration of glycan chains was composed). (B) The ability of all phages in the BASEL
1706 collection to infect different enterobacteria was studied qualitatively (lysis host range; top) and, more
1707 stringently, based on the ability to form plaques (bottom). Top: The observation of lysis zones with high-
1708 titer lysate ($>10^9$ pfu/ml) in at least three independent experiments is indicated by colored bars. Bottom:
1709 The infectivity of BASEL collection phages on diverse enterobacterial hosts was quantified as efficiency
1710 of plating (EOP). Data points and error bars represent average and standard deviation of at least three
1711 independent experiments. Since the data obtained with *Salmonella* Typhimurium 12023s and SL1344 were
1712 indistinguishable, we only show the results of one representative strain (*S. Typhimurium* 12023s).

1713 **Data reporting**

1714 All data generated or analyzed during this study are included in this published article.

1715 **Accession numbers**

1716 The annotated genome sequences of all 66 newly isolated phages as well as T3(K12) have been
1717 submitted to the NCBI GenBank database under accession numbers listed in S5 Table.

1718 **Funding Disclosure**

1719 This work was supported by Swiss National Science Foundation (SNSF) Ambizione Fellowship
1720 PZ00P3_180085 (to AH), SNSF National Center of Competence in Research (NCCR) AntiResist, and a
1721 generous contribution of the Stiftung Emilia-Guggenheim-Schnurr of the Naturforschende Gesellschaft in
1722 Basel (NGiB; to AH). AS was supported by a Biozentrum PhD Fellowship. S.M. and H.H. were supported
1723 by the Institute of Medical Microbiology, University of Zürich. The funders had no role in study design,
1724 data collection and analysis, decision to publish, or preparation of the manuscript.

1725 **Competing Interests**

1726 The authors do not declare any competing interests.

1727 **Supporting Information Captions**

1728 **S1 Table. List of all bacterial strains used in this study.**

1729 The abbreviations in the selection column indicate the drug and its concentration that were used.
1730 Amp = ampicillin, Cam = chloramphenicol, Kan = kanamycin, Zeo = zeocin; 25 / 50 / 100 refer to 25 µg/ml,
1731 50 µg/ml, and 100 = 100 µg/ml, respectively. The following mutants of the KEIO collection were used for
1732 qualitative top agar assays but are not included in the strain list because no phage showed any growth
1733 phenotype on them: *ompW::kanR*, *phoE::kanR*, *flgG::kanR*, *fepA::kanR*, *hofQ::kanR*, *cirA::kanR*,
1734 *fhuE::kanR*, *fiu::kanR*, *ompN::kanR*, *pgaA::kanR*, *chiP::kanR*, *ompL::kanR*, *yddB::kanR*, *fecA::kanR*,
1735 *uidC::kanR*, *nanC::kanR*, *yfaZ::kanR*, *bglH::kanR*, *bcuC::kanR*, *cusC::kanR*, *gfcE::kanR*, *mdtP::kanR*,
1736 *ompG::kanR*, *ompX::kanR*, *yfeN::kanR*, *csgF::kanR*, *wza::kanR*, *flu::kanR*, *nmpC::kanR*, *eaeH::kanR*,
1737 *ydiY::kanR*, *yiaT::kanR*, *yaiO::kanR*, *mdtQ::kanR*, *pgaB::kanR*, *mipA::kanR*, *pldA::kanR*, *yzcX::kanR*,
1738 *ydeT::kanR*, *blc::kanR*, *gspD::kanR*, *yjgL::kanR*

1739 **S2 Table. List of all oligonucleotide primers used in this study.**

1740 **S3 Table. List of all plasmids used in this study.**

1741 The abbreviations in the selection column indicate the drug and its concentration that were used.
1742 Amp = ampicillin, Cam = chloramphenicol, Kan = kanamycin, Zeo = zeocin; 25 / 50 / 100 refer to 25 µg/ml,
1743 50 µg/ml, and 100 = 100 µg/ml, respectively.

1744 **S4 Table. Construction of all plasmids generated in this study.**

1745 **S5 Table. List of all phages used in this study.**

1746 The table lists all details regarding the taxonomic classification, isolation / source, host receptors,
1747 and genomic features of all phages used in this study. As *Caudovirales*, all these phages are classified as
1748 *Viruses* / *Duplodnaviria* / *Heunggongvirae* / *Uroviricota* / *Caudoviricetes* / *Caudovirales*, so only the
1749 classification on the level of family and below as defined by the ICTV
1750 [<https://talk.ictvonline.org/taxonomy/>; reference 142] is listed. For the reference phages, genome sizes and

1751 estimation of RM system recognition sites are based on the reference genomes in NCBI GenBank as
1752 indicated. Note that for phage T5 the reference genome includes the 10²219bp terminal repeat twice, unlike
1753 all other *Markadamsvirinae* genomes that we listed. The P2*vir* phage had been isolated as a spontaneous
1754 mutant of a P2 *cox3* lysogen (supposedly unable to excise [148]) and was analyzed by whole-genome
1755 sequencing (as described in *Materials and Methods*), revealing few single-nucleotide differences to the
1756 reference genome, the expected *cox3* mutation, and a one-basepair insertion in the lysogeny repressor gene
1757 *C* that results in a premature stop codon. Recognition sites of RM systems were identified using Geneious
1758 Prime 2021.0.1. The numbers include the two orientations of palindromic recognition sequences separately
1759 and do not account for the fact that the counts are not fully comparable, e.g., because type III RM systems
1760 require two unmodified recognition sites in head-to-head orientation for cleavage [49]. Given the high
1761 number of type III RM recognition sites in all genomes because of their short length (5 nt in case of both
1762 EcoCFT_II and EcoP1_I, see Fig 3B), this limitation is largely theoretical.

1763 **S6 Table. List of all phage genomes used in the *in silico* analyses.**

1764 **S1 Text. Construction of bacterial mutant strains.**

1765 **S2 Text. Generation of the Maximum-Likelihood phylogenies shown in this article.**

1766 **S3 Text. Technical considerations regarding the composition of the BASEL collection
1767 and the phenotyping of bacterial defense systems.**

1768 **S1 Figure. Supplemental data for Figs 4 and 5.**

1769 (A) Maximum-Likelihood phylogeny of *Drexlerviridae* and the *Dhillonvirus* genus of *Siphoviridae*
1770 based on several core genes with bootstrap support of branches shown if > 70/100. It is clearly apparent
1771 that *Drexlerviridae* are split into two major clades, one formed by *Braunvirinae* and *Rogunavirinae* and
1772 another one formed by *Tempevirinae*, *Tunavirinae*, plus a few other groups. Given that the phylogenies
1773 strongly agree on all major branches, the root of the *Drexlerviridae* phylogeny shown in Fig 4B was placed
1774 between these two major clades. (B) The locus encoding lateral tail fibers was analyzed in a sequence

1775 alignment of the thirteen *Drexlerviridae* phage genomes of the BASEL collection (see *Materials and*
1776 *Methods*). It is clearly visible that the upstream and downstream regions (encoding genes involved in
1777 recombination as well as primase / helicase proteins for genome replication) are highly conserved and fully
1778 syntenic, with exception of small insertions in a few sequences. Conversely, only the most 5' end of the
1779 largest lateral tail fiber protein gene is very similar among all analyzed genomes (green circle), while the
1780 rest shows neither synteny nor clear homology across all genomes. **(C)** The *bona fide* RBP loci downstream
1781 of the *gpJ* homolog are shown for all small siphoviruses (*Drexlerviridae* and *Siphoviridae* of *Dhillonvirus*,
1782 *Nonagvirus*, and *Seuratvirus* genera) where we had experimentally determined the terminal receptor
1783 (together with selected representatives where previous work had determined the receptor specificity). **(D)**
1784 The *bona fide* RBP locus of *E. coli* phage RTP was aligned to the homologous locus of phage
1785 AugustePiccard (Bas01) as described in *Materials and Methods*. For the region comprising *rtp44* and *rtp45*
1786 of phage RTP, the pairwise identity of the two nucleotide sequences is ca. 93%.

1787 **S2 Figure. Supplemental data for Fig 6.**

1788 **(A)** The locus encoding lateral tail fibers was analyzed in sequence alignments of the five
1789 *Dhillonvirus* phage genomes of the BASEL collection (top) and the seven *Nonagvirus* + *Seuratvirus* phage
1790 genomes of the BASEL collection (bottom) as described in *Materials and Methods*. In both cases two clear
1791 dips in overall sequence similarity are obvious, once at the *bona fide* RBP locus and then at the lateral tail
1792 fiber locus downstream of the far 5' end of its first gene. **(B)** Schematic comparison of representative *bona*
1793 *fide* RBP loci as shown in S1C Fig to the corresponding allele of *E. coli* phages JenK1, HdK1, and HdsG1
1794 that does not match clearly match any of them.

1795 **S3 Figure. Supplemental data for Fig 7.**

1796 **(A)** The locus encoding lateral tail fibers was analyzed in a sequence alignment of the
1797 *Demereciviridae: Markadamsvirinae* phage genomes of the BASEL collection as described in *Materials*
1798 *and Methods*. Sequence identity is high upstream and downstream of the lateral tail fiber locus (with
1799 exception of presence / absence of a few putative homing endonucleases) but drops considerably at the

1800 lateral tail fiber genes. Note that, as described previously, the lateral tail fibers can either be composed of a
1801 single large polypeptide or by two (or more) separate proteins [51, 60]. The same diversity in architecture
1802 of lateral tail fibers can also be seen at the corresponding loci of small siphoviruses (S1B and S2A Figs).
1803 **(B)** The illustration shows a phylogeny of the RBPs of all *Markadamsvirinae* phages shown in Fig 7B.
1804 Briefly, the RBP genes of all genomes (invariably encoded directly upstream of the terminase genes) were
1805 translated, aligned, and then used to generate a phylogeny as described in *Materials and Methods*. Three
1806 clear clusters emerge, one including all phages known to bind BtuB (left), one including all phages known
1807 to bind FepA (top right), and one including all phages known to bind FhuA (bottom right). Based on similar
1808 analyses by others [62], we conclude that the position of RBPs in these clusters is predictive of terminal
1809 receptor specificity of the phages encoding them.

1810 **S4 Figure. Supplemental data for Fig 8.**

1811 **(A)** Top agar assays with different surface protein mutants of the KEIO collection in comparison
1812 to the ancestral *E. coli* K-12 BW25113 strain were performed with serial tenfold dilutions of all
1813 *Tevenvirinae* phages used in this study (undiluted high-titer stocks at the bottom and increasingly diluted
1814 samples towards the top). The phages show strongly or totally abolished growth on each one of the mutants
1815 which identifies the primary receptor of each phage (also indicated by the color code highlighted on the
1816 right). **(B)** Top agar assays of reference strain *E. coli* K-12 Δ RM carrying empty vector pBR322_ Δ Ptet or
1817 pAH213_rexAB were performed with serial tenfold dilutions of phage T4 wildtype, a T4 variant encoding
1818 an apparently hypomorphic *rIIAB* fusion (see (C)), and phage T5 (as control). The *rIIAB* mutant of phage
1819 T4 is unable to form plaques on the *rexAB*-expressing host and shows only “lysis from without” [98], while
1820 the T4 wildtype and phage T5 are not affected. **(D)** A T4 phage mutant was erroneously obtained from a
1821 culture collection instead of the wildtype and encoded a peculiar *rII* allele with fusion of the *rIIA* and *rIIB*
1822 open reading frames (as revealed by whole-genome sequencing). Since such a mutant seems unlikely to
1823 arise spontaneously during shipping, we find it likely that this phage strain is related to the *rIIAB* fusion
1824 mutants employed for discovery of the triplet nature of the genetic code that were once commonly used

1825 [concisely reviewed in reference 149, 150]. Notably, position and size of the deletion fusing *rIIA* and *rIIB*
1826 are indistinguishable from the sketch drawn by Benzer and Champe for the *rIIAB* fusion mutant *rI589*
1827 which was used in the aforementioned work [151]. Unlike T4 wildtype, the *rIIAB* fusion mutant is
1828 susceptible to *rexAB* when ectopically expressed from a plasmid vector (see (C)) and therefore validates
1829 functionality of the *rexAB* construct.

1830 **S5 Figure. Supplemental data for Fig 9.**

1831 The illustration shows a sequence alignment of the locus encoding lateral tail fiber genes in phage
1832 rV5 and new isolates DrSchubert, AlexBoehm, and JeffSchatz that broadly cover the phylogenetic range
1833 of this genus (Fig 9B). It extends from the tail tape measure protein of phage rV5 (*gp49*) to the last large
1834 lateral tail fiber gene (*gp27*) [70, 71]. Note that most genes are highly conserved including the lateral tail
1835 fiber component with sugar deacetylase domain (compare Fig 9D; around position 8'000 in this alignment)
1836 or the short tail fiber locus (compare Fig 9E). Only the three largest lateral tail fiber genes show considerable
1837 allelic variation that is very strong for two of them (positions 10'000-14'000 and 16'000-19'000) and
1838 moderate for another one (positions 29'000 to 34'000).